Archean dome-and-basin style structures form during growth and death of intraoceanic and continental margin arcs in accretionary orogens

Timothy Kusky [a,b,*], Brian F. Windley [a,c], Ali Polat [a,d], Lu Wang [a], Wenbin Ning [a], Yating Zhong [a]

[a] State Key Lab for Geological Processes and Mineral Resources, Center for Global Tectonics, School of Earth Sciences, China University of Geosciences, Wuhan 430074, China
[b] Three Gorges Research Center for Geohazards, China University of Geosciences, Wuhan 430074, China
[c] Department of Geology, University of Leicester, Leicester LE1 7RH, UK
[d] Department of Earth and Environmental Sciences, University of Windsor, Ontario, Canada

ABSTRACT

Determining whether plate tectonics or some other mode of planetary dynamics operated in the early Archean is one of the most contentious and debated areas of Earth Sciences today. The Paleo- Mesoarchean dome-and-basin structures of the Eastern Pilbara craton are widely used as an example of an early Archean terrane supposedly unlike any produced by plate tectonics in the current mode of active-lid plate tectonics on Earth. In contrast, we produce a synthesis of the structural, magmatic and sedimentological development of the Eastern Pilbara craton from 3600 to 2800 Ma, and through comparative tectonic analysis, show that the craton developed following a typical orogenic sequence from an immature oceanic arc-dominated accretionary orogen, with the oldest rocks of the craton represented by slabs of primitive circa 3590 Ma gabbro - anorthosite - ultramafic rocks, and 3522–3426 Ma oceanic crust and overlying dominantly hydrothermal deep-water cherts imbricated in thrust piles and giant recumbent nappes. These were intruded by juvenile arc magmas including gabbros, diorites, and TTG suites, most of which intruded as sills into structurally favorable sites between 3484 and 3416 Ma. These oceanic crust and overlying sedimentary litho-tectonic assemblages of gabbro/ basalt/ komatiite/ chert, and TTG-diorite-dominated plutonic rocks were deformed into imbricate and antiformal thrust stacks intruded by suites of sheet-like TTG magmas during late regional shortening-related deformation at 3318–3290 Ma, then soon-after, folded by upright folds during continued contractional deformation. The intrusive style, compositions, and relationships to structures suggest that the late magmatic suites represent a massive slab-failure magmatic event similar to those formed during arc accretion and slab failure events in the North and South American Cordilleras, and older orogens of all ages. Late-orogenic shortening deformed these sheet intrusions into large domal structures, synchronous with or soon-after late- to post-orogenic cross-cutting steep-walled circa 3274–3223 Ma plutons vertically intruded the cores of some of the domes, forming nested plutons akin to the Cretaceous Sierra Crest Suite of the Sierra Nevada batholith, and deformed equivalents in Phanerozoic orogens. In a much younger magmatic event, a wide swath of the craton was affected by circa 2851–2831 monzogranite intrusions, after which the magmatic events of the Archean of the Eastern Pilbara were terminated by the circa 2772 Ma Black Range dolerite dike swarm, that preserves evidence for rapid APW drift during its intrusion.

The Eastern Pilbara represents only a very small preserved Paleo-Mesoarchean crustal remnant, measuring a mere 200×200 km^2, yet has been frequently used to model the presumed tectonic behavior of the entire planet for much of the Archean. In this synthesis, we show that the scale of the craton renders its significance in this literature greatly exaggerated. The Eastern Pilbara is only 1/3 the size of just the Sierra Nevada batholith. Considering the entire Eastern, Central and Western Pilbara belts, the scale and tectonic zonation of lithotectonic assemblages is remarkably similar to that of the California section of the North American Cordillera, from arc root (Eastern Pilbara. cf. Sierra Nevada), to fore-arc overlap basin (de Gray Basin, cf. Great Central Valley Sequence), to an accretionary complex (Western Pilbara, cf. Franciscan). The duration of different magmatic and deformational events, confined to three main pulses in 300 Ma, including about six total magmatic suites over 500 Ma, is similar to that of different pulses and/or accretionary events in the western American Cordilleran

* Corresponding author at: State Key Lab for Geological Processes and Mineral Resources, Center for Global Tectonics, School of Earth Sciences, China University of Geosciences, Wuhan 430074, China.
E-mail address: tkusky@gmail.com (T. Kusky).

examples, such as the peri-Gondwanan Famatinian (Cambro-Ordovician) and Pampean (Cambrian) arcs which were later affected by Permian and Mesozoic intrusives from the Peruvian coastal batholith, and form part of the present day active Andean margin of South America.

From this analysis, we firmly conclude from four degrees of similarity of the full data set of field, structural, temporal, and compositional data that the evolution of the craton is readily and rather simply explained by the plate tectonic paradigm. Thus there is no scientific justification to suggest that the geological characteristics of the Eastern Pilbara require any different imaginative or fantastic type of planetary heat loss mode during the interval of its formation from 3600 to 2800 Ma. The Eastern Pilbara is simply an exceptionally well-preserved small fragment of a poly-phase root of a continental margin accretionary orogen that evolved from accretion and magmatism from some of Earth oldest telescoped oceans and included arcs, in a regime of accretionary-style plate tectonics. Comparison with other well-preserved Eo-Mesoarchean terranes shows a common trait, that of derivation from immature introceanic accretionary orogens, building Earth's first continents.

1. Introduction

One of the most hotly contested and debated, and hence most important, topics in Earth Sciences today is determining when the present mode of a planet with a plate-dominated mobile lid became active on Earth, and whether any different type of planetary tectonic behavior preceded the present mode (National Academies of Sciences, Engineering, and Medicine, 2020). Solutions to this fundamental problem can be sought through numerical modeling (e.g., Sizova et al., 2015; Korenaga, 2018, 2021; Lenardic, 2018a, 2018b), sampling of relict mineralogical or geochemical traces of the earliest history of Earth (Harrison, 2020; Turner et al., 2020), or examining the geological record of Earth's oldest-preserved terranes (e.g., Kusky et al., 2018; Windley et al., 2021). In this contribution we focus on the archival rock record of one of Earth's oldest preserved cratons, the Pilbara of western Australia, which is widely cited as an archetypical remnant of a pre-plate tectonic mode of planetary heat loss, characterized by dome-and-basin structures, in which granite-cored domes are interpreted in some models as a manifestation of heat loss by overturn of a soft deformable stagnant lid, where heavy, tens-of-kilometers-thick volcanic piles are overplated on the planetary surface, then sink, partially melt, and domes rise into the soft "mushy" lid. The dome-and-basin pattern is said to have no comparison or Earthly analogs in the record of present, Phanerozoic, or Proterozoic mobile lid plate-tectonic mode of planetary heat loss (e.g., Nebel et al., 2018; Hawkesworth et al., 2020; Smithies et al., 2021). Since these dome-and-basin structures, with long-lived granitoid domes penetrating a cover of deformed volcano-sedimentary rocks are so widely regarded as the hallmark signature of a distinctive map pattern and tectonic regime preserved in Earth's oldest cratons, we ask if this speculation is correct, and test it using the rock record.

We note that gneiss domes, or dome-and-basin structures with cores of higher-grade gneiss, granite or migmatite surrounded by variably deformed and metamorphosed volcano-sedimentary sequences, are typical structures in the cores of orogenic belts of all geological eras (Suess, 1875; Argand, 1924; Collet, 1927; Heritsch, 1929; Eskola, 1949; MacGregor, 1947, 1951; Leo, 1991; Robinson et al., 1991; Windley, 1995; Kusky and Vearncombe, 1997; Whitney et al., 2004, 2013; Kusky et al., 2018; Lamont et al., 2019), yet their origin and significance has proven to be controversial through the ages. In recent literature, many works have ignored the classical geology of orogenic belts of all ages, and also the geological relationships of the Archean dome-and-basin regions being analyzed, and instead rely on numerical models, geochemical proxies, or greatly simplified views of the geological structure of these small cratonic regions, so a myth has emerged that dome-and-basin structures (a.k.a. gneiss domes), such as those in the Eastern Pilbara craton of northwest Australia, represent a unique map pattern only found in Archean terranes (e.g., Smithies et al., 2021). From that incorrect assumption, have stemmed many misconceptions about the nature of early Earth tectonics, and its similarity or difference from the tectonic regime operating on Earth at present. In this work, we aim to correct this misconception.

One of the most-cited arguments for a major secular change in tectonic regime from the current mobile lid back to a so-called stagnant lid regime on Earth is the supposed unique map pattern of domes-and-basins in Early Archean terranes, the eastern Pilbara being the most cited example (e.g., Kröner, 1984; Choukroune et al., 1995; Van Kranendonk et al., 2004, Van Kranendonk et al., 2007; Bédard, 2006; Bédard et al., 2013; Debaille et al., 2013; Sizova et al., 2015; Lin et al., 2013; Nebel et al., 2018; Hawkesworth et al., 2020). It is claimed that the map pattern in some cratons of regions comprised of granitic domes surrounded by metavolcanic and metasedimentary rocks represents a "supracrustal sequence" deposited on top of a granitoid substrate, and because of their density contrast in a regime of high geothermal gradients, the heavier supracrustal rocks sank down gravitationally between the uprising domes, leading to a so-called dome-and-basin or dome-and-keel architecture. This was further extended by numerical models (Sizova et al., 2015; Johnson et al., 2014, 2019) that showed that conditions can be derived where it is numerically possible for dense upper crust to sink into the mantle by so-called "drip tectonics," leading to the suggestion that the Archean tectonic regime was dominated by vertically-rising solid-state diapirs (sensu Ramberg, 1967; Weinberg and Podladchikov, 1995), and downward-sinking greenstones (Van Kranendonk et al., 2015; Wiemer et al., 2018).

The ideas of greenstones sinking between vertically rising diapirs, were first clearly elucidated by MacGregor (1947, 1951) in his "gregarious batholiths" concept for parts of the greenstone-gneiss terrain of Zimbabwe, and expanded to the Pilbara by Glikson (1979). The "gregarious batholith" concept was in turn a derivative of the earlier geosyncline concept, elucidated by Han Stille (1924), in his treatise "Grundfragen der vergleichenden Tektonik". However, like Pilbara, in the greenstone belts of Zimbabwe there are well-documented large-scale early thrust-imbricated nappes including granitoids that were later refolded into domes, and intruded by late granites forming zoned plutons, such as those that typify modern orogens (Stowe, 1968, 1971, 1974; Coward et al., 1976; Key et al., 1976; Kusky and Kidd, 1992; Kusky and Winsky, 1995; Kusky, 1998; Hoffman and Kusky, 2004; Sawada et al., 2020). To address this common belief among the Precambrian communities that the map patterns and geological relationships of the Eastern Pilbara Terrane represent a unique set of geological, structural and temporal relationships, we present a description and discussion of how and in what tectonic settings remarkably similar relationships have developed on Earth in the Phanerozoic mobile-lid tectonic regime. We then directly compare a few definitive examples (and there are many more) with the same features in the Eastern Pilbara Terrane. We then posit that the remarkably well-exposed and beautifully weathered East Pilbara terrane does not represent the vestige of a vastly different or unique planet preserved by chance from 3.5 Ga ago, but rather that it represents a well-exposed and weathered cross-section of the mid-crust of a typical continental margin arc that evolved from an early intra-oceanic accretionary orogen, to a collisional orogen intruded by late granitic magmas, to a stable craton in a mobile-lid plate tectonic regime.

2. Basins-and-domes formed during crustal growth in accretionary orogen magmatic arcs: examples from the American Cordillera

The roots of oceanic and continental magmatic arc are exposed in numerous orogens, and we posit that there are at least four orders of similarity between modern accretionary orogens and Archean dome-and-basin provinces, including 1) rock types and sources, 2) structures, including early accretionary structures, deformed into domes-and-basins, 3) map-scale patterns of variation, and 4) temporal-scales of evolution of magmatic and structural systems. Therefore, following recent documentation that most orogens in the Archean were accretionary in nature (Kusky and Polat, 1999; Kusky et al., 2018; Windley et al., 2021), we look to the present-day accretionary-collisional plate mosaic for the most-likely modern analogues to Archean orogens, to search for similarities and differences between similar systems of vastly different ages. While searching for similarities, we also recognize some differences, produced largely by increased heat production on early Earth (Arevalo et al., 2009; Lenardic, 2018a, 2018b), and different chemical and biological systems extant at the time.

Continental crust is built through a series of accretionary and plutonic events in accretionary orogens, from initial formation as parts of intra-oceanic arc systems, to more mature continental margin arc systems, and finally intruded by late- to post-orogenic plutons related to slab failure and breakoff, crustal thickening, and orogenic collapse (Kusky, 1989; Şengör et al., 1993; Kusky and Polat, 1999; Stern, 2010; Ducea et al. (2015a, 2015b), Pfiffner and Gonzalez, 2013, Hildebrand et al., 2018; Hildebrand and Whalen, 2014a, 2014b, 2020; Windley et al., 2021). Through these processes rocks in the orogens form over protracted amounts of time, typically starting for tens to 100 Ma within intra-oceanic systems (Arculus, 2003; Kelemen et al., 2003; Pearce and Stern, 2006; Stern, 2010; Reagan et al., 2010, 2013, 2017; Maunder et al., 2020; Ning et al., 2020; Dai et al., 2020; Bonner et al., 2020), then being part of continental margin accretionary orogen/arc systems for up to hundreds of millions of years (Paterson et al., 2011; Jagoutz and Kelemen, 2016), and experiencing multitudes of intrusive episodes at mid-crustal levels, each causing intrusion of steep-sided compositionally intermediate plutons (mostly TTGD), rising between or folded together with roof pendants, between or during regional deformation events, eventually forming continental crust comprised of a nest of domal plutons with remnants of older infolded volcano-sedimentary sequences (Komatsu et al., 1989; Brown et al., 2000; Stern, 2010; Kusky, 1989; C-T. Lee et al., 2007; Hildebrand, 2013; Ducea et al., 2015a; Kusky et al., 2018; Hildebrand et al., 2018; Windley et al., 2021). The plutonism in some cases, such as in the southern Andean arcs, can be superimposed in successive arcs built one on top of another with co-magmatic and intervening deformation events (Dewey, 1977; Draper et al., 1996; Chemenda et al., 1997; Pubellier et al., 1999; Teng et al., 2000; Clift et al., 2003; Vignaroli et al., 2008; Kusky, 2011; Kusky et al., 2018, 2020), over hundreds of millions of years, such as the Cambro-Ordovician Famatinian arc, which is now dissected over its 1500 km length by magmatic suites of the Permian-Mesozoic peri-Gondwana subduction system, and the modern Andean arc, thus showing magmatic activity in different pulses or "supersuites" for the past 500 Ma (Otamendi et al., 2009, 2012; Demouy et al., 2012) with a hot partially molten crust lasting over much of that time-frame, which has huge implications for interpreting the metamorphic and igneous history of Archean gneiss-dome terranes. In this section, we briefly describe the geological evolution and dome-and-basin map patterns of four typical areas of continental margin-type arc systems that have experienced complex histories, and have produced map patterns that are strikingly similar to those of the Archean "dome-and-basin patterns" of the famous 200 km × 200 km Eastern Pilbara craton. However, all the examples we choose here are Phanerozoic.

For comparison with the Eastern Pilbara, in this section we focus on some of the map relationships between accreted rocks of the North American Cordillera, and the Cordilleran Batholiths, in particular the Sierra Nevada and Coast Ranges Batholiths (Figs. 1, 2). We emphasize that the relationships we describe are about the structural and intrusive relationships and map patterns of the plutons, gneiss domes, and country rocks within the accreted terranes along the ancient continental margin of North America. We therefore focus on the map patterns, rock types, and compare their similarities and differences with map patterns, rock types and other relationships with the plutons and gneiss domes in the Paleo-Meso Archean granitoid gneiss domes of the East Pilbara craton. In this simple description therefore, we rely heavily on published geologic maps, geochronology, structural relationships and petrology, but we do not elaborate on the details of on-going debates about the origins of specific accreted terranes in the Cordilleran accretionary orogen, or subduction polarities during different accretion events, or similar interesting and important topics. For discussions of these topics, we provide abundant references in the text, and suggest recent reviews with diverging models such as Hildebrand (2013), and Pavlis et al. (2019).

2.1. Sierra Nevada Batholith, USA

The Sierra Nevada batholith (Figs. 1, 2) is about the same width as, but three times longer than the Eastern Pilbara dome-and-basin terrane. The rock types within the batholith belt, and the relationships of the plutonic rocks with surrounding older and contemporaneous volcanic assemblages is so similar to the Eastern Pilbara, that we highlight the salient features in this section. The "batholith" forms a NNW-trending 600 km-long composite assemblage of arc- and slab-failure-related plutonic, volcanic and sedimentary rocks, which exhibits distinct zonation in structural character, petrologic, and geochronologic systems, including a general west-east variation from mafic to felsic plutonic compositions with a concomitant decrease in age and nature of roof-pendant inclusions (Chapman et al., 2012). The depth of exposure increases markedly to the south. The batholith is composed of many hundreds of individual plutons that either have sharp generally steep mutual contacts with each other, or are separated by thin screens or roof pendants of older metamorphosed rocks, caught between the walls of the plutons, with which they generally have concordant contacts (Bateman, 1992; Hildebrand, 2013). Compositions range from gabbro to leucogranite but by far the most common rock types are tonalite, granodiorite, and granite (Ross, 1989). Most individual plutons were emplaced at mesozonal-epizonal depths based on their generally narrow hornblende hornfels metamorphic aureoles (Bateman, 1992) with crystallization at 3–4 kbar (~10–15 km), except in the south where this rises to >6 kbar (~ >20 km); the eastern margin of the pluton has crystallization pressures of 1–2.5 kbar (~3–10 km) (Nadin and Saleeby, 2008).

Cretaceous plutonic rocks and associated wall-rock supracrustal sequences of the Sierra Nevada can be divided into a western group or facies deformed at ~100 Ma, consisting of arc-related volcano-sedimentary sequences and related plutons (Saleeby et al., 1990; Memeti et al., 2010), and an eastern group or facies of circa 99–82 Ma tonalitic-granodioritic plutons of the Sierra Crest magmatic suite (Coleman and Glazner, 1998). Hildebrand et al. (2018) relate the older, western belt to arc-related magmatism, whereas the eastern belt is attributed to slab-failure magmatism, both of which ceased by 83 Ma (Saleeby et al., 2008).

Continental-margin and Andean arcs such as the Western North American batholiths, including the Sierra Nevada (Fig. 1) are broadly similar to intraoceanic arc systems (Stern, 2010; Jagoutz and Kelemen, 2016), but also some fundamental differences, and are the present-day locus of the largest amount of intermediate composition magmatism on Earth. They have crustal thicknesses that vary from ~30–70 km (the Sierra Nevada is towards the thicker end of the spectrum), and compositions between andesite and dacite representing an average between new mafic material added from the mantle, and products of upper
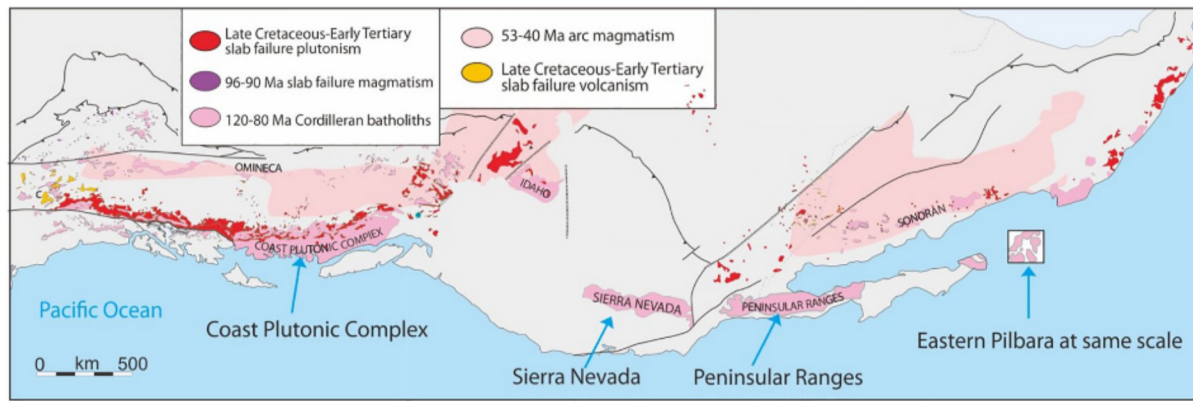
Fig. 1. Map of western North America (north towards upper left) showing Cordilleran-type batholiths of the North American Cordillera, along with post-collisional slab-failure magmatic rocks, and younger 53–40 Ma arc magmatism (modified from Hildebrand, 2013). The small box on right near Baja contains a greatly simplified map of the Eastern Pilbara Terrane (Fig. 4) drawn at the same scale as North America, and showing only the granitoid domes, tilted so that N is to the left. Note that the 200 × 200 km area of granitoid gneiss domes of the Eastern Pilbara (colored in pink) would fit into any of the major Cordilleran batholiths, including the Coast Plutonic Complex, Sierra Nevada, or Peninsular Ranges Batholiths. (For interpretation of the references to colour in this figure legend, the reader is referred to the web version of this article.)

crustal differentiation, and/or episodes of slab-failure magmatism from successive arc accretion events. Fig. 3 shows a generalized petrotectonic model for continental margin arcs, based larely on the Sierra Nevada example. Continental margin accretionary orogens with their arcs tend to have long life-spans (including multiple separate events), from tens to hundreds of millions of years (compared to ~50–60 Ma for most intra-oceanic arcs; Paterson et al., 2011) and they witness frequent lateral migration of the axis of magmatism, periods of extension or contraction, periods of quiescence and magmatic flare ups, times of lithospheric thickening and postulated times of foundering of their deep roots (Ducea et al., 2015a,b, 2020a, b). Importantly, most continental-margin accretionary-orogen arcs do not form during a single subduction event, but represent a collage of accreted arcs formed above a succession of subducting slabs over this long interval.

Many of the variations in continental-margin accretionary-orogen arcs are related to the age, angle, and temperature of the subducting slab (Fig. 3), relative velocities between over-riding and under-riding plates, and subduction of anomalous features such as seamounts, or spreading ridges. Continental-margin arcs are similar to intraoceanic arcs in that their magmas are fundamentally derived from dehydration of a subducting slab driving partial melting of the mantle wedge (Fig. 3), but they also differ from intraoceanic arcs in some fundamental ways (Jagoutz and Kelemen, 2016). First, they are compositionally richer in silica, have longer life spans, and typically experience greater variations in tectonic style than intraoceanic arcs, with episodes of upper plate extension (back- or fore-arc basin formation), contraction (fold-thrust belt formation, crustal thickening), strike slip faulting, fore-arc accretion, and fore-arc erosion. Because of their complex evolution including successive accretion of exotic arcs, migrating magmatic fronts, periods of extension and contraction, continental-margin and Andean arcs tend to have very wide areas (hundreds of km) of thickened crust and regions influenced by processes in the continental margin accretionary orogens containing the various accreted arcs, and underlying mantle wedge and/or subducting plates (C-T. Lee et al., 2007; Hildebrand, 2013; Ducea et al., 2015a). Importantly, these processes all produce a complex orogenic structure, with belts of accreted oceanic material (ocean plate stratigraphic, or OPS sequences, ophiolites), oceanic arcs, all intruded by multiple generations of intermediate, generally TTG-type plutonic rocks (Fig. 3). Many are intruded between or during deformation events, as sheets, that get folded into domes, and many form successively "nested" plutons, with progressively more K-rich plutons intruding as steep-walled domal structures into olded previously deformed magmatic suites. The result, at mid-crust depths (Fig. 3) is a map pattern of long-lived structurally complex magmatic and structural domes,

surrounded by down-folded "basins" or roof pendants of oceanic-like OPS. The map pattern is remarkable like that of Archean dome-and-basin provinces.

The Sierra Nevada Batholith (Figs. 1, 2) is instructive to students of Archean geology, who wish to interpret the structural basins and domes of the eastern Pilbara and elsewhere as downwarps of the crust, where the hypothesized process of sagduction takes the upper supracrustal rocks, where they become gravitationally unstable, and partially melt when they sink into the mushy lower crust or mantle, generating the late domal granitoids. In the pre-plate tectonic era of geosynclines, Bateman and Wahrhaftig (1966) made a comprehensive review of the geology of the Sierra Nevada batholith, and concluded that "the volcano-sedimentary wall rocks (supracrustals for the Archean workers, or the "framework rocks" of Bateman and Wahrhaftig) formed a large synclinal structure that downwarped, reaching deep in the crust where it was warm and thus partially melted in its axial zones, which in turn led to the upwelling of the magmatic suites of the Sierra Nevada Batholith". Such is still the widespread interpretation of many domal granitoids with surrounding volcano-sedimentary sequences in the Archean, but this idea has been left far behind in the Sierras with the recognition of plate tectonics. While the geosynclinal, or sagduction type models have been completely abandoned with modern studies on the pluton formation and emplacement mechanisms, there is still considerable research on the relative roles of folding induced by plate motions, vs. more localized deformation patterns caused by the rising subduction- or slab-failure-related plutons and consequential sinking of the roof pendants and other wall rocks, and the roles of pluton expansion or ballooning during multiple intrusive events (e.g., Pitcher, 1993; Saleeby, 1999; Saleeby et al., 2008; Fiske and Tobisch, 1994; Paterson and Farris, 2008).

2.2. Western Sierra Nevada Metamorphic Belt, USA

The northwestern side of the Sierra Nevada batholith (Figs. 2, 4a) is marked by Paleozoic-Mesozoic arc and accretionary complexes that strongly resemble the "supracrustal" assemblages of the Eastern Pilbara, in terms of the rock types, early structures, and how they participate in the growth of the orogen and interact with multiple stages of magmatism to eventually produce dome-and-basin structures. The accretionary complexes young generally westward (Saleeby et al., 1989; Hacker, 1993). These include the Paleozoic Shoo Fly complex of the Northern Sierra terrane, made of west-vergent thrusts of Ordovician-Silurian sedimentary rocks with Ordovician-Devonian ophiolitic mélange, cut by the elliptical circa 385–364 Ma Bowman Lake batholith (Hanson et al., 1988; Hildebrand, 2013), interpreted by most workers to have
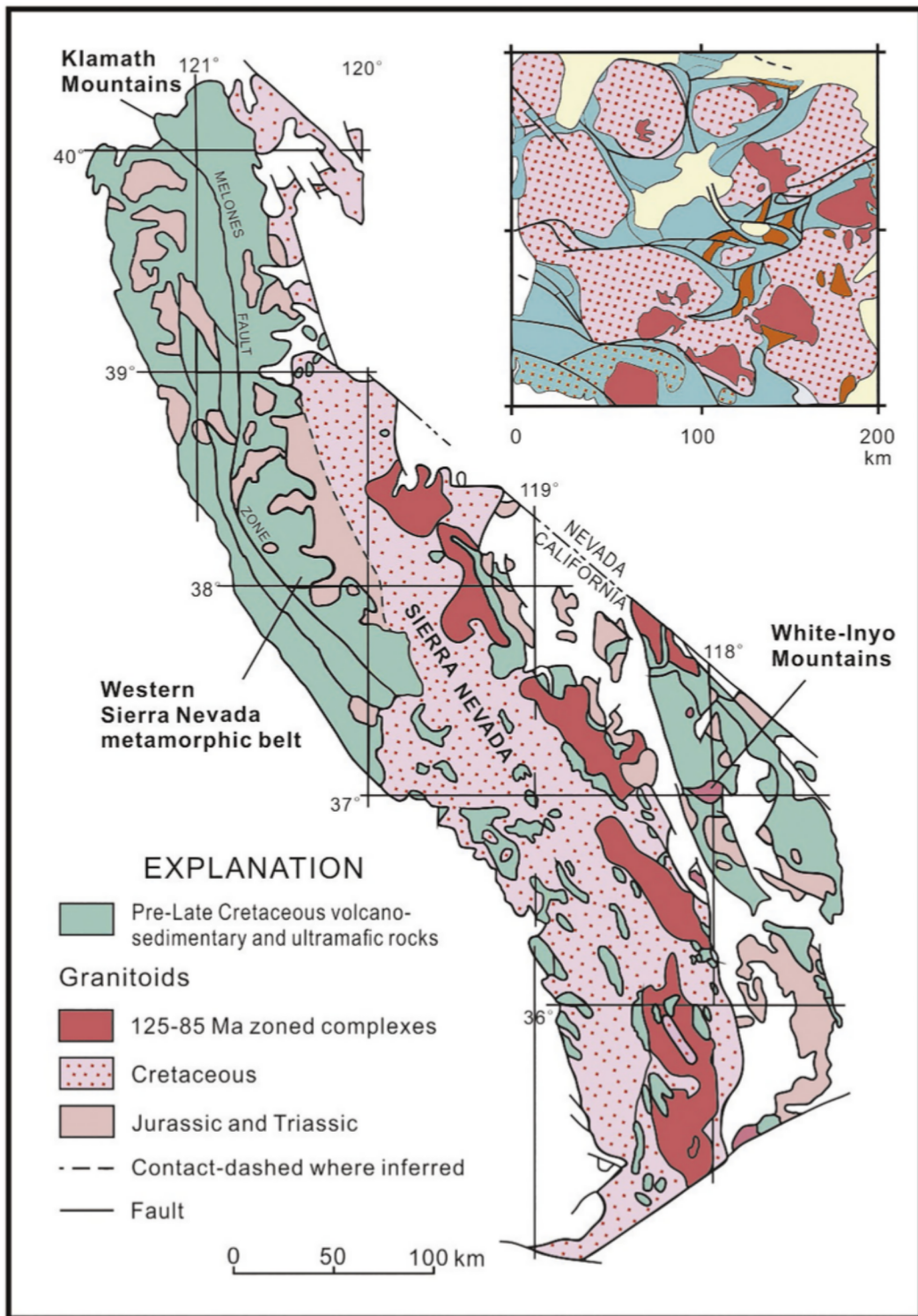
Fig. 2. Simplified map of the Sierra Nevada batholith and adjacent areas showing major plutonic suites and roof pendants, Klamath Mountains, and Western Sierra Metamorphic Belt, showing the locations of Figs. 3 a,b, and other features discussed in text. Compiled from Bateman (1992); Snelling and Gates (2009), after Irwin and Wooden (2001), and Saleeby and Busby-Spera (1993), Dunne et al. (1978) and Saleeby et al. (1978). Note locations of Western Sierra metamorphic belt, Klamath Mountains, discussed in the text. Inset map shows the map of the Eastern Pilbara Terrane at the same scale, with major rock groups colored the same for comparison.

formed by eastward subduction beneath North America, but have alternatively been interpreted as a peri-Gondwanan terrane that accreted after migrating through the Pacific (Wright and Wyld, 2006). These were overthrust by younger Paleozoic to Mesozoic calc-alkaline arc sequences of the Sierras, formed by subduction beneath North America (Burchfiel and Davis, 1975). West of the Northern Sierra

terrane, the Feather River peridotite, consisting of ultramafic tectonite, serpentinite, dunite, metagabbro, amphibolite, and metasedimentary rocks, occupies a suture marked by a thrust contact with the Calaveras mélange of the Central Belt (Smart and Wakabayashi, 2009) to the east (Figs. 2, 4a). The Central Belt includes a tectonic mixture of mélanges including the Calaveras, and lenticular structural slices of ultramafic,
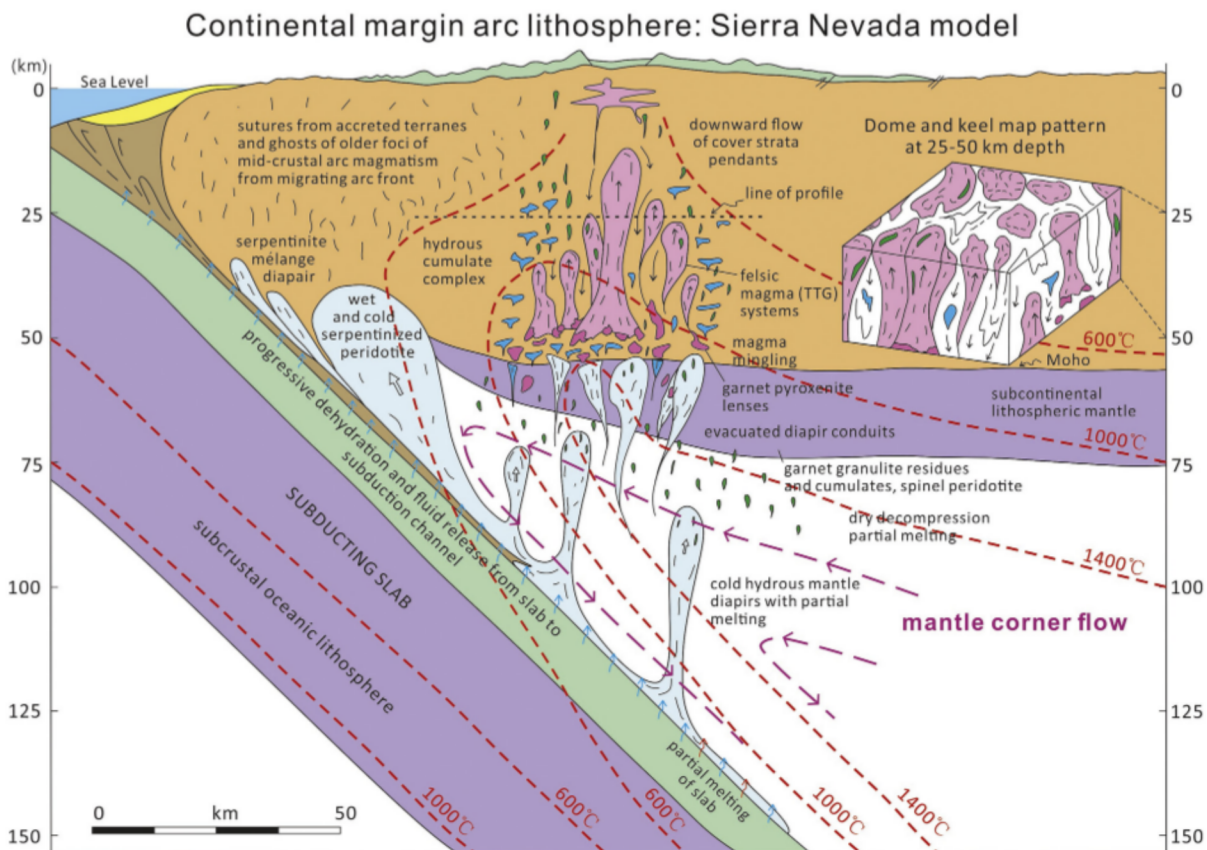
Continental margin arc lithosphere: Sierra Nevada model

Fig. 3. Model of a thickened continental-margin Andean-style arc and subduction system based largely on the Sierra Nevada batholith (Fig. 2). Model is developed from multiple previous works, including most notably Saleeby et al. (2003) and Ducea et al. (2010, 2015a, 2015b), Marschall and Schumacher (2012) and Zeelmer et al. (2015). Dehydration of the subducting slab and sedimentary/volcanic material in the subduction channel hydrates the mantle wedge and fluxes it with LILE, leading to partial melting, the formation of serpentinite (plus entrained material) diapirs and subcrustal relamination. Corner flow in the mantle wedge brings new mantle under hypersolidus flow to be metasomatized by the slab-derived flux. These processes form a lower crust/upper mantle hydrous cumulate complex derived from the slab flux melting, with possible additions of slab or subduction channel melts (adakites, etc.) under appropriate thermal conditions such as a warm slab-top geotherm. Dehydration melting and remelting of this complex and older residual material produce large volumes of TTG (felsic) magmas that rise in multiple steep-walled plutons, leaving garnet pyroxenite (arclogite) residues along the Moho. The plutons may rise under conditions of hot sub-solidus flow of the wall rock, although migmatization is common, so many plutons may rise as hypersolidus crystal liquid mushes that leave combinations of magmatic and tectonic foliations, depending on the depth of crystallization (generally between 15 or 20 to 50 km depth). Studies of deep arc roots show deformation is assisted by melts along grain boundaries, and many of the chemical signatures in deep mafic granulites from arc roots (such as Fiordland) show a significant melt flux during deformation and upward melt percolation (Stuart et al., 2016, 2018; Daczko et al., 2016). The line of profile for the 3-D block diagram (inset on the upper right of diagram) is at 25 km, showing typical dome-and-basin type outcrop patterns found in rocks from arc roots exposed at these depths, such as those discussed in the text from the Sierra Nevada batholith, Coast Ranges batholith, the Mojave Desert section of the southern Sierras, the Western Sierra Metamorphic Belt, and Klamaths, and are remarkably similar to those of the basin and domes of the Eastern Pilbara and other similar tectonic settings in some Archean cratons.

plutonic, volcanic, and sedimentary rocks (Dilek, 1989). Following this belt to the east (Fig. 4a) are two fault-bounded arc sequences, the Lake Combie and Slate Creek complexes.

The Calaveras Complex (Fig. 4a) includes structural units of Permian-Triassic-Jurassic basaltic to andesitic pillows, chert, volcaniclastics and phyllite with blocks of marble, forming a mélange beneath the Feather River ophiolite decorating the Foothills suture (Schweickert and Bogen, 1983). The fault-bound Jurassic Slate Creek complex includes a basal serpentinite matrix mélange, a middle unit of amphibolitic gabbro, tonalite and metadiabase, and an upper volcanic unit of greenstones and volcaniclastics (Day et al., 1985; Fagan et al., 2001). These are thrust over the Fiddle Creek complex, then all intruded by the circa 167 Ma Scales plutonic complex (this is the bright red Jurassic pluton labeled 167 on Fig. 4a, and the other numbered plutons refer to their determined ages. See Hildebrand, 2013 for details on the geochronology) and other circa 160–150 Ma plutons (Day and Bickford, 2004). The Middle Triassic Fiddle Creek complex includes a lower ophiolitic mélange with large "ophiorags" with intrusions of diorite, and diorite dikes, and units of chert-argillite associated with volcaniclastic

sandstones and olistostromes (Hacker, 1993). The Lake Combie complex (Fig. 4a) is similar-to the Slate Creek complex with a lower ultramafic unit in structural contact with an upper sheet of mafic flows, breccias, and volcaniclastic rocks (Day et al., 1985). The Smartville ophiolite/arc complex forms the westernmost belt of the Western Sierra Nevada Metamorphic Belt, and contains lower ophiolitic serpentinized ultramafics, gabbros, pillow basalts and sheeted dikes, overlain by 1.5–2 km of andesitic volcanics with minor dacites and clastic rocks (Day and Bickford, 2004). The lower volcanics are tholeiitic, whereas the upper ones are calc-alkaline and intruded by a circa 163–159 Ma sheeted dike complex, suggesting extension of the arc complex (Dilek, 1989).

The Western Sierra Metamorphic Belt is cut by a series of large oval-shaped Early Cretaceous (circa 140–142 Ma) plutons, especially in the area north of Lake Oroville (39 30 N: Fig. 4a), that are structurally similar to the dome-and-basin structures of the Eastern Pilbara. These may be related to an extensional arc phase (Hildebrand, 2009), and are associated with deposition of shallow marine and terrigenous clastic sequences in the arc (Lackey et al., 2008; Gehrels et al., 2009). In contrast to the older Jurassic intrusives, this suite clearly cross-cuts the
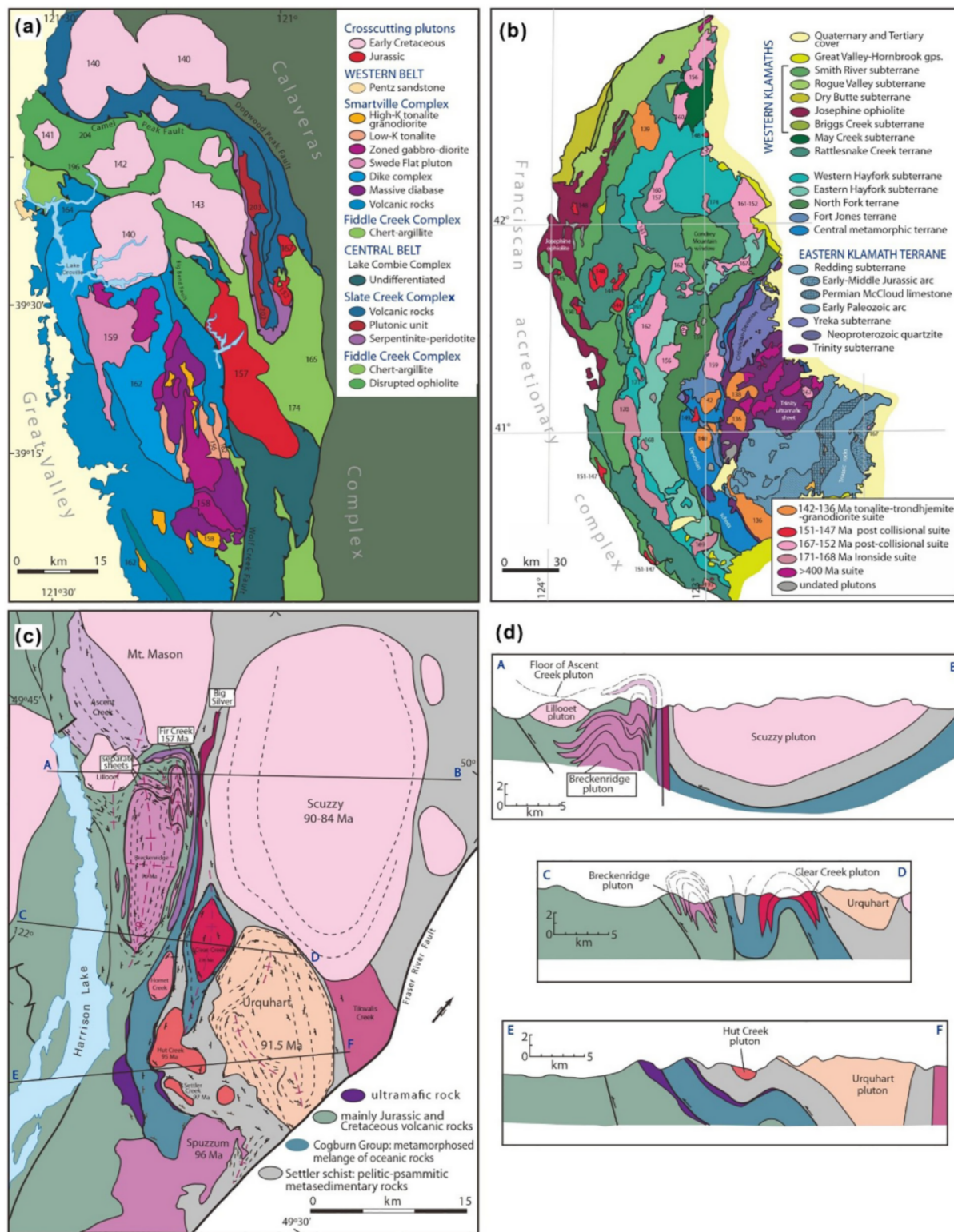
Fig. 4. Maps (modified after Hildebrand, 2013) of the (a) Western Sierra Metamorphic Belt (modified from Day and Bickford, 2004), (b) Klamath Mountains (modified from Irwin (2003), Snoke and Barnes (2006) and Allen and Barnes (2006), (c) map and (d) parts of the Coast Range Batholith in the Harrison Lake area in southern British Columbia (modified from Brown and McClelland (2000) and Brown et al. (2000). Note that the outcrop patterns in these accretionary orogen examples show that the crustal architecture was built by thin early thrust-sheets of mafic and ultramafic units initially thickening the crust, intruded by early concordant plutons (e.g., 96 Ma Spuzzum and Breakenridge, light purple in c), which were later folded, cut by strike-slip faults, then intruded by a younger suite of 90–84 Ma oval-shaped sub-horizontally floored plutons (e.g. Scuzzy) that were displaced downwards by up to 10 km after initial intrusion by inflation by additional magmas, further thickening the arc. (For interpretation of the references to colour in this figure legend, the reader is referred to the web version of this article.)

regional structures including some of the main terrane-bounding faults including the Dogwood Peak fault at the base of the Calaveras Complex, and the Big Bend fault between the Fiddle Creek and Smartville Complexes (Fig. 4a).

2.3. Klamath mountains

Farther north the Klamaths (Figs. 2, 4b) contain an east-dipping imbricate stack of accreted terranes (Irwin, 1972) that correlate in a general sense with the western Sierras described above. The oldest is the Eastern Klamaths, consisting of the Yreka, Trinity, and Reading belts. The Trinity is made of serpentinized peridotite cut by Neoproterozoic and Paleozoic trondhjemite and gabbro overlain by mafic volcanics, whereas the Yreka belt includes a series of imbricate nappes of metasediments, ultramafics, amphibolites, mélange, and quartzite (Hildebrand, 2013). The Reading belt includes early Paleozoic, Permian, and Triassic-Jurassic arcs that probably correlate with similar belts in the Western Sierras to the south (Fig. 2). The large Trinity thrust (Fig. 4b) separates the Eastern Klamaths from the Central Metamorphic Terrane (Fig. 4b), with a blueschist-bearing accretionary wedge (Hacker and Peacock, 1990). The North Fork terrane in the Central Metamorphic terrane includes meta-ophiolites, mafic volcanics, cherts, and limestones. The Western Klamath terranes to the west consist of Permian-Triassic mélanges, broken formation, ophiolites, and arcs. These are intruded by a multitude of plutonic domes and sheets (Fig. 4b), including olivine-clinopyroxene ultramafic complexes, diorites and monzodiorites, siliceous hornblende-bearing plutons, and gabbroic to quartz-diorite plutons (Wright and Wyld, 1994). Still farther west in the western Klamaths (Fig. 2, 4b), the Josephine ophiolite complex separates the Rogue Chetco arc from the Rattlesnake complex, and both were thrust over the basinal flysch of the Galice Formation between 153 and 150 Ma (Miller et al., 2003).

The entire Klamaths were intruded by numerous Jurassic-Cretaceous domal plutons (Fig. 4b), that strongly resemble the basin-dome structures that are found in the Eastern Pilbara and other cratons. These include circa 167–152 Ma ultramafic-gabbroic-dioritic-tonalitic-trondhjemitic-granodioritic plutons of the Wooley Creek Suite (Allen and Barnes, 2006), a 151–147 Ma suite of ultramafic to granodioritic plutons emplaced in late stages of deformation, and circa 140 Ma TTG (tonalite, trondhjemite, granodiorite) plutons that form semi-circular domes generally 10–30 km in diameter (Fig. 4b), similar to the late TTG plutons of the Pilbara craton. The younger plutons show evidence for mixing of magmas from different sources, and contamination by older crust (Barnes et al., 2006).

2.4. Coast Range Plutonic Suite

The Coast Range Plutonic Suite (Fig. 1) is part of a huge belt of batholiths that extends in the North American Cordillera from Washington in USA to Alaska, and is correlated with the Peninsular Ranges batholith to the south, and the plutonic belts in the South American Andes (Hildebrand, 2013; Ducea et al., 2015a). The belt is typically about 50–175 km wide (similar to the eastern Pilbara terrane) and made of many discrete and composite plutons. The Coast Range plutonic suite includes at least two tectonically juxtaposed belts. The western belt is built on the amalgamated Alexander - Wrangellia terranes, with discrete plutonic intervals recorded at 177–162 Ma, 157–142 Ma, and 118–100 Ma (Hildebrand, 2013) whereas the eastern belt experienced fairly-continuous intrusion from 180 to 110 Ma (Gehrels et al., 2009). The circa 100–90 Ma plutons (Fig. 4c) that contain large titanite and epidote crystals were intruded at >25 km depth during deformation, with some of the pre-92 Ma plutons clearly folded (Fig. 4c) and metamorphosed (Brown and McClelland, 2000), but the younger ones are not obviously deformed or metamorphosed. Other plutons, for instance in the Harrison Lake area (Fig. 4c) were emplaced at relatively shallow levels as subhorizontal sheets, that were inflated by up to 10 km by

younger intrusions, before folding, thus showing that both magmatic inflation and structural thickening by thrusting contributed to thickening of the arc crust (Brown et al., 2000). These mid-crustal plutons, and their contact relationships with suites of surrounding mafic, ultramafic, volcanic, and sedimentary supracrustal rocks are similar in composition, structural style, and metamorphic relationships to the 3450–3420 Ma Tambina plutonic suite of the Eastern Pilbara terrane, described below. These intervals of plutonism were followed by an interval of later Cretaceous - Paleocene plutonism in a 1000 km-long belt east of the Coast shear zone, characterized by plutons and steeply-dipping sills of foliated tonalite, and intrusive bodies that are zoned inwards from diorite, to tonalite and granodiorite (Crawford et al., 1987; Evenchick et al., 2007).

The Coast Ranges batholith exhibits some of the detailed processes that created the mid- to lower-crustal sections of a continental margin arc. Because some of the plutons were emplaced as sheet like bodies at >25 km depth in Jurassic and Cretaceous magmatic pulses, they were complexly folded along with their wall rocks, forming large domes with intervening synforms of strongly deformed volcano-sedimentary sequences, and all were deformed into gneisses and metamorphosed under amphibolite-granulite facies conditions (Crawford et al., 1999). As we describe below in section 3.4, these conditions are virtually identical to the intrusion conditions of the Tambina Suite of the Eastern Pilbara, intruded at circa 3450–3420 Ma. Much later in the Tertiary, the belt underwent rapid exhumation at 65–60 Ma involving at least 15 km of exhumation, accompanied by a tonalitic magmatic bloom with multiple sources of melts (Hollister et al., 2008), which Hildebrand (2009) associated with slab failure. Slab failure magmatism (Hildebrand et al., 2018) is an important part of the development of an arc that is rarely considered in discussions of the evolution, exhumation, doming and the intrusion of late granitoids in Archean cratons (e.g., see Nebel et al., 2018).

3. Domes-and-basins of the Early Archean Pilbara Craton. A unique geodynamic mode for Earth?

3.1. Regional relationships

In NW Australia the 3.59–2.77 Ga Pilbara Craton, one of the planet's smallest, contains several remarkably well-preserved, little-deformed, low-grade Paleoarchean greenstone belts, and is well-known for its granitoid gneiss domes in the east (Glikson, 1979; GSWA (Geological Survey of Western Australia), 1990, 2016; Van Kranendonk et al., 2007; Hickman, 2012, 2016). Broadly, the Pilbara is divisible into the Western, Central, and Eastern tectonic zones (Fig. 5), plus the poorly exposed Kurrana Terrane in the southeast, which is probably a part of the Eastern Terrane. The East Pilbara Terrane is the oldest (with some components in the range of 3.59–3.22 Ga), and is remarkable in that it contains ten gneiss domes that record three major (and several minor) magmatic events that span a time interval of more than 300 Ma, with other sporadic magmatic events extending to a length of >500 Ma, a history remarkably similar in multi-stage duration to the North American Cordillera, and more so- the Andes with its predecessor peri-Gondwanan Pampean (Cambrian) and Famatinian (Cambro-Ordovician) arcs, later affected by Permian to Mesozoic intrusives of the Peruvian coastal batholith (Demouy et al., 2012; Otamendi et al., 2012). The earliest known magmatic rocks in the Pilbara are 3.58–3.59 Ga gabbros and ultramafics that only occur as a small raft in the Shaw dome (Fig. 5), with the main magmatic intrusive rocks with ages between 3.48 and 3.42, and 3.32–3.30 Ga belonging to the tonalite-trondhjemite-granodiorite suite. Younger granitic suites with ages of 3.33–3.22 Ga become more K-rich with decreasing age (Champion and Smithies, 2007), a feature typical of orogens and particularly of nested plutons of all ages including the Cretaceous Tuolumne Suite of the Sierra Nevada, described above (e.g., Bateman, 1992; Coleman and Glazner, 1997). The Eastern Pilbara overlaps in age with the Karratha Terrane of the West
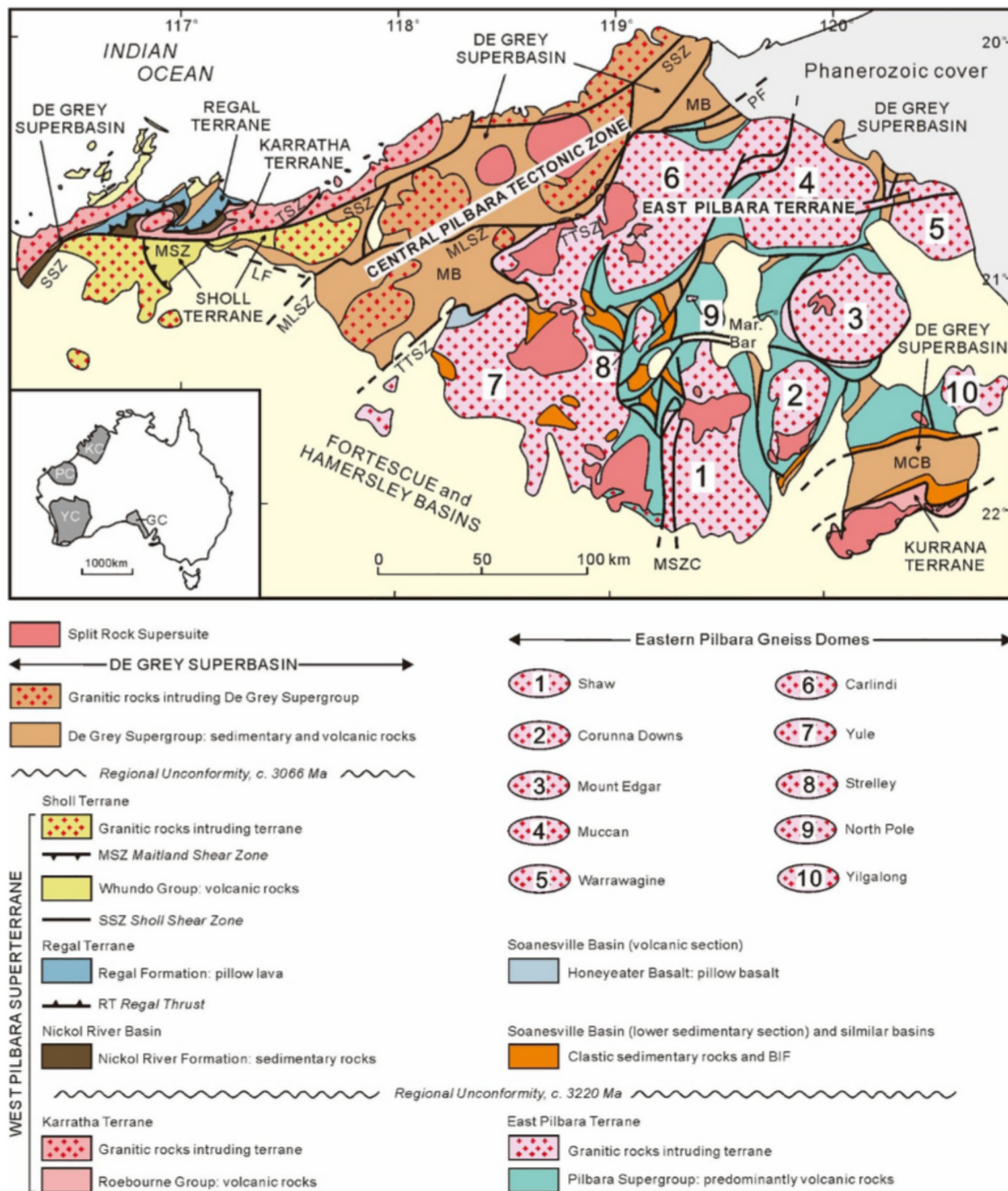
Fig. 5. Map of the Pilbara craton, modified from Hickman (2016). Names of granitic/gneiss domes are: 1-Shaw, 2-Corunna Downs, 3-Mount Edgar, 4-Muccan, 5-Warrawagine, 6-Carlindi, 7-Yule, 8-Strelley, 9-North Pole, 10-Yilgalong. Main shear zones and Basins of the Western and Central Pilbara include: MSZ- Maitland Shear Zone; MSZC- Mulgandinnah shear zone complex; SSZ-Sholl Shear Zone; MB-Mallina Basin; MLSZ- Mallina Shear Zone, PF-Pardoo Fault (part of TTSZ); TTSZ-Tabba Tabba Shear Zone. Shear zones of Eastern Pilbara discussed in text are keyed to later figures.

Pilbara Superterrane (3.28–3.07 Ga) and both the Eastern and Western Pilbara Terranes are overlain by 3.06–2.93 Ga rocks of the De Gray Superbasin (Hickman and Van Kranendonk, 2004; Hickman, 2016; Petersson et al., 2019), which covers most of the Central Pilbara Tectonic Zone and is preserved in other scattered locations around the Eastern Terrane (Fig. 5).

3.2. Western Pilbara Terrane

The Western Pilbara Superterrane (Hickman, 2016) comprises several components or terranes (Fig. 5) including the Karratha Terrane, which includes the Roebourne Group volcanics rocks and > 3.22 Ga

intrusive granitoids, pillow basalts of the Regal Terrane thrust over clastic sedimentary deposits of the Nickol River Formation along the Regal Thrust (Fig. 5), and the Scholl Terrane that consists of volcanic rocks of the Whundo Group emplaced along the Maitland Shear Zone (Hickman, 2016). The bulk structure of the terrane is thus an east-vergent thrust stack with linear belts of volcanic and sedimentary units that extend across the exposed width of the craton, imbricated, and then intruded by granitoids before 3.22 Ga (Fig. 5).

The Western Pilbara Terrane contains several greenstone belts, the most prominent of which is the 3.3–3.2 Ga, 3.5 km-thick Cleaverville belt, which in the revised nomenclature of Hickman (2016) is the Regal Formation, a part of the Roebourne Group in the Roebourne Greenstone

Belt of the Karratha Terrane shown on Fig. 5. On the coast and offshore islands, the Regal Formation consists of basaltic greenstones with pillow lavas, breccias and hyaloclastites, overlain by iron-rich bedded cherts i. e. banded iron formation (BIF), ferruginous and siliceous mudstones, and at the top sandstone/ mudstone/ conglomerate turbidites (Kato et al., 1998). The rocks have been repeated by thrusts into well-defined duplexes (Ohta et al., 1996), the unravelling of which provides the original ocean plate stratigraphy (OPS). The basalts are low-K tholeiites richer in FeO but otherwise similar-to modern MORB (Ohta et al., 1996). The metamorphic grade of the basalts increases downwards corresponding to ocean-floor metamorphism of modern mid-ocean ridges (Shibuya et al., 2007, 2010).

On the coast and on Dixon Island (Fig. 5) the Regal Formation (Cleaverville Group in the terminology of Ohta et al., 1996 and Kato et al., 1998) comprises imbricated cyclic packages of pillow basalts cut by dolerite dykes and sills (feeders to higher basalts, rhyolite flows (up to 900 m thick), pyroclastic breccias and felsic ash-fall tuffs, rhyolite tuffs (150 m) that are cut by black hydrothermal chert veins up to 2 m wide, as well as white silica dykes, bedded black cherts up to 100 m-thick, and overlying unconformable clastic sediments. The lithostratigraphy including the overall OPS is very similar to that of a modern immature island arc like Izu-Bonin, or more evolved examples in Japan (Taira, 2001). This mode of evolution is consistent with Pacific-type accretion envisaged by Krapez and Eisenlohr (1998). There has been no controversy about the interpretation of the Mesoarchean belts in West Pilbara in terms of their OPS and modern plate tectonic style of development, it is *nemine contradicente*. The Western Pilbara is therefore interpreted as a circa 3.3–3.2 Ga accretionary orogen (Kusky et al., 2013, 2016, Kusky et al., 2018; Windley et al., 2021) that records the early growth of the Pilbara craton, in a manner remarkably similar to the accreted oceanic terranes described from the Western Sierra Metamorphic Belt and Klamaths of the western USA, and the Coast Ranges of British Columbia (see above in section 2).

3.3. Central Pilbara Tectonic Zone and the De Gray Superbasin

Following the nomenclature of the Geological Survey of Western Australia (GSWA) the Central Pilbara Tectonic Zone (Fig. 5) is a tectonomagmatic belt that separates the Eastern and Western Pilbara Terranes, whereas the De Gray Superbasin is defined as a circa 3066–2919 Ma lithostratigraphic unit that covers portions of the Western, Eastern and the Central Pilbara Terranes, but is mostly preserved in the Central Pilbara Tectonic Zone (Hickman, 2016). The main units of the De Gray Superbasin are the 3228–3176 Ma Soansville Basin, the 3130–3110 Ma Whundo basin, the 3066–3015 Ma Gorge Creek Basin, the 3009–2991 Whim Creek greenstone belt, and the large 3015–2931 Mallina basin (Hickman, 2016). The basinal deposits and volcanic sequences of the Whim Creek greenstone belt were intruded by the following Supersuites: the circa 3274–3223 Cleland, the 3130–3093 Railway, the 3023–3012 Ma Orpheus, the 3006–2982 Ma Maitland River, the 2954–2919 Ma Sisters, and the 2851–2831 Split Rock (Fig. 5).

The De Gray Superbasin, which includes the De Gray Supergroup (Fig. 5) covers most of the Central Pilbara Tectonic Zone, has an age range of 3066–2919 Ma, and is generally divisible into the Gorge Creek, Whim Creek, and Mallina Groups. The Gorge Creek Group consists largely of sandstone, conglomerate, and psammitic to pelitic schist with minor basalt at the base, whereas the Whim Creek Group includes basalt, felsic volcanics, slate, and minor tuff (GSWA, 1990). The Gorge Creek Group is characterized by large variations in thickness of individual units, with rapid facies variations with chemical sediments near the base, but which are almost absent higher in the group. From exposures of presumed Gorge Creek Group in the Eastern Pilbara, Eriksson (1981) suggested deposition in an alluvial plain to submarine fan. The Whim Creek Group that is generally 500–1000 m thick includes basalt to andesite at the base, succeeded by tuffaceous and volcaniclastic deposits

with tuffaceous and agglomeratic rhyolites, overlain by 200 m of slate intercalated with tuffaceous andesite, dacite, and quartzite (GSWA, 1990). The Mallina Group in the Mallina Basin (Fig. 5) includes circa 3010 Ma volcaniclastic rocks, which include arkoses, graywacke and conglomerate at its base, but which is dominated by 2970–2955 Ma siliciclastic turbidites that consist of fine- to medium-grained, interbedded graywacke and shale, interpreted to have been deposited in a submarine fan in a cratonic basin (Smithies et al., 2001). Smithies (2002) reported 2970–2955 Ma boninite-like compositions in highly schistose rocks near the base of the succession, which consist of chlorite-tremolite-actinolite schists and epidote-talc-plagioclase schists that contain remnants of spinifex and cumulate textures. These volcanic-sedimentary rocks are associated with high-Mg diorites (sanukitoids) forming part of the Mallina mafic suite, which has geochemical features remarkably like modern boninites and sanukitoids from juvenile arcs, suggesting generation by subduction by 3.0 Ga (Smithies et al., 2004).

3.4. East Pilbara terrane

The East Pilbara terrane (3.59–3.16 Ga), roughly the shape of a 200 × 200 km (40,000 km^2) block (Fig. 5) contains three main 3.53–3.23 Ga volcano-sedimentary groups collectively known as the Pilbara Supergroup (Fig. 5). This term includes the Warrawoona, Kelly, and Sulphur Springs Groups which are complexly deformed and wrap around ten different composite granitic/gneiss/greenstone domes, each of which ranges from ~35 to 120 km in diameter, with shear zones or younger intrusives ubiquitously separating the gneiss/granite domes from the greenstones. The Sulphur Springs Group is locally, especially along the western margin of the Eastern Pilbara, overlain by a siliciclastic succession known as the Soansville Group (3228–3190 Ma, GSWA, 2016), including sandstones, turbidites, conglomerates, and shale and BIF capped by basalts and komatiites of the Honeyeater basalt (Brenner et al., 2020).

The gneiss domes of Eastern Pilbara (Fig. 5) are the archetype for the Archean dome-and-basin architecture that forms one of the basic structural styles and framework for many models of Archean tectonics (e.g., Macgregor, 1951; Glikson, 1979; Condie, 1981; Kröner, 1984; Kusky and Vearncombe, 1997). Some models suggest that the domes are vertically-penetrating diapirs that rose through and deformed a sinking but coherent stratigraphic cover of volcanic and sedimentary rocks (e.g., Collins et al., 1998; Williams and Collins, 1990; Van Kranendonk et al., 2007, 2014; Nebel et al., 2018; Hawkesworth et al., 2020), whereas others suggest that the domes are largely Type 1 fold interference patterns, similar to the arguments for the origin of the Paleozoic-Mesozoic granitoid gneiss domes in the southern Sierras (Blewett, 2002; Blewett et al., 2004; Hildebrand, 2013), or a combination of the different processes (Zegers and van Keken, 2001; Van Kranendonk et al., 2007).

In this section, we describe the geology of the most significant, best-studied, and well-exposed domes of Eastern Pilbara, and document how the domes development is intricately related with structural events during structural stacking of the early structural assemblage of the oldest basement, including imbrication of oceanic-type basement and OPS. In the domes, this early accretion is followed by successive intrusion by early oceanic arc and later continental arc-related magmas, along with accretion-related deformation that formed the domal structures. We make direct comparisons with the Cordilleran accretionary orogen batholith systems of the western Americas. The similarities are striking.

3.4.1. Lithotectonic assemblage of the Eastern Pilbara craton- stratigraphic or lithostructural?

The main volcano-sedimentary group of the Eastern Pilbara is the ~3525–3426 Ma Warrawoona, which Van Kranendonk et al. (2007, 2015) suggested consists largely of a pile of mafic lavas more than 12 km thick. The type section at Marble Bar (Mar. Bar in the Eastern Pilbara on Fig. 5) is suggested to be 15–20 km thick (Hickman, 1983, 2012), or

even 45 km in some models (Johnson et al., 2014; Smithies et al., 2021), while others have suggested that the volcano-sedimentary sequence is not stratigraphic, but is a structural or litho-tectonic sequence duplicated by numerous thrusts, folds, and strike-slip related structures (Krapez, 1993), and no thrust sheets are more than 6 km thick. The geochronological data are summarized by Hickman (1983, 2012, 2016) and Nijman et al. (2017), using stratigraphic correlations and nomenclature, showing that the ages and stratigraphic/structural correlations of the Warrawoona lithotectonic sequence are still not agreed upon by the stratigraphers, suggesting perhaps some structural complications have been overlooked.

In the stratigraphic models, the ~3350–3300 Ma Kelly Group sits on top of the Warrawoona Group, starting with carbonate/chert/siliciclastic rocks of the <3426 Ma Strelley Pool Formation, and consists of komatiites and basalts of the circa 3350–3335 Ma Euro Basalt, the felsic volcanic and basaltic Wyman Formation, and the komatiites, basalts and minor felsic volcanics of the Charteris Basalt (Hickman, 2012). These are overlain unconformably by the 3255–3235 Ma Sulphur Springs Group, consisting of basal siliciclastics of the Leilra Formation, komatiites and basalts of the Kunagunarinna Formation, then felsic volcanics, BIF, and chert of the Kangaroo Caves Formation (Hickman, 2012). The Soansville Group is placed above the Warrawoona in the stratigraphic nomenclature of GSWA (2016) and includes lower units (up to 3500 m thick) of sandstones, turbidites, conglomerates, with chert and BIF, overlain by basalts and komatiite (up to 1050 m) of the 3192–3176 Ma Honeyeater basalt (Van Kranendonk et al., 2010; Brenner et al., 2020).

In contrast to the "layer-cake" stratigraphic models, numerous structural studies have shown that the so-called "supracrustal" "supergroups" of the Eastern Pilbara "Superterrane" are not intact stratigraphic sequences, but are litho-tectonic complexes assembled during at least two periods of accretion tectonics, followed by extensional and strike-slip tectonic activity during which time most of the granitoids were emplaced and multiply deformed along with the volcano-sedimentary sequences (Bickle et al., 1980, 1985; Boulter et al., 1987; Krapez, 1993; Kusky and Vearncombe, 1997; White et al., 1998).

3.4.2. Components and structures of the domes-and-basins of the Eastern Pilbara craton

The granitoid gneiss domes of Eastern Pilbara (Figs. 5, 6, 7, 8) are composed of multiple generations of smaller plutonic suites that are exposed in a dome-and-basin-pattern eroded to the present level. Many show complex refolded deformation patterns with infolded and mylonitized inliers of multiply-folded (Bickle et al., 1985) roof pendants or inliers of adjacent volcano-sedimentary litho-tectonic assemblages, such as those mapped in detail on the margins of the Shaw batholith (Fig. 7). The structural style is reminiscent of the isoclinally infolded roof pendant synforms in the Sierra Nevada and Coast Ranges batholiths (Chapman et al., 2012; Hildebrand, 2013), described above in section 2. The domes are generally broad, open-tight structures with moderate dips (35–70 degrees, mostly 45–75 degrees) of outward contacts (Figs. 6, 7, 8) and with structurally overlying sequences, except where modified in late steep shear zones (e.g., Kloppenberg et al., 2001a). The domes are not simply vertically-walled intrusive diapirs as commonly assumed, and do not represent "birds eye views of the opposite ends of drips" (Nebel et al., 2018; Hawkesworth et al., 2020), or vertically-walled intrusive contacts as implied by such models. In this section we show that the domes represent a Type-1, fold interference pattern of an imbricated allochthonous cover, thrust over and intruded by multiple generations of magmas during crustal growth and thickening in a growing accretionary orogen, and later modified into essentially their current form by circa 2960–2930 Ma transpressional strain.

3.4.3. Igneous rock suites of the dome complexes

The oldest rocks in the East Pilbara Terrane are the spatially-limited 3.59–3.58 Ga (zircon U—Pb ages of leucogabbro and gabbro of 3588+/− 5 Ma, and 3578 +/− 1 Ma: Petersson et al., 2019) Mount Webber

gabbro and associated ultramafics and anorthosite from the Daltons pluton in the NW part of the Shaw dome (Fig. 7), which Petersson et al. (2019) correlated with TTG's of the same age from the Muccan dome (Fig. 8), with circa 3467 Ma zircons from the Owens Gulley diorite (Kemp et al., 2017) of the Warrawigine dome (Fig. 5). The main preserved magmatic pulses or flare-ups occurred during six major 20–30 Ma intervals separated by 10–100 Ma quiet intervals (ages follow the nomenclature of GSWA, 2016 and modification by Gardiner et al., 2017), at 3484–3462 Ma (Callina Supersuite), the 3451–3416 Ma (Tambina Supersuite), the 3324–3277 Ma (Emu Pool Supersuite), the 3274–3223 Ma (Cleland Supersuite), the 2954–2919 Ma (Mount Billroth and Sisters Suites), and the 2851–2831 Ma (Split Rock Supersuite) (Buick et al., 1995; Nelson, 1999; Bagas et al., 2005; Van Kranendonk et al., 2007; GSWA, 2016; Gardiner et al., 2017; Petersson et al., 2019).

The oldest supersuite, Callina, (excluding the small 3.58–3.59 Ga Webber gabbro) consists of a moderately deformed to migmatitic circa 3484–3462 Ma (GSWA, 2016) tonalite-trondhjemite-granodiorite (TTG) suite, especially well-represented in the Carlindi and Muccan domes, in the Shaw batholith, and to a lesser extent in the Mount Edgar, Corunna Downs, Yule, and Warrawagine domes (Figs. 5, 6, 7, 8). Some of the tonalites have large "clotty" hornblende" phenocrysts (GSWA, 2016). Most units within the Callina Supersuite are interleaved gneisses with moderate to strong foliations, intruded by sheets of massive to foliated muscovite-metamonzogranite and pegmatites (GSWA, 2016).

The 3451–3416 Ma Tambina Supersuite includes banded metatonalite and metagranodiotic gneiss, metatrondhjemite, and less-abundant metamonzogranite, metasyenogranite, and migmatites (GSWA, 2016). Some of the tonalitic bodies have hornblende schlieren, biotite-hornblende phenocrysts, migmatites, and are extensively intruded by sheets of pegmatitic leucogranite and granite. Xenoliths of amphibolite or larger pendants and rafts of greenstones are common. The Tambina Supersuite appears slightly more voluminous than the Callina (Figs. 6, 7, 8) consisting mostly of sodic tonalite and granodiorite; it was emplaced at mid-crustal levels and then apparently buried to ~25 km depth and metamorphosed in the amphibolite facies (Collins and Van Kranendonk, 1999), and deformed in many places (e.g. the Fig Tree gneiss along the south margin of the Mount Edgar Dome, Figs. 6, 11) to a gneissic fabric (Kloppenburg, 2003). The Callina Supersuite is roughly contemporaneous with felsic extrusive rocks of the Duffer Formation in the volcano-sedimentary package, whereas the slightly younger Tambina Supersuite overlaps in age with rhyolitic rocks of the Panorama Formation (Van Kranendonk et al., 2006).

The 3324–377 Ma (GSWA, 2016) Emu Pool Supersuite consists of many small plutons and sills that collectively form most of the outcrop area of some of the domes in the eastern part of the block, such as the Mount Edgar and Corunna Downs domes (Figs. 6), but is conspicuously absent or scarce in domes (e.g., Carlindi, Shaw, Figs. 7, 8) in the western part of the East Pilbara block. It includes mostly metagranodiorite to biotite-meta-monzogranite (GSWA, 2016), but ranges in composition from trondhjemite to syenogranite (Gardiner et al., 2017), and rare muscovite-garnet syenogranite (Davitt Syenogranite, GSWA, 2016). Most of these plutons are moderately to weakly foliated, with many local sills or seriate intrusions of monzogranite and muscovite granodiorite. Some of the plutons have mafic xenoliths, biotite-hornblende xenoliths, and xenoliths of the Tambina Supersuite and were intruded by monzogranites of the Cleland Supersuite at 3274–3223 Ma (GSWA, 2016).

The Cleland Supersuite (3274–3223 Ma) includes mostly weakly metamorphosed monzogranite, seriate intrusions of granodiorite, biotite-muscovite granodiorite, and tonalite, with local gabbro and dolerite, and rare associated pegmatite dikes (GSWA, 2016). Monzogranites contain hornblende and biotite and have local granophyric textures and some phases are foliated and have greenstone xenoliths

The Sisters Supersuite (2954–2919 Ma) in the Shaw and Muccan domes (Figs. 7, 8) includes biotite and K-feldspar porphyritic monzogranites, magnetite-bearing biotite monzogranite, metamonzogranite intruded by pegmatites and granitic dikes, and some phases show
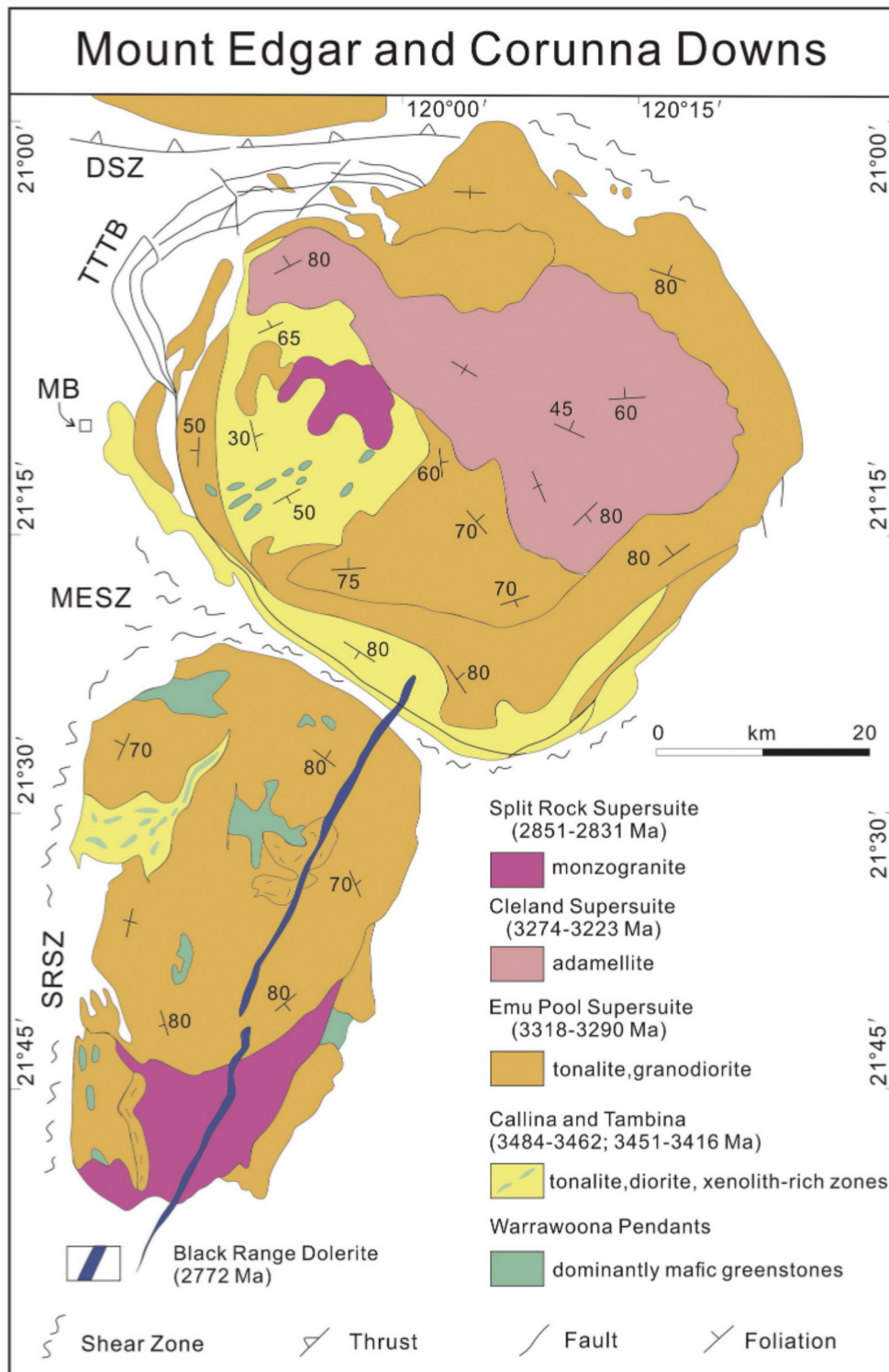
Fig. 6. Geological map of the Mount Edgar and Corunna Downs domes. Compiled from GSWA (1990, 2016)); McNaughton et al. (1993); Zegers (1996); Davids et al. (1997); Van Haaften and White (1998); White et al. (1998); Hickman (2012, 2016); Gardiner et al. (2017); and Nijman et al. (2017). Map shows the poly-phase nature of the plutonic rocks that compose the gneiss domes of the Eastern Pilbara. Note the older suites (e.g. Callina and Tambina Supersuites) form sheet-like bodies presently rotated into a steep attitude, concordant with the surrounding volcano-sedimentary sequences, reminiscent of the structures of the Coast Ranges Batholith (Fig. 4c). These field relations and map patterns show that these suites intruded as sheet-like bodies concordant to layering (bedding and bedding-parallel shear zones) in the volcano-sedimentary litho-tectonic package, and were later folded into the domal patterns during subsequent steep-sided intrusion events and additional upright folding events. The small stocks of the Coppin Gap Granite (Emu Pool Supersuite) within the Marble Bar greenstone belt (north center of figure) are shown above to have intruded during deformation at 3317–3314 Ma into extensional jogs in the Talga Talga antiformal stack, and they fed along shear planes into the larger sheet-like bodies of the Emu Pool Suite, which also form a folded sub-horizontal sill, structurally beneath the Talga Talga antiformal stack when the stack was unfolded about an ESE axis (Figs. 9, 10). The sub-horizontal sill was apparently fed from the funnel-like stock of Emu Pool granodiorite beneath the sill complex (Joorina Granodiorite of Fig. 10). Thus, the map patterns and structural relations show clearly that the intrusion of the early phases of magmas was structurally controlled, and that they later attained their dome-like forms during folding and later intrusions. Structural analysis of the Mount Edgar and Corunna Downs domes (e.g., Zegers et al., 1996; Kloppenberg et al., 2001a; Roberts, 2020), show that they have strongly sheared gneiss-greenstone contacts (dome side down senses of shear, Roberts, 2020), interpreted by Zegers et al. (1996) to have formed during lateral escape and extensional doming during regional *E*-W contraction at circa 3.3 Ga, with the Mt. Edgar shear zone (MESZ) between the domes representing a mid-crustal detachment associated with crustal thickening, partial melting, and intrusion of the granitoids during extensional collapse of the orogen. Gneisses of the Emu Pool Supersuite of the Muccan Dome Complex appear on the northern margin of the map, thrust over the Coppin Gap greenstone belt along the Doolena shear zone (DSZ). Abbreviations as follows: DSC-Doolena shear zone, MESZ- Mount Edgar shear zone, SRSZ-Split Rock shear zone (Coongnan belt), TTTB- Talga Talga thrust belt (see Figs. 9, 10).
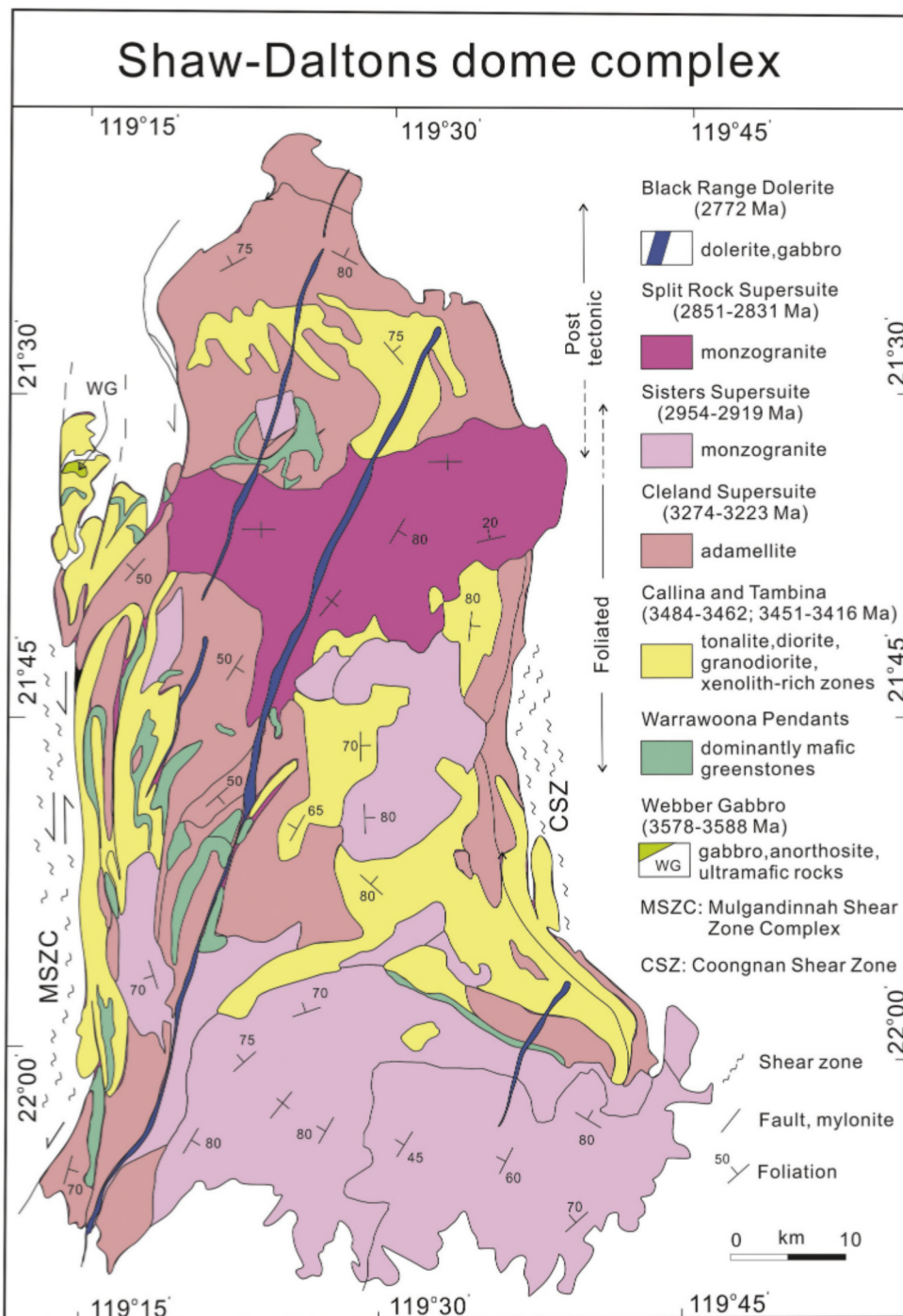
Fig. 7. Geological map of the Shaw dome complex. Compiled from Bickle et al. (1983, 1985); Cooper et al. (1982); GSWA (1990, 2016); Zegers (1996); McNaughton et al. (1993); Davids et al. (1997); Hickman (2012, 2016); Gardiner et al. (2017), Petersson et al. (2019); and Nijman et al. (2017). Note that especially along the western side of the dome the volcano-sedimentary sequences of the Warrawoona tectono-lithological package are thrust together with the rocks of the Callina and Tambina Superuites during early thrusting of the gneisses over the greenstones, then later refolded during doming of the Complex at 2960–2930 Ma during transpressional motion along the MSZC. Abbreviations: MSZC- Mulgandinnah shear zone complex; CSZ-Coongnan shear zone/ greenstone belt and Split Rock shear zone. WG- Mount Webber gabbro suite (Fig. 13 shows a detailed map of the Daltons area around the Mount Webber gabbro).

excellent magmatic textures including flow-alignment of phenocrysts and abundant schlieren (GSWA, 2016). Also present in the Sisters Supersuite are biotite-titanite and porphyritic biotite monzogranites. The Sisters includes the Indee Suite of metamorphosed hornblende-biotite granodiorite, and foliated tonalite, as well as the Millindinnah intrusion of gabbro, pyroxenite, and peridotite, and the Shay intrusion comprises metamorphosed gabbro, norite, and pyroxenite (GSWA, 2016).

The Split Rock Supersuite (2851–2831 Ma; GSWA, 2016) (and related rocks) consists of post-deformation highly fractionated monzogranites, syenogranite plutons, and Sn-Ta-Li-Be pegmatites, which intrude the Eastern Pilbara Terrane, the Kirruna Terrane, and the Central Tectonic Zone (Fig. 5). The granites include porphyritic muscovite-biotite monzogranites, leucocratic monzogranite, and coarse-grained to pegmatitic granites. The younger granitoid suites, like those of the Klamaths and Sierras described in section 2 above, become more potassic with decreasing age, and include the 3.32–3.29 Ga Emu Pool Supersuite, and monzogranites to syenogranites of the Cleland Supersuite. Post-3.2 Ga granitoids are known as the Mount Billroth, Sisters and Splitrock Supersuites (Hickman, 2016), with ages of 3.20–2.83 Ga. The circa 2851–2831 Ma Split Rock Supersuite roughly forms a NW-trending 150 km-wide by 200 km-long belt across the Eastern Pilbara and Central Pilbara terranes (Fig. 5), and is characterized by highly-fractionated, Si-rich (>73%) monzogranites and associated pegmatites
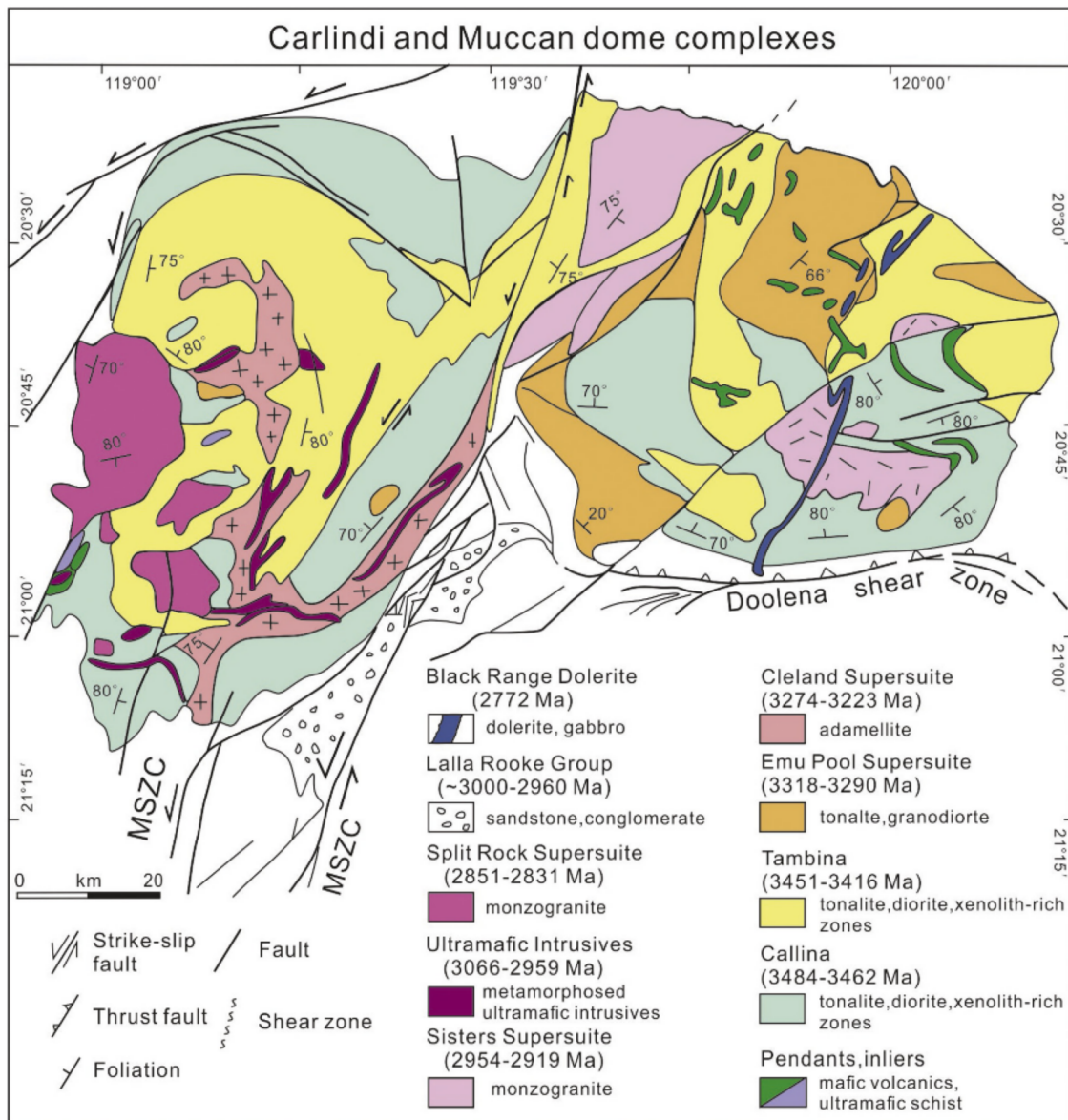
Fig. 8. Geological map of the Carlindi and Muccan dome complexes. Compiled from GSWA (1990, 2016); Zegers (1996); Van Haaften and White (1998); White et al. (1998), and Hickman (2012, 2016). The map pattern shows no resemblance to vertically intruded diapirs, but rather they are a series of folded sill complexes of the Emu Pool, Cleland, and Sisters Supersuites which intruded the older Callina and Tambina Supersuites that form the bulk of the domes, and were later folded into transpressional shear domes during motion along the sinistral MSZC at 2960–2930 Ma. Sandstones and conglomerates of the Lalla Rookh Group were deposited in a small foredeep-type transpressional basin south of the Carlindi and Muccan domes during this late transform motion, likely concurrently with thrusting to the south of the Muccan dome over the Coppin Gap greenstone belt on the Doolena shear zone. Acronyms: MSZC- Mulgandinnah shear zone complex.

with high LILE contents, enrichment in Y, depletion in Sr, and high LILE contents, consistent with derivation from melting of older crust (Champion and Smithies, 2001).

The last significant Archean igneous event of the Eastern Pilbara was intrusion of the NE striking dolerite dykes of the Black Range swarm at circa 2772 Ma (Figs. 6, 7, 8). These dykes are doleritic to gabbroic, and have been interpreted to have intruded near the surface, forming phreatomagmatic basaltic boulder conglomerates contemporaneous with the circa 2775 +/− 10 Ma Mt. Roe Basalt of the Fortescue Group (van Kranendonk et al., 2006). The correlation of the basaltic boulders in the Fortescue Group with the dykes was disputed by Evans et al. (2017), who nonetheless related both to Neoarchean rifting of the Pilbara, during its rapid drift across the polar circle at circa 2772 Ma.

3.4.4. Mount Edgar, Muccan and Corruna Downs domes; thrust nappes, duplexes, and antiformal stacks during doming

Most models for the formation and evolution of the Eastern Pilbara use relationships around the Edgar Dome, to discuss proposed diapirism, vertical tectonics of plumes rising through thick piles of volcanic rocks, and many other features. The type section for these stratigraphic and structural relationships is at Marble Bar, on the west side of the Edgar Dome (Figs. 5, 6). Presumed stratigraphic thicknesses of 15–45 km of the Warrawoona Group in many recent models for drip tectonics, sagduction, etc., for the early evolution of the Pilbara Craton, are based on the well-exposed type section as the best example to suggest that these extraordinarily thick piles of mafic/ultramafic volcanic rocks exist (Nijman et al., 2017; Hawkesworth et al., 2020; Smithies et al., 2021). However, at Marble Bar on the western side of the Mount Edgar Dome, and through the Talga Talga River and Bamboo Creek areas between the

Edgar and Muccan Dome Complexes (Fig. 5), the volcano-sedimentary sequence has been mapped (White et al., 1998) as a structural package consisting of twelve major (and many smaller) shear-zone-bounded lithological packages (Fig. 9), not an intact stratigraphic sequence. The older tectonic slices (2–8) of White et al. (1998) are little-deformed internally but occur in a gently to moderately west-dipping domal culmination named the Talga Talga antiform that formed during the first early E-W accretionary event (Van Haaften and White, 1998), and was later reactivated during extension (Zegers et al., 1996; Nijman et al., 2017). Slice 2 mapped by White et al. (1998) consists of the Lower and Upper North Star basalt units in the lowermost structural horses of the Talga Talga antiformal stack (Fig. 9), and slice 3 is made of the Mount Ada basalt. The structures related to emplacement of these structural horses in the duplexes of the antiformal stack (sensu Boyer and Elliot, 1982) were intruded along extensional jogs in the thrusts during deformation (Fig. 10), by magmas of the 3317–3314 Ma Coppin Gap granodiorite (GSWA, 2016) of the Emu Pool Suite of the Mount Edgar batholith (Williams and Collins, 1990), then overthrust by slices 4–8 that include rocks of the Duffer Formation, and others of the Salgash Subgroup of the Warrawoona Group (Nijman et al., 2017). Some of these granitoids form km-sized en-echelon elliptical plugs between shear zones mappable at the regional scale (Fig. 9) whereas others are smaller and confined to local extensional jogs on the faults (Van Haaften and White, 1998). This antiformal stack, named the Talga Talga antiform (Van Haaften and White, 1998), was later overridden by slices 9–12 along and north of the Doolena shear zone, that form a large thrust south of the Muccan dome (Fig. 9). These thrust sheets are composed of internally deformed metasediments, and are in turn overthrust from the north by slice 1 (which is internally deformed, and includes Gorge Creek-type sediments unconformably overlying the Muccan dome) and parts of the Muccan Dome.

The relationships within the Talga Talga antiformal stack (Van Haaften and White, 1998) are the key for understanding the structural development of the Eastern Pilbara basement, the relationships of the structures, and to the emplacement of the granitic domes. The antiformal stack developed in the circa 3525–3426 Ma Warrawoona lithotectonic succession, including the Talga Talga succession (North Star Basalt, Mount Ada Basalt, and the Salgash Succession (Towers Formation, Apex Basalt, Panorama Formation, and Euro Basalt), which are separated by felsic volcanics of the Duffer Formation. The shear zones are generally layer (bedding) parallel schistose zones, but converge at the southern end of the antiformal stack where they continue into the Mount Edgar Shear Zone (Fig. 9). Many of the shear zones are thin, but in the North Star Basalt they are up to 75–85 m thick, and cut the basalt at angles of up to 30 degrees (Van Haaften and White, 1998). Importantly the shear zones preserve kinematic indicators and stretching lineations (Van Haaften and White, 1998) that indicate consistent thrust-sense transportation to the ESE and are not radially-folded by the dome structure (Fig. 10) so their origins and relationships of the structures to the Mount Edgar dome show that the thrust stacking and intrusion of the Emu Pool Suite was not related to the doming. The McPhee Reward Formation of early workers was found by Van Haaften and White (1998) to be a mafic mylonite and is a major shear zone (Figs. 9, 10) that was important in building the regional antiformal stack. Failure *to-the-present-day* to recognize this and other shear zones, and to regard them as stratigraphic units has led to highly-unusual interpretations such as calling the anomalously thick antiformal stack a "blob" or "birds eye view of a drip" (i.e., Nebel et al., 2018; Hawkesworth et al., 2020) in stratigraphic maps of the greenstones around Marble Bar (Fig. 5), and demonstrates that the widespread use of measured stratigraphic sequences through an antiformal stack with multiple (at least 12) thrust horses, without recognizing the structural breaks, will lead to erroneously thick perceptions of stratigraphic thickness (e.g., Van Kranendonk et al., 2007, 2015). *Unfortunately, Marble Bar is the type section of the Warrawoona Group (Hickman, 1983) and incorrect stratigraphic thicknesses of 15–45 km have been propagated*

through the literature and are a major reason that so many models of early Earth tectonics suggest that the planet behaved in a drastically different way than at present. Additional major shear zones (up to 300 m thick) occur in the Duffer Formation and Mount Ada Basalt, such as the Duffada shear zone (Figs. 9, 10), and like the other early shears, was intruded by both *syn*-shearing hornblende granodiorite sheets (circa 3304 ±10 and 3314 +/− 13 Ma, U—Pb SHRIMP, Williams and Collins, 1990; Warrulinya Suite) sheets, and later by a post-deformation micaceous granodiorite. Some granodioritic sheets along the shear zones feed intro small cogenetic en-echelon stocks along the northern margin of the structure (Fig. 9). Interestingly, the hangingwall shear zones (with intrusions) show higher-temperature shearing fabrics (with hornblende development) than the footwall shear zones, perhaps related to the syn-shearing intrusive sheets (Van Haaften and White, 1998), or perhaps representing a dynamothermal aureole.

The Talga Talga antiformal thrust stack formed during early horizontal contractional deformation, (with early extensional structures locally shown along some faults) with the hangingwall transported to the ESE (Figs. 9, 10a), which was intruded by syn-thrusting, hornblende-bearing granodiorite sheets of the Coppin Gap granodiorite (Emu Pool Supersuite) along extensional zones in the shear system at 3317–3314 Ma (Van Haaften and White, 1998; White et al., 1998; GSWA, 2016), then re-oriented by NW-SE shortening along conjugate shears, and finally contracted and re-oriented at ~2950 Ma by N-S shortening, forming additional thrusts, all in turn cut by cross-cutting late plutonic rocks (mica-bearing granodiorite and sugary-textured granite) of the Mount Edgar batholith along the eastern margin of the antiformal stack. Thus, the early generations of intrusions are sheet-like bodies intruded along extensional segments of oblique thrust systems, which were re-oriented into antiforms and synforms and dome-like structures, but there are no radially-oriented stretching lineations or any other structures that might suggest intrusion of the Mount Edgar or other batholiths by solid state diapirism (Van Haaften and White, 1998).

The geometry of the Talga Talga antiformal stack and associated intrusions (Figs. 9, 10) is instructive to understand the mechanisms of intrusion of the granitoids across the Eastern Pilbara. The circa 3317–3314 Ma granodiorite stocks on the northern limb of the Talga Talga antiformal stack (Coppin Gap Granodiorite of Fig. 9) were intruded into extensional gashes in the oblique thrust system (Van Haaften and White, 1998), and then fed along the shear planes. They correlate with the large sill-like bodies of the circa 3324–3277 Ma Emu Pool Suite sills (numbers 10, 11, 16, 19, 20, of the Coppin Gap, Kennell, Jenkin, Mullugumya and Zulu Granodiorites of Fig. 10) along the edges of the Mount Edgar Batholith, which form the lower plate to the Talga Talga antiformal stack. If the stack is unfolded to its circa 3300 Ma configuration (Fig. 10b), the small stocks are located in the gashes in the system in the upper plate, but the large ring of Emu Pool granodiorites in the granite complex form a large sub-horizontal sill in the lower plate in its unfolded state, in a large tensional structure that fed up into the antiformal stack of Talga Talga (Fig. 10c,d,e). When the later folding and doming of the Mount Edgar Complex occurred, probably partly concurrently with intrusion of the Cleland or Sisters Supersuites, the large subhorizontal sill was folded into a dome, into which the younger intrusives expanded. The intrusion mechanisms of the early tonalites and granodiorites along thrust planes in the Talga Talga antiformal stack and Mount Edgar Dome are similar to those described from the Neoarchean Point Lake antiformal stack and fold thrust belt of the Slave Province (Kusky, 1991, 1992), and from the Tertiary arc-trench system of Japan by Komatsu et al. (1989), who showed how peraluminous tonalites were intruded along thrust planes into gabbro-diorite complexes during sub-horizontal accretionary tectonics and granulite facies metamorphism. In a significantly different interpretation, Nebel et al. (2018) noted that the younger granites in the Mount Edgar Dome are more K-rich than the older ones, and suggested therefore, that the younger intrusions and "doming" represent the start of plate tectonics on Earth, a criterion and suggestion later adopted by Hawkesworth et al.
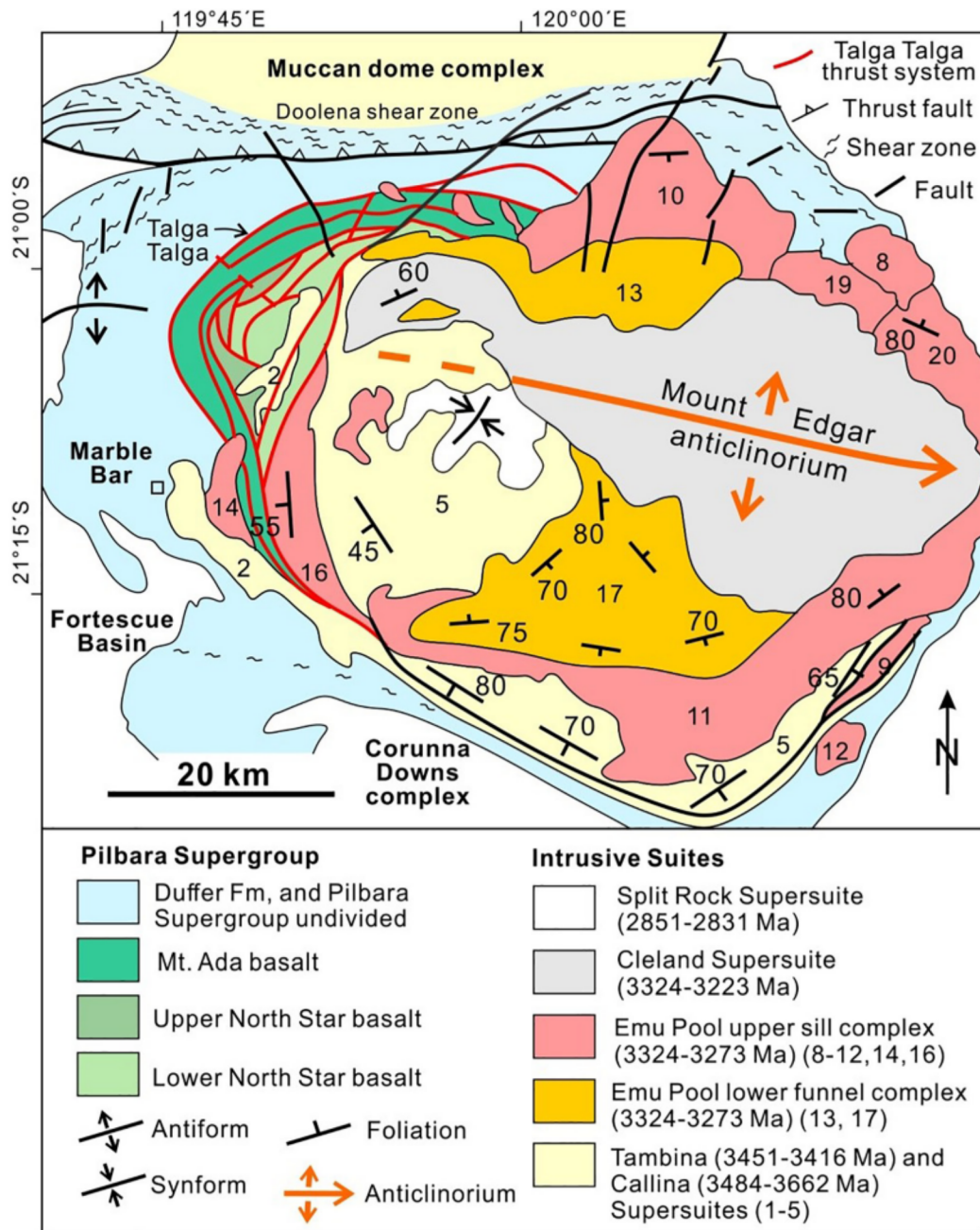
Fig. 9. (a) Simplified structural map of the Marble Bar - Doolena Gap greenstone belts (nomenclature of Hickman, 2012) and adjacent Mount Edgar granitoid gneiss dome complex, showing the division of the structurally lower parts of the belt into twelve major (and several minor) shear-zone-bound structural packages. The lower thrust sheets that form the Talga Talga antiformal stack continue to the south through the Marble Bar area (Fig. 5), where the thrusts merge in a tip line and become highly deformed in the high-strain zone between the Mount Edgar and Corunna Downs dome complexes. Map compiled from White et al. (1998), Van Haaften and White, (1998), Nijman et al. (2017), Gardiner et al. (2017), and Blewett et al. (2004). The Mount Edgar dome complex is not a simple diapir, but consists of at least 23 individual gneissic and plutonic units (Gardiner et al., 2017) that are exposed in an antiformal culmination (Mount Edgar anticlinorium) whose major fold axial surface strikes WNW. Dips of units are generally moderately (45–75 degrees) outwards, except where affected by later steep shear zones (e.g., Kloppenberg et al., 2001a). The oldest plutonic rocks are the dioritic-granitic gneisses of the circa 3484–3462 Ma Callina Supersuite (numbers 1–3 in yellow), and the 3451–3416 Ma Tambina Supersuite orthogneisses (4,5 in yellow). The most voluminous rocks in the dome are the multiple sill-like intrusions of the 3324–3277 Ma Emu Pool Supersuite that were at least locally intruded during thrusting of the greenstone belt over the complex. Based on map patterns and structural relationships, we divide the Emu Pool into an upper sill complex, plutons 8–12, 14, 16, that now form moderately-to-steeply-dipping sheets around the edge of the dome, but when unfolded (Fig. 10) form a subhorizontal sill parallel to the thrust faults that was intruded by the Coppin Gap granodiorite member (10 in the northern part of the map) during deformation. This sill complex is succeeded downward by a funnel-shaped complex (when unfolded, see Fig. 9), which is made of the Munganbrina and Joorina plutons (13, 17) that generally have foliations defined by shape-preferred orientations of feldspars parallel to the funnel walls. These are all intruded in the center of the dome by the late, steep-walled Bishop Creek Monzogranodiote of the 3274–3223 Ma Cleland Supersuite and the 2851–2831 Ma Monzgranite of the Spilt Rock Supersuite (Moolyella Monzogranite, not colored). (For interpretation of the references to colour in this figure legend, the reader is referred to the web version of this article.)
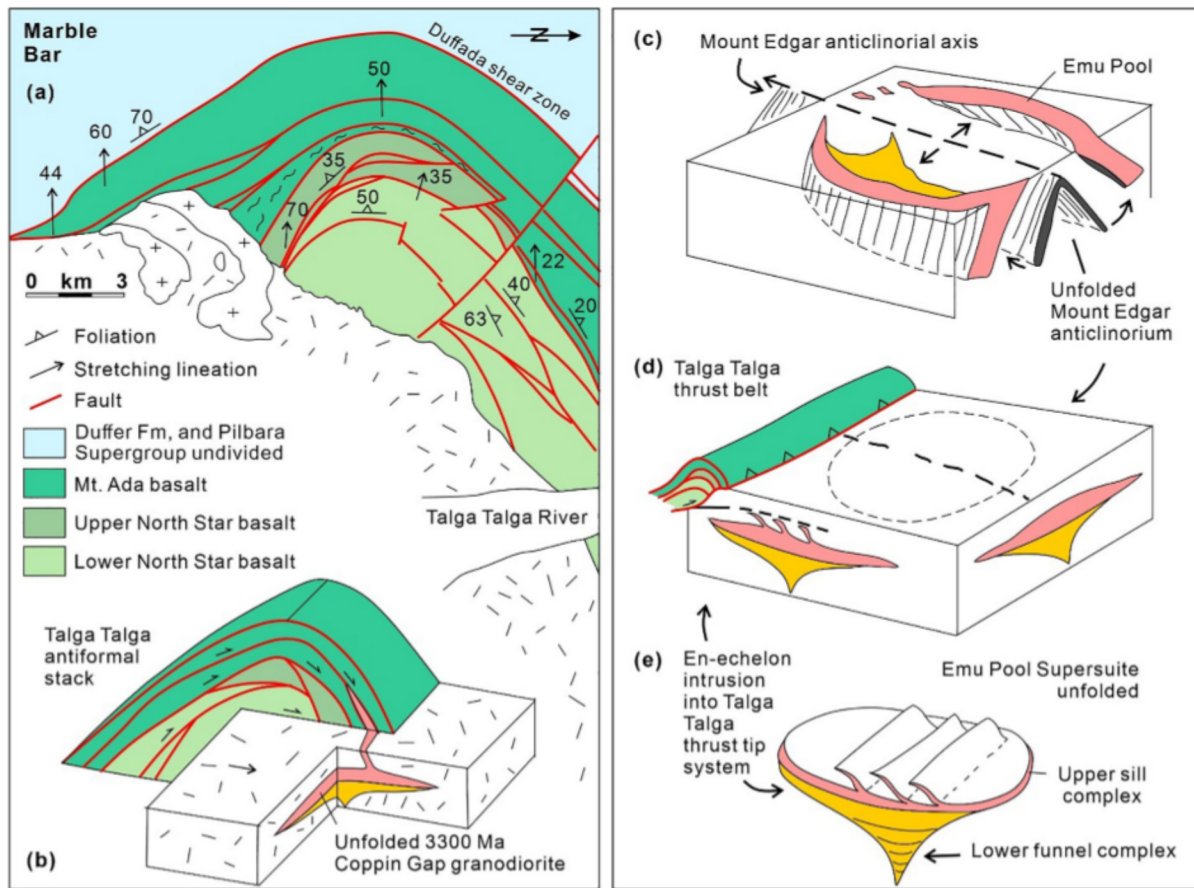
Fig. 10. (a) Structural map of the Talga Talga antiformal stack. Note the thick shear zone between the North Star basalt units and the Mt. Ada basalt, is known as the McPhee Reward shear zone (formerly regarded as a formation). Note the stretching lineations are not folded by the dome structure. (b) Geometry of the Talga Talga antiformal stack shows a pre-doming structural evolution stage with *syn*-thrusting, hornblende-granodiorite sills of the Coppin Gap suite (Emu Pool Supersuite) that intruded along transtensional segments of the thrust planes at circa 3317–3314 Ma, and were then deformed, and rotated and intruded by granitoids of the Mount Edgar dome by 2950 Ma (structural data from Van Haaften and White, 1998, age from GSWA, 2016). Only the section near Marble Bar is shown, see Fig. 9 for location. (c) conceptual block diagram showing the orientations of the sill-like and deeper funnel-like suites of the Emu Pool Supersuite in their present orientations, the geometry of the large Mount Edgar anticlinorium, and the direction it will be unfolded, for (d) unfolded geometry of the Emu Pool Supersuite, showing how it forms a shallow sill complex below the Talga Talga antiformal stack (numbers 10, 11, 16, 19, 20, of the Coppin Gap, Kennell, Jenkin, Mullugumya and Zulu Granodiorites), being fed by the deeper funnel-shaped Emu Pool bodies (17-Joorina granodiorite, and 13-Munganbrina monzogranite). (e) simplified view of the Emu Pool magmatic system at circa 3300 Ma.

(2020).

3.4.5. North Pole and Strelley domes; imbricate thrusts systems domed in transpression

The North Pole and Strelley Domes (Fig. 5) are large structures, but generally preserve higher structural levels than the Mount Edgar and other majors domes, and therefore reveal additional information about the early thrust stacking of the Pilbara Supergroup lithotectonic assemblage, and the relationships between the types of deformation, its causes, and the relationships between plutonism and deformation. We describe the geology of the North Pole-Strelley Domes here. In the North Pole Dome area (NP on the eastern part of Fig. 5), where the lower part of the Warrawoona Group is well exposed, there is a domal structure with a 2 × 5 km wide circa 3459 +/− 18 Ma adamellite/monzogranite (GSWA, 2016; Nijman et al., 2017) in its core, flanked by rocks of the lower Warrawoona Group (North Star and Mt. Ada basalts) on the limbs of a doubly-plunging NE-striking fold, which forms a ~ 20 degree acute angle with the sinistral Mulgandinnah shear zone complex (MSZC on Figs. 5, 11), consistent with uplift and tilting of the dome during circa 2960–2930 Ma transpression along the shear zone (section 3.5), to expose an oblique section through the older litho-structural section. From here, Kitajima et al. (2008) demonstrated through detailed

structural mapping at a scale of 1:5000 (covering an area of 10 × 30 km, Fig. 11) that the OPS succession consists, not of a single stratigraphic unit (Van Kranendonk et al., 2007, 2015; Nijman et al., 2017), but of a ~ 6 km-thick pile of imbricated pillowed basaltic greenstones with units of komatiites, bedded tuffaceous cherts (>30 m), local felsic volcanics, and conglomerates and sandstones at the top of one of the latest units. They defined 5 units in a lower thrust stack, plus two higher structural slices (Fig. 11), each capped by bedded chert, and each unit is separated by thin layer-parallel thrusts and clear, small duplexes along the bedding-parallel thrusts. The lower two units contain basaltic greenstones (MORB chemistry) with mid-ocean ridge-type hydrothermal metamorphism, intruded by more than 2000, white chert-barite dykes up to 10 m-thick and > 1 km long (downwards) and black chert dykes that increase upwards in width and abundance to cap the barite-bearing chert beds (Nijman et al., 1998; Terabayashi et al., 2003; Kitajima et al., 2008). The silica dykes are interpreted as the fossil pathways of hydrothermal fluids (Kitajima et al., 2001a, 2001b). The metamorphic grade of the greenstones increases downwards through the units (prehnite-pumpellyite, transitional to greenschist) comparable to that of modern ocean-floor metamorphism (Terabayashi et al., 2003).

To constrain the ages of their detailed litho-structural maps, Kitajima et al. (2008) used CL images to confirm that the zircons are euhedral
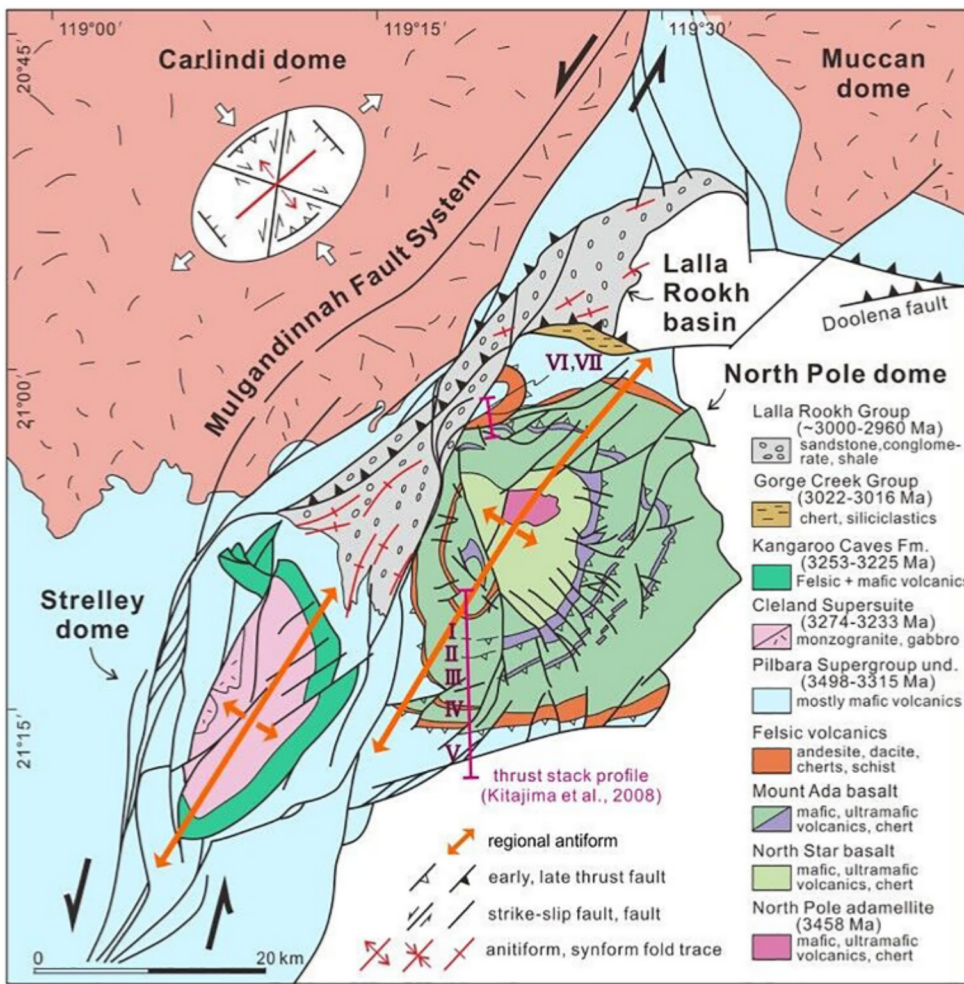
Fig. 11. Geologic and tectonic map of the North Pole and Strelley dome areas, showing the relationships of the domes to the sinistral Mulgandinnah shear zone system. Map is compiled from: GSWA (2016: 1:250,000); Kitajima et al. (2001a, 2001b, 2008); Krapez and Barley (1987); White et al. (1998); and Nijman et al. (2017). The map shows the lower part of the Warrawoona Group where, on the flanks of the North Pole dome, Kitajima et al. (2001a, 2001b, 2008) mapped the group as a series of seven older-over-younger thrust sheets. The circa 3000–2960 Ma Mulgandinnah shear zone complex (MSZC) is associated with thrust faults that define parts of the margins of the *syn*-deformations Lalla Rookh foredeep-style basin, which is affected by a series of NE-striking transpressional folds, and links with the Doolena thrust fault system that thrusts the Muccan dome to the south over the Warrawoona lithotectonic assemblage. The similarly-oriented NE axes of the Strelley and North Pole domes are also attributed here to doming associated with motion along the MSZC. Since the core of the Strelley dome is occupied by 3228 +/− 2 Ma (GSWA, 2016; Nijman et al., 2017) Strelley hornblende-biotite monzogranite of the Cleland Supersuite, doming must have occurred after its intrusion, along with motion on the transpressional MSZC. Lower panel (modified after Kusky et al., 2016) show the formal Warrawoona formational names and columnar lithotectonic section of the lithotectonic assemblage of basalts, gabbros, komatiites, cherts and felsic volcanics of the lower five thrust sheets exposed along the southern margin of the North Pole dome (location shown on map), and the interpreted tectonic setting of duplexed oceanic crust and OPS that formed the lithotectonic stack.
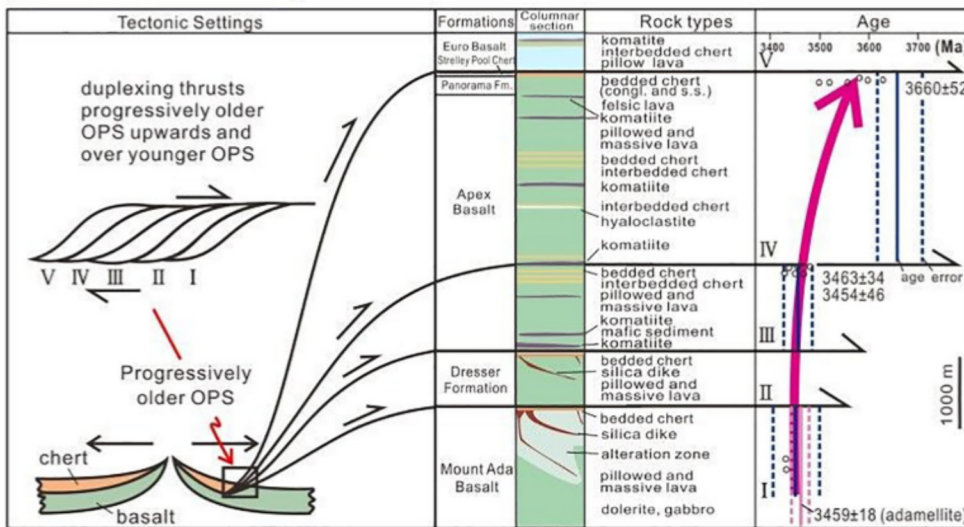
igneous crystals (i.e. not inherited or metamorphic), and in-situ LA-ICP-MS dating, showing that rocks previously dated using TIMS and MC-ICPMS methods at 3458+ 9.1/−4.2 and 3454 +/− 46 Ma, respectively (Thorpe et al., 1992, and Amelin et al., 2000) are 3660 +/− 52 Ma, and then they dated tuffaceous chert units progressively down in the section as 3463 ±34 Ma, and 3454 +/− 46 Ma. Thus, zircon ages from the tops of Units III and IV (Fig. 11) and the underlying monzodiorite as reported by Kitajima et al. (2008) demonstrate that the five units decrease in age progressively downwards with jumps across the mapped thin thrust zones. Kitajima et al. (2008) argued that the overall downward-younging structural sequence combined with the right-way-up stratigraphy of all individual units, each separated by thrust duplexes, is so similar in structure and lithology to that in modern circum-Pacific accretionary complexes, that this provides robust evidence that the Lower Warrawoona Group is a subduction-accretionary complex with prominent OPS that formed by ridge-trench horizontal shortening

and was imbricated during accretion by layer-parallel thrusting. The early history of the formation and accretion of the Lower Warrawoona Group is thus remarkably similar to that of the accreted ocean floor OPS units with ophiolites described above from the Klamath Mountains, Coast Ranges, and the Western Sierra Metamorphic Belt in Section 2 above, suggesting that both formed initially in intra-oceanic accretionary arcs.

The ages from the tops of Units III and IV reported by Kitajima et al. (2008) showing that the five units decrease in age progressively downwards were questioned by Nijman et al. (2017), who used stratigraphic correlations and previously reported TIMS/MC-ICPMS ages (Thorpe et al., 1992; Amelin et al., 2000) to suggest that the high-resolution in-situ LA-ICP-MS ages of circa 3660 +/− 52 Ma are "anomalous," and preferred the previously-believed ages of 3458 + 9.1/ −4.2 Ma and 3454 +/− 46 Ma, which are consistent with their stratigraphy-based divisions. At the same time, Nijman et al. (2017) recognized that the basalts and cherts at North Pole are duplicated in an east-vergent imbricate thrust system, with piggy-back thrusts, and kinematic indicators ubiquitously indicating west over east shear and duplication of units. We point out that new 3588 +/− 5 Ma - 3578 +/− 1 Ma ages from the Webber gabbro - ultramafic -anorthosite complex (Petersson et al., 2019) of the Shaw dome, and 3591 +/− 36 Ma and 3576 ±22 Ma trondhjemites from the Muccan dome (Wiemer et al., 2018), overlap in age within error with the 3660 +/− 52 Ma age reported by Kitajima et al. (2008), so the ages are no longer anomalous as suggested by Nijman et al. (2017), but instead represent remnants of the Eastern Pilbara's oldest known ultramafic-cumulate-gabbroic-tonalitic-trondhjemitic igneous suite, now correlated with the oldest basaltic thrust slice in the accretionary stack, which we interpret below (sections 4.2, 4.3) as the original oceanic basement of the entire Eastern Pilbara block.

The Strelley Dome to the south of the North Pole dome (Fig. 11) is cored by the circa 3228 +/− 2 Ma (GSWA, 2016, Nijman et al., 2017) Strelley hornblende-biotite monzogranite of the Cleland Supersuite, and hosts the 3253–3225 Ma Kangaroo Caves Formation, and higher units of the Sulphur Springs Group. The Soansville Group rests over the Sulphur Springs Group of the Warrawoona lithotectonic assemblages, the upper part of which includes the circa 3180 Ma Honeyeater Basalt, for which Brenner et al. (2020) have determined paleolatitudes, and through comparison of previously determined paleomagnetic poles of the Euro basalt from the Warrawoona Group, constrain a paleolatidinal drift of ~2.5 cm/yr from 3350 to 3180 Ma for the Eastern Pilbara, suggesting modern plate-tectonic latitudinal motion of oceanic plates by 3.2 Ga.

3.4.6. Shaw-Daltons dome; multiple shortening events associated with plutonism and dome growth

The Shaw Dome (Fig. 5) forms an elongate NNE striking dome in the southern part of the Eastern Pilbara, and is bounded on the west by the major circa 3000 Ma Mulgandinnah Shear Zone system, and on the east by the Coongnan Shear Zone (Fig. 8). The Shaw-Daltons Dome is also widely used as an example of an "inverted drip" formed in a non-plate tectonic vertical diapiric type of global tectonic behavior, so we describe the geology, and relationships between the structures and plutonism here. Bickle et al. (1980, 1983, 1985) reported early pioneering structural studies of greenstone-gneiss dome relationships in Eastern Pilbara from analysis of structures around the Daltons pluton area of the NW Shaw Batholith (Figs. 7, 13) aimed at understanding the doming and intrusion mechanisms. They suggested early thrusting of the gneiss complex over the greenstone belt, with subsequent recumbent folding of the tectonically-stacked gneiss-greenstone assemblage, forming a giant recumbent nappe with a 10 km amplitude, covering an area of 200 km^2, with a 70 km^2 area of the inverted northern limb exposed in the Daltons area (Figs. 13, 14). Bickle et al. (1980, 1983, 1985) documented two subsequent upright tight to isoclinal folding events (their D$_3$ and D$_4$) that formed a Type III fold interference pattern of hook-shaped basins and domes (Fig. 13) that was later re-oriented by

late steep shear zones of the Mulgandinnah shear zone system (Figs. 7, 13, 14), with the end result being a series of elongate domal antiforms, antiformal synclines, and synformal anticlines (Figs. 13, 14), bounded by banded multi-component (including greenstones) gneiss that resembles the gneisses of Archean granulite-gneiss belts (Windley and Bridgwater, 1971; Windley et al., 1981). A similar structural sequence was reported for the Mount Edgar Batholith by Collins (1989).

Our new cross sections (Fig. 14), based in part on Bickle et al. (1980, 1985) show clearly that the uplift and doming of the Shaw Batholith was a consequence of multiple horizontal shortening events, rather than the intrusion of a pluton being the cause of the deformation of the volcano-sedimentary sequence. This is demonstrated by the facing of the major D$_2$ recumbent fold nappe (Fig. 14) towards the batholith, which shows that it formed during early thrust-nappe tectonics (Kusky and Vearncombe, 1997). The formation of regional-scale inverted recumbent nappes involving both the gneiss dome rocks and the volcanosedimentary sequence is a characteristic of thick-skinned thrust-nappe tectonics in the internal zones of convergent orogens of all ages (Coward, 1983; McClay, 1992; Poblet and Lisle, 2011), and their documentation in the tectonically interleaved basement gneiss units comprised of the ~3.6 Ga Webber gabbro, 3.5–3.4 Callina and Tambina gneisses, with the >3.5–3.4 Ga lower Warrawoona lithotectonic assemblage demonstrates the operation of thrust/nappe tectonics by 3.4 Ga. Later generations of upright folds likewise are characteristic of convergent orogens, and have no relationship to any postulated doming by diapiric processes as widely proposed for Eastern Pilbara.

Cooper et al. (1982) demonstrated that the intrusions were multi-phase, and intruded at different stages of the structural evolution. Early intrusions include migmatitic and banded gneisses (Callina and Tambina Supersuites, or arc-phase magmatism) with sheet-like forms, which contain an early foliation that is now generally parallel to the dome margins. These were intruded by early- to *syn*-tectonic plutonic sheets and dikes of porphyritic granodiorite and adamellite (Emu Pool Supersuite, or slab-failure phase magmatism), that were strongly foliated by the second deformation event, and then both of these broad suites were intruded by later post-tectonic plutons (the "tin-granites" of early literature, e.g., Glikson, 1979) which have sharp cross-cutting intrusive contacts, and typically have many large xenoliths and roof pendants of the migmatitic and syn-tectonic suites enclosed within the younger bodies (Cooper et al., 1982). Structural fabrics within the second generation syntectonic suites define L-S shape-preferred orientations, which are consistent with emplacement of the granitoid sheets during compression, but they do not have any structures that could be related to postulated diapirism or doming other than that they were re-oriented by late domal-style folds. Cooper et al. (1982) concluded that the Corunna and Shaw domes acquired their domal form only after magma emplacement during early horizontal contraction, and noted that the early lineations related to thrusting are not domed but remain subhorizontal, and they concluded that the granitoids did not rise by diapiric doming, but that early complex folds and shear zones are truncated by late cross-cutting granitoids.

3.4.7. Carlindi, Muccan, and Corunna domes; domed early thrusts with sheet-like intrusions

The volcano-sedimentary lithotectonic assemblage on the southern side of the Carlindi gneiss dome (dome number 6 on Fig. 5) is known as the Coonterunah Succession (part of the East Strelley greenstone belt of the nomenclature of the Pilbara Craton Mapping Project; Hickman, 2012), which includes a bi-modal assemblage of volcanic rocks, intensely folded banded Fe-rich cherts, and banded iron-mylonites that strongly resemble the banded iron-mylonites from the Zimbabwe craton (Kusky and Winsky, 1995; Hoffman and Kusky, 2004). Buick et al. (1995) suggested that the formation of the Fe-mylonites is related to an early accretionary/collisional event at 3515 +/− 2.7 Ma, and pre-dates the formation of the main Warrawoona Succession.

Strongly deformed circa 3460 Ma volcano-sedimentary rocks form

the Coongan Belt are situated between the Shaw and Corunna Downs dome complexes (Domes 1 and 2 on Fig. 5). The western margin of the belt is a several-km wide moderately *E*-dipping thrust-sense shear zone (Split Rock / Coonggan shear zone) that separates mylonitic gray gneisses of the footwall from intrusive sheets of circa 3450 Ma foliated granodiorites of the Shaw batholith in the hangingwall (Zegers et al., 1996, Davids et al., 1997). The shear zone and Coongan belt are in turn truncated by cross-cutting circa 2850 Ma adamellites (Davids et al., 1997), and the eastern margin is intruded by younger circa 3300–3200 Ma granodiorites and adamellites of the Corunna Downs dome. Structures in the Coongan Belt show that it consists of isoclinally folded structural slices of the 3460 Ma Duffer Formation of the Warrawoona Group, emplaced over relatively undeformed slices of circa 3329 Ma volcanics of the Wyman Formation (McNaughton et al., 1993), which in turn rest allochthonously on top of an older succession of the Duffer Formation that preserves evidence of early-extension at 3470–3450 Ma (Zegers et al., 1996 Van Haaften and White, 1998; White et al., 1998). Thus, like the Coonterunah Succession, and the type Warrawoona succession at Marble Bar, the Coongan Belt is not a coherent stratigraphic sequence, but rather is a series of allochthonous sheets structurally emplaced during an early series of contractional events, with intervening extension, and these events were associated with sheet-like intrusions that later became strongly sheared and mylonitized, and infolded with the volcano-sedimentary rocks, and deformed into intermediate composition gneisses that were then intruded by younger granitoids.

3.5. From early accretion tectonics to crustal thickening with collision, slab failure magmatism, and transpressional slicing

We show above that the main early thrusting event in Eastern Pilbara was at circa 3300 Ma, coeval with intrusion of the Emu Pool granodiorite sheets, and formation of the Talga Talga antiformal stack, with the repeated thrust sequence south of the Muccan dome in the Coppin Gap greenstone belt, in the Coongan belt, and elsewhere in the eastern Pilbara. Early thrusting and accretion may have occurred as early as 3470 Ma in the North Pole thrust stack (Kitajima et al., 2008), but Buick et al. (1995) document an even older accretion/thrusting event at circa 3515 Ma in the East Strelly greenstone belt (Coonterunah Succession) south of the Carlindi dome (Fig. 5). In their structural/stratigraphic traverse across the Eastern Pilbara from North Pole, Marble Bar and into the Mount Edgar Batholith, Nijman et al. (2017) recognized an early deformation event that preceded the deformation which produced the main greenstone belt map patterns. This event is well-shown by repeated and folded basalt/chert units, imbricate thrusting, by bedding-parallel shear zones with both extensional and contractional structures, but which were interpreted to be largely extensional in nature; Nijman et al. (2017, p. 1098) suggested that these structures formed by slumping at the base of a slope, with the Marble Bar basalts and cherts representing a submarine fan deposit. We note, however, that submarine fans are not typically composed of disharmonically deformed basalt/chert packages, but rather should include units such as turbidites with Bouma sequences, contourites, or pelagic shales. Additionally, from the map and outcrop patterns, we note that the basalt/chert lithological packages have a remarkable similarity to extensional and contractional structures documented from early accreted, basalt/chert packages in OPS in younger accretionary orogens such as the Mesozoic McHugh Complex of Alaska (Kusky and Bradley, 1999), the early Paleozoic Laohushan Complex in the Qilian orogenic belt (Fu et al., 2020), the Calaveras and related mélanges of the Western Sierras (Hildebrand, 2013), and many other accretionary mélanges of all ages (Kusky et al., 2013, 2020).

During continued post-3300 Ma thrusting, some thrust surfaces were steepened and rotated (perhaps associated with crustal thickening, as per Kusky and Vearncombe, 1997), and developed an oblique transcurrent and localized second phase of extensional and escape structures, and related core complex-type structures so enhancing the domal

structures including Mount Edgar (Zegers, 1996; White et al., 1998), that were associated with the earlier emplacement of circa 3300 Ma granitoids. This second, partitioned or localized deformation was affiliated with bi-modal volcanic rocks and clastic sediments of the circa 3022–3016 Ma Gorge Creek Group (Krapez̆ and Barley, 1987). The extension in some orientations was synchronous with overall thrusting such that the extension-related sediments and volcanics became incorporated in the growing thrust stack, and other sediments were deposited in small syn-orogenic foredeeps (Fig. 11) in front of the emergent thrusts (White et al., 1998), then cut by post-deformation granitoids. In stratigraphic nomenclature (Van Kranendonk et al., 2007; Hickman, 2016) these units are known as the Gorge Creek Group.

Zegers (1996) and Zegers et al. (1996) documented a second main episode of thrusting at 3000–2930 Ma, which involved NNW to SSE thrusting of allochthonous sheets of dominantly metasedimentary rocks of the Gorge Creek Group over the previously stacked thrust piles. Late stages of this event at 2930 Ma were associated with transcurrent transfer zones that re-activated older N-S structures including the large Mulgandinnah Shear Zone Complex (MSZC on Figs. 5, 11) (Zegers et al., 1996; White et al., 1998), which led to deposition in several basins represented by the Lalla Rookh Group (Krapez, 1993), which formed additional 020–070 trending folds, and uplift of the Shaw dome relative to the adjacent Tambourah greenstone belt to the west (Figs. 5, 11). This phase of deformation was also associated with movement along the terrane-bounding fault (the Tabba Tabba Shear Zone Fig. 5) between the Eastern and Central Pilbara, suggesting perhaps that the two terranes were accreted at circa 3.0 Ga (Smith et al., 1998).

All the detailed structural studies summarized above have a similar history- that is, at least two early phases of intense horizontal shortening were associated with accretion by 3300 and 3000 Ma, with more limited evidence of older events. These accretionary events were responsible for the growth of Eastern Pilbara, and associated intrusions were largely sheet-like filling extensional structures related to the deformation events, or they were related to post-orogenic extensional phases of deformation, or to changes in the strike of major steeply-inclined structures. Late intrusions of the circa 3274–3223 Cleland Supersuite, and the 2851–2831 Ma Split Rock Supersuite are steep-sided, cross-cutting plutons that truncate structures, but there is a profound paucity of structural evidence to support any solid state diapirism or role of doming plutons in the formation and growth of the cratonic crust. Furthermore, the complex structure, not considered in many recent studies (led by Van Kranendonk et al., 2007, 2015) relied on the presence of a relatively intact stratigraphy, separated only by unconformity surfaces, which were correlated across the craton. This imagined stratigraphy has been shown to have internal inconsistencies (Shepard et al., 2017; Krapez et al., 1987; White et al., 1998; Nijman et al., 2017), which is readily explained by the structural data that show that a craton-wide, 15–45 km-thick stratigraphic sequence simply does not exist.

In summary, the Pilbara Craton contains remarkably well-preserved ultramafic schist-basalt-chert-clastic successions, whose early history can convincingly be interpreted in terms of OPS and ridge-trench tectonics (e.g., Kusky et al., 2013, 2016, Kusky et al., 2018). However, this environment is incompatible with the current popular idea favored by e. g. Van Kranendonk et al. (2007, 2015 and earlier papers) according to which the Early Archean, East Pilbara block evolved by several massive mantle plume outpourings that created a continuous 12–15, or even 45 km-thick lava pile, or with eruption onto a continental basement (Green et al., 2000; Johnson et al., 2014), or a volcanic arc setting (Barley, 1993), or an oceanic plateau setting (Condie, 1997). The case for horizontal shortening (plate interaction) was demonstrated by Blewett (2002) from structural studies around Marble Bar and extended across the whole of the Pilbara Craton, following the earlier ideas of Bickle et al. (1980). We emphasize the fact that it is the OPS in Pilbara, and the structural stacking and repetition of different oceanic units including basalts, cherts, and clastic sediments, that are exactly analogous to the early history of accreted oceanic sequences of the Western

Sierra Metamorphic Belt, the Klamath Mountains, Coast Ranges of British Columbia (section 2 above), and other accretionary orogens worldwide (Hildebrand, 2013; Kusky et al., 2013, 2018, 2020; Windley et al., 2021) which clearly document their formation in an accretionary orogen, and which grew through later stages of arc magmatism, slab failure magmatism, and extensional collapse magmatism into a stable craton. This also provides the most definitive and diagnostic evidence for plate tectonics in the early Earth (Windley et al., 2021), a feature that is not taken account of in most models of Early Archean evolution.

3.6. Intrusion and doming mechanisms of the East Pilbara domes

While the majority of the works cited above are concerned primarily with petrological and geochronological aspects of the East Pilbara domes and with speculations on how events from the upper-middle crust recorded in the domes may relate to the volcano-sedimentary sequences, most have taken for granted proposals that the domes rose vertically through the overlying crust as solid-state or migmatitic diapirs (e.g., Hickman, 2012; Van Kranendonk et al., 2007, 2015), which formed the granitic domes with intervening synclinal volcano-sedimentary sequences. A simple test of the diapir model is whether the domes are fairly symmetrical from outside to inside (Weinberg and Podladchikov, 1995). The dome that shows the most concentric zoning from oldest at the margins to youngest in the center is Mount Edgar (Fig. 6), which has oldest rocks of the Tambina and Callina Suites along the edges and western side that were intruded by sills of the Emu Pool Supersuite that now form a folded rim around the edges. Above we demonstrated that these were intruded as *syn*-deformational sills related to thrusting, and not as diapirs. Moreover, the Corunna Downs, Shaw, Muccan and Carlindi domes show no features that can reasonably be interpreted as vertically intruded diapirs. The fold interference patterns of the Shaw Dome (Fig. 7) provide clear evidence of formation through multiple solid-state folding and thrusting events, the first two of which were related to sub-horizontal nappe emplacement, followed by two upright folding events, the last of which was related to sinistral movement on the craton-scale Mulgandinnah shear zone. The Calindi dome (Fig. 8) has a core of the most ancient gneisses intruded by a folded rim-sill of younger intrusives, and the Muccan Dome (Fig. 8) consists of moderate to steeply-dipping sill complexes that are folded and truncated by faults or younger rocks at its margins. Also, we showed above that the North Pole Dome (Fig. 11) preserves a tilted section through the thrust packages of the Warrawoon, exposed by virtue of its tilting during transpressional folding during the 2960–2930 Ma strike-slip tectonics exemplified by the Mulgandinnah shear zone system, and thus the uplift is related to horizontal, not vertical, movements.

Concentrically zoned plutons are common in Phanerozoic orogens, as in the case of nested plutons, like the Sierra Crest magmatic suite (exemplified by the Toulumme suite) that extends along the length of the Sierra Nevada, and a similar example being the Mount Edgar batholith. However, the domes of the Pilbara are each remarkably different (Figs. 5, 6, 7, 8), with the Mount Edgar dome being the most symmetric (and highly used in models), but others expose deeper levels or are just different, such as the Shaw dome (Fig. 7), where the exposed gneisses and plutons show complex fold interference patterns that are closely related with early thrusting of the gneiss over adjacent greenstones (Bickle et al., 1980, 1985) and with later transpressional strains related to strike-slip motion on the bounding Mulgandinnah Shear Zone (Fig. 7); these could not have formed by vertical diapirism. The Carlindi and Muccan domes do not exhibit any type of radial patterns (Fig. 8). We therefore reject the diapiric hypothesis as the main intrusion and doming mechanism of the Pilbara dome-and-basin structures.

Some features of some of the late-stage plutonic phases, particularly the circa 3274–3244 Ma Cleland and 2851–2831 Ma Split Rock Supersuites show features of magmatic diapirs, plugs, and sills rising through mid-crustal levels, like those suggested for some of the deep-seated plutons of the Sierra Nevada and Coast Ranges (Hildebrand and Whalen, 2014a, 2014b) described above (Section 2). However, numerous structural studies have demonstrated that the most significant contributors to the domal characteristics of the eastern Pilbara were the result of horizontal contraction with associated folding and faulting that involved both the volcanosedimentary sequences and the solid gneissic rocks of the domes. Sheet-like strata-parallel intrusions (Figs. 6, 7, 8) and later steep-walled plutons were folded and thrust together with the volcano-sedimentary sequences, and refolded by regional upright folds, all contributing to the outcrop pattern of the domal granitoids and volcano-sedimentary synclinal keels between them (Bickle et al., 1980, 1985; Krapez, 1984, Krapez, 1993; Boulter et al., 1987; Krapez and Barley, 1987; Zegers, 1996; Zegers et al., 1996; Van Haaften and White, 1998; White et al., 1998; Barley and Pickard, 1999; Blewett, 2000a, Blewett et al., 2004; Kloppenberg et al., 2001a; Nijman et al., 2017). Other aspects of the domal structures were developed with later additional shortening during younger orogenic events, strike-slip tectonics, orogenic collapse and core complex formation. Discussions of East Pilbara concerning emplacement mechanisms of the granitic gneiss and granite domes are thus very similar to those about the Paleozoic-Mesozoic Coast Ranges plutons, Sierra Nevada batholith, and Klamaths, described above in section 2.

3.7. Doming by multiple deformation events or solid-state diapirism?

A number of structural studies since the pioneering work of Bickle et al. (1980) have also confirmed that the structures of the domes of Eastern Pilbara are not simple solid-state or magmatic diapirs. Zegers (1996) and Zegers et al. (1996) reported detailed structural analyses, which suggested that the domes saw their first phase of formation during circa 3460 Ma extension with the domes representing the lower plate that was exhumed during formation of core complexes with associated migmatization, and were later modified by folding and strike-slip structures. This was followed by Kloppenberg et al. (2001a) who completed detailed structural studies around the Mount Edgar Dome (Fig. 6) demonstrating that the stretching lineations were unidirectional around the western and southern margins of the dome, inconsistent with a domal (radial) pattern. They interpreted the structural patterns to result from lateral NE-SW extensional-escape at 3.31 Ga along a mid-crustal detachment fault (Mount Edgar Shear Zone, Fig. 6), which formed during overall E-W contraction associated with crustal thickening and partial melting along with extensional collapse and extrusion of the granitoids along the Mount Edgar shear zone. Kloppenberg et al. (2001a) compared the structural evolution of the East Pilbara domes to post-orogenic (post-accretion phase in our model) collapse, and showed that the structural data are inconsistent with solid state diapiric rise of the plutons, and inconsistent with convectional overturn or sagduction of the crust (c.f. Collins et al., 1998; Wiemer et al., 2018). Interestingly, Kloppenberg et al. (2001a) documented excision of a ~ 9 km section of upper crust during the extension, a number remarkably similar to the 5–10 km of excision of the upper crust associated with late Cretaceous gravitational extensional collapse of the southern Sierra Nevada batholith (Chapman et al., 2012), implying that the lithospheric rheological response to extensional collapse (e.g., Dewey, 1988; Kusky, 1993) was similar between the Paleoarchean and the Late Cretaceous, and by implication that the compositional and thermal structures were also similar.

The observations of Kloppenberg et al. (2001a) were complimented and modified by a detailed structural traverse from the North Pole to the Mount Edgar Dome (Fig. 5). Nijman et al. (2017) showed that at 3.31 Ga, early extensional and contractional deformation was supplanted by regional NW-SE contraction forming NW over SE shear zones and ramp-flat thrusts, and that the deformation related to the present dome-and-basin pattern did not begin to develop until the third (D$_3$) event, constrained to be between 3.18 and 2.9 Ga (Nijman et al., 2017). Roberts (2020) and Roberts and Tikoff (2021) applied quantitative microstructural and AMS (anisotropy of magnetic susceptibility) studies to the

margins of the Mount Edgar dome, and found that the sense-of-shear was dominantly dome-side-down relative to the Warrawoona (Talga Talga) thrust system. Interestingly, the AMS fabrics also reveal early fold-nappe structures within the dome within the border sill-phases (Callina and Tambina suites), making map patterns similar to that in the Shaw Dome (Fig. 10 of Roberts and Tikoff, 2021).

Kloppenberg et al. (2001a) also documented an early pre-domal phase of deformation at 3.46–3.45 Ga associated with gabbroic intrusions, and noted that these early-deformed gabbroic rocks contain xenoliths of schistose ultramafic rocks that were deformed prior to their incorporation in the gabbro at 3.46–3.45 Ga, hinting at an early ultramafic basement to the Eastern Pilbara. This astute observation was recently confirmed by the discovery of the 3.59–3.58 Mount Webber gabbro and associated ultramafic rocks (Petersson et al., 2019), that represent the oldest basement of the Pilbara Mesoarchean accretionary orogen.

3.8. Fold-interference patterns

Blewett et al. (2004) presented a structural synthesis of the dome-and-basin pattern of Eastern Pilbara demonstrating that the most deeply eroded domes are granitoid gneiss-dominated, and the shallower-level domes are greenstone-dominated (Figs. 5). They showed that the pattern of shallow-level (i.e. North Pole, Strelley; Fig. 11) and deep (i.e. Shaw; Fig. 7) domes is a result of a Type-I (dome-and-basin)

fold interference pattern formed during the multiple stages of horizontal compression described above, and not directly related to the intrusion of the late-stage granites, which are only present when the fold interference pattern brings up the level of intrusion of these granitoids. The regional fold interference pattern is thus similar to those described above from the North American Cordillera, Appalachians, and from places in other orogens such as the Caledonides (Tobish, 1966), Alpine-Himalayan system (Xu et al., 2020), and nearly every orogen of all ages globally (Windley, 1995; Teyssier and Whitney, 2002; Whitney et al., 2004; Kusky et al., 2018).

The regional pattern of folds within the domes includes volcano-sedimentary tectonostratigraphic sections, where they are folded together as shown in Fig. 15. The general first-order pattern is that of a Type-1 basin and dome ("egg carton") fold interference pattern, but it was modified by strike-slip faults, especially the Mulgandinnah shear zone complex (MSZC) that divides the Eastern Pilbara into two halves (Figs. 15). The dome-and-basin pattern was most likely formed initially during the two main contractional events, the early circa 3460 Ma E-W contraction and the later NW-SE contraction that was associated with the syntectonic intrusion of the 3300 Ma Coppin Gap granodiorite of the Emu Pool Supersuite, together with formation of the Talga Talga thrust system (Figs. 9, 10). This was followed by D₃ contraction at 3.18–2.9 Ga (Nijman et al., 2017). A late but major cause of the present-day domal structure was the formation of a regional transpressional fold system related to sinistral movement along the craton-wide Mulgadinnah Shear
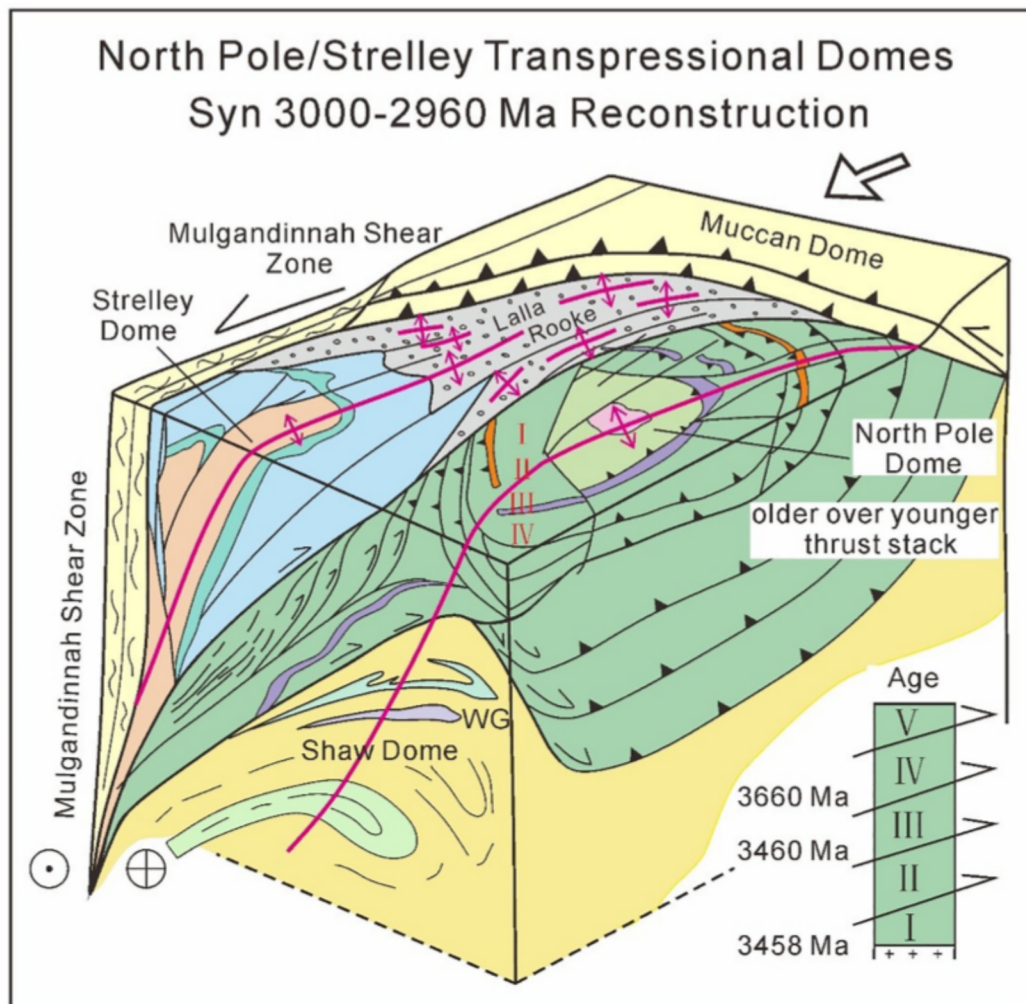

Fig. 12. A permissible reconstruction of the North Pole and Strelley Domes at circa 3000 Ma, showing their formation as transpressional uplifts of previously imbricated thrust stacks, during sinistral motion along the Mulgandinnah Shear Zone.

Zone system at circa 2960 Ma-2930 Ma, that is during the D_3 interval (Krapez̆ and Barley, 1987). Many of the dome complexes are cut by even younger monzogranites belonging to the circa 2851–2831 Ma Split Rock Supergroup, but these are generally late steep-sided intrusions that are generally distributed in a NW-trending, 200 km × 150 km belt that extends across the craton, but they show little to no relationship to locations in the centers, margins, or outsides of the dome complexes (Fig. 5).

We note that the elongate domal structures of the western part of Eastern Pilbara have their long axes oriented NE-SW, oblique to the orientation of the sinistral Mulgandinnah shear zone complex (MSZC; Figs. 5, 6, 7, 8, 11), suggesting that the domal structures may in part have been acquired during the strike-slip deformation at circa 2960–2930 Ma (Fig. 12) in a manner similar to oblique folds in many transpressional systems of all ages globally (e.g., Wilcox et al., 1973: Dolan and Mann, 1998; Wallace, 1990). This is supported by the

structural studies of Zegers (1996) who showed that the MSZC is a major ductile sinistral-oblique shear zone with a motion that ceased by 2934 +/− 2 Ma, and that the oblique component of motion caused relative uplift of the Shaw dome relative to the adjacent Tambourah greenstone belt to the west. Zegers (1996) documented that movement along the MSZC formed a series of 020–060 oriented folds between the major strands of the faults, which is parallel to the major oblique folds that we show in Fig. 15 in the Yule and Carlindi domes parallel to this trend. Strains associated with this transpressional system also include thrusting along the E-W Doolena thrust system, uplift of the Muccan dome relative to the Coppin Gap greenstone belt, which likely caused additional uplift of the Mount Edgar Complex to the south along its NW-SE anticlinorial axis (Fig. 15). Documentation of major transcurrent faults across the preserved width of Eastern Pilbara at circa 3000–2934 Ma raises the distinct possibility that the current width of the Eastern Pilbara may in fact be duplicated by strike-slip structural slicing (sensu Şengör and
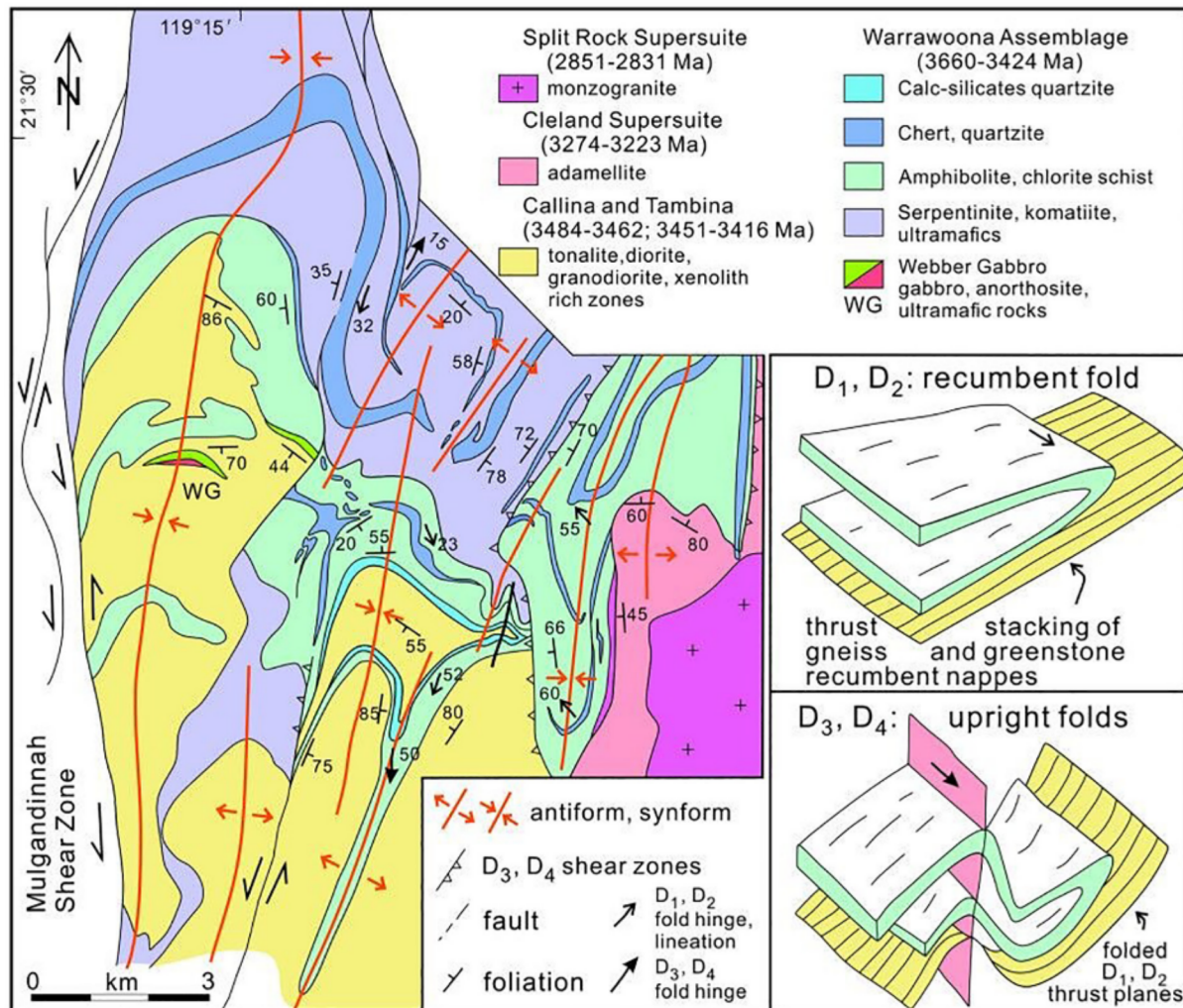

Fig. 13. Map of the NW part of the Shaw dome, of the Daltons "pluton" (see Fig. 7 for location), showing volcano-sedimentary rocks of the greenstone belts complexly folded and sheared together with the gneisses of the dome, forming a Type III fold interference pattern formed by early subhorizontal thrusting and recumbent folding (map is modified and adapted from Bickle et al., 1980, 1983, with additional data from GSWA 2016). The location of the Webber Gabbro (WG) is based on the sample location map of Gardiner et al. (2017) but the boundaries are at present not well constrained. The horse-shaped basement-cored recumbent nappe in the center of the map covers ~200 km², with an inverted sub-horizontal limb preserved over >70 km². The gneiss complexes were not folded into the domes until late in the structural history, during the formation of late upright folds, the second generation of which is related to sinistral motion on the Muldandinnah shear zone. The inset shows the Type III fold interference patterns forming based on the geometry of structures in the area, with a high angle between the axial surfaces of two main folding generations (grouping D_1, D_2, and D_3, D_4), but with similar orientation of hinges as in co-axial deformation histories (Ramsay and Huber, 1987; Fossen et al., 2019). In this case the interference results from the interference of early subhorizontal axial surfaces formed during thrusting of the gneiss over the greenstones with recumbent folding of the tectonically stacked sequence, followed by two episodes of upright folding. Such sequences are characteristic of nappe emplacement in orogens of all ages, and inconsistent with structures formed from diapiric emplacement of gneiss of plutonic domes.

Natal'in, 1996a, 1996b) and prior to 2934 it may have been a single, 400 km × 100 km long terrane.

The volcano-sedimentary successions in Eastern Pilbara wrap around the granitic domes, strongly resemble the map patterns produced by arc-related folded plutons of the Sierras, Coast Ranges, and Klamaths described above. However, the origin of the East Pilbara domes has proven to be very controversial. It is commonly assumed, for instance, that Eastern Pilbara had an old Eoarchean or Hadean continental basement (Van Kranendonk et al., 2007; Hickman and Van Kranendonk, 2012), yet no such old rocks have ever been identified, and this hypothesis was based only on cryptic evidence, predominantly the presence of detrital zircons with ages up to 3.8–4.0 Ga or older (Tessalina et al., 2010; Petersson et al., 2019) in the younger sedimentary successions, and on xenocrystic zircons in the Muccan dome (Wiemer et al., 2018). The oldest rocks identified in the East Pilbara Terrane are the 3.59–3.58 Ga Mount Webber gabbro suite, which is a primitive structurally dismembered ultramafic/ cumulate gabbro/ leucogabbro/ anorthosite complex that occurs as a several hundred-meter long raft in the South Daltons pluton within the Shaw Batholith Complex (Petersson et al., 2019). The Webber gabbro is roughly contemporaneous with circa 3.59 Ga TTGs from the Muccan Granite dome (Wiemer et al., 2018), so Petersson et al. (2019) named this ultramafic - gabbro - anorthosite - TTG event the Mount Webber event for the Eastern Pilbara Terrane, and suggested that this is the oldest basement of the craton. Accordingly, the oldest basement formed in an oceanic accretionary orogen, was intruded by multiple generations of *syn*-deformation, and by arc- and slab failure-related plutons that were deformed into domes, which were subsequently accentuated during late-stage strike-slip regional deformation.

3.9. Magmatic sources; arc or slab-failure magmatism?

With analogies to the Western Sierra Nevada Metamorphic Belt, Klamaths, and other orogens described above, based on the field litho-structural relationships, we ascribe the earliest phase of magmatism (3580–3590 Ma Webber gabbro-anorthosite-ultramafic suite) to sea-floor spreading and formation of oceanic lithosphere, with the accreted rocks of the Warrawoona Group representing the slices of oceanic crust as ophirags. During and after accretion these rocks were intruded by diorites and granitoids of the 3484–3462 Ma Callina Supersuite, and the 3451–3416 Ma Tambina Supersuite (Figs. 6, 7, 8, 9, 10). These resemble arc-type magmas of the Mesozoic Cordillera, and the Amoonoosuc arc of the Paleozoic Appalachians, but like the younger examples, these suites form only a minor part of the preserved magmatic complexes of the exposed domes in Eastern Pilbara. Felsic volcanic rocks are time-equivalents of the Callina Supersuite, and rhyolites of the Panorama Formation are temporally equivalent with the Tambina Supersuite (Van Kranendonk et al., 2006). Similar relationships with contemporaneous plutonic and volcanic suites are common in magmatic arcs of all ages (see section 2 above).

A large proportion of the magmatic rocks in the eastern half of the Eastern Pilbara dome complexes are part of the 3324–3277 Ma, syn- to late-kinematic, Emu Pool Superuite as exemplified by the Mount Edgar and Corunna Downs domes (Fig. 6). These syn-deformational TTG plutons were intruded as sill-like bodies that were folded into domes, and then refolded at least twice as described below. The composition of these magmas and the close relationships between plutonism and late stages of the early deformation are remarkably similar to the slab failure-related suites described above (e.g. Sierran Crest magmas of the Sierra Nevada), so we tentatively suggest here that the Emu Pool Supersuite of
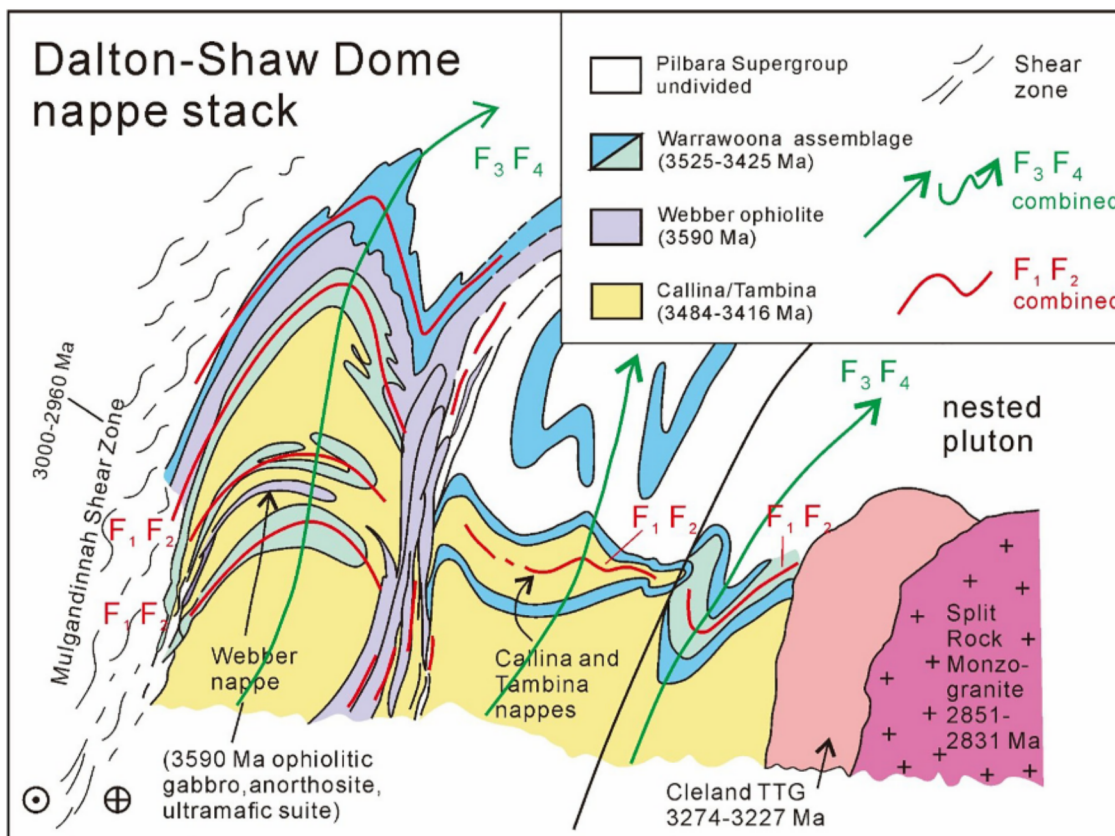

Fig. 14. Interpretative down-plunge view of the structural stack of nappes in the Shaw-Daltons area of the Shaw Dome. Note the early F_1 F_2 nappes involve thrusting of the gneiss over the greenstones, then refolding of the entire stack of nappes during late upright folds F_3 and F_4, forming the domal structures. Center part of cross-section modified after Bickle et al. (1980, 1983) with additional data from GSWA (2016).
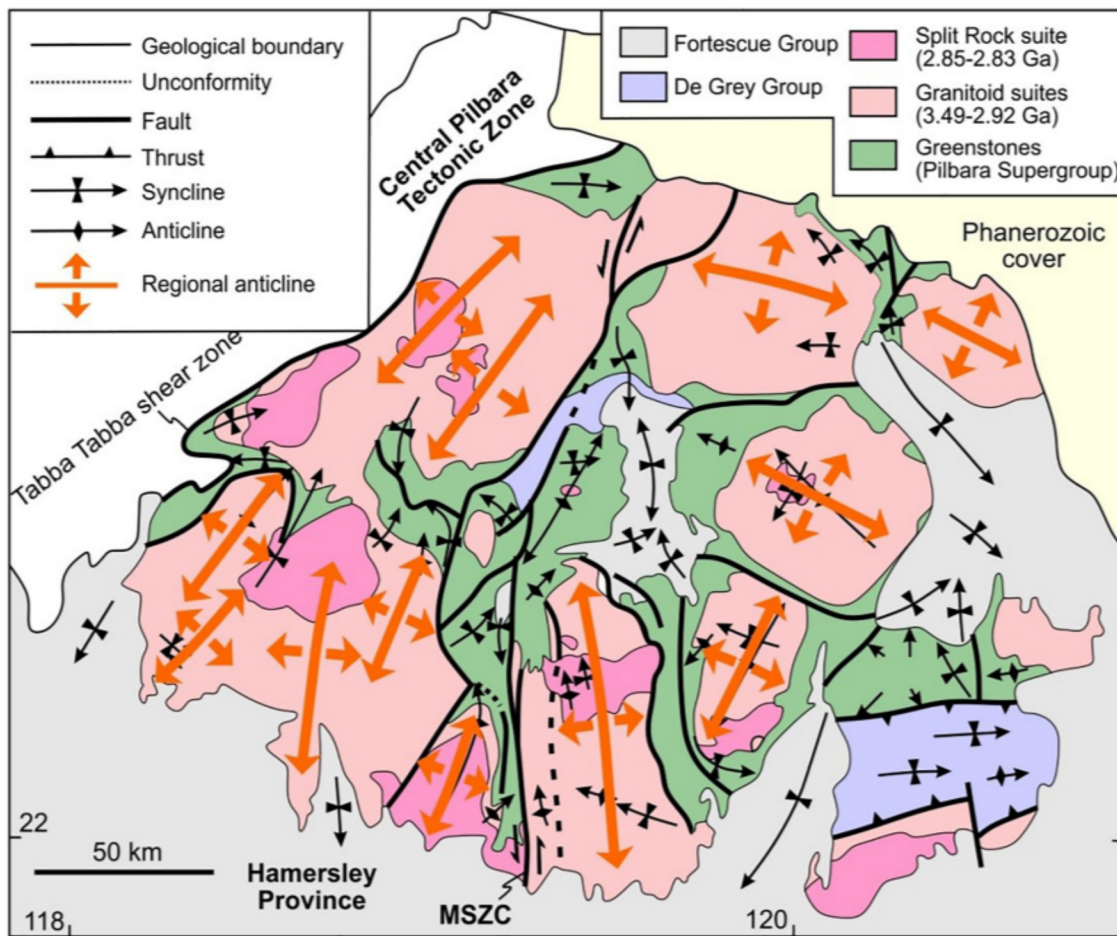
Fig. 15. Simplified map of the domes and basins of the Eastern Pilbara, compiled and expanded on that of Blewett et al. (2004) from Hickman (1983), Blewett et al. (2000a, b), Van Kranendonk et al. (2002), Nijman et al. (2017), Zegers (1996), Krapez and Barley (1987) and White et al. (1998). The folds and overall structural patterns and relationships can be interpreted to show a first order regional Type-I fold interference pattern. NE-SW oriented folds with circa 50 km wavelengths have a geometric and spatial relationship with the sinistral Mulgandinnah shear zone complex (MSZC), interfering with NW-SE oriented structures, especially in the Mount Edgar and Muccan domes, influenced the Doolinah thrust system that may have formed contemporaneously with the MSZC. The large-scale folds expose a range of deep and shallow crustal levels, and a great diversity in pluton emplacement mechanisms in different stages of plutonism at different depths.

the Eastern Pilbara was also related to slab failure, after accretion of the Warrawoona oceanic basement, and after the Callina-Tambina arc-related magmatism.

The zoned lithological patterns of some of the intrusive suites in Pilbara, such as in the Mount Edgar dome are strikingly similar-to the "nested" zoned plutons of the circa 100 Ma (Cretaceous) Tuolumne intrusive suite (Fig. 16) of the Sierran Crest event of the Sierra Nevada batholith (Memeti et al., 2010; Žák and Paterson, 2005). These nested granitoid complexes become progressively younger and more leucocratic inwards (Calkins, 1930; Bateman, 1992; Coleman and Glazner, 1997, 1998), typically with the oldest tonalite and granodiorite in the outer rims, in sharp contact with younger hornblende porphyry granodiorites, and with K-feldspar megacrystic granites and granodiorites in the cores of the domes (Fig. 16). The zones and associated lobes are thought to form by batches of melt during continuous magma generation that did not mix and amalgamate, or in some cases they represent distinct pulses of magma that show shifts in locus within individual plutons, as well as across the length of the 600 km-long Sierra Nevada batholith (Memeti et al., 2010). These nested plutons formed in a regional "pulse" named the Sierra Crest magmatic event (Coleman and Glazner, 1998), which lasted for about 10 Ma along the axis of the batholith (Nadin and Saleeby, 2008), which Hildebrand et al. (2018) attributed to slab-failure magmatism. We note that while it may be difficult to discern such short-term shifts in magmatic foci in Eastern

Pilbara, which is only 1/3 the size of the Sierra Nevada batholith (let alone the 15,000 km strike length of similar Late Cretaceous slab failure-related nested plutons in the entire North and South American Cordilleran orogens (Hildebrand and Whalen, 2014a, 2014b), some of the individual domes (e.g., Figs. 6, 7) do clearly preserve nested structures similar to those of the Sierra Crest suite (Mount Edgar and Warrawagine). Others such as Carlindi, Muccan, Yule and Yilgalong (Figs. 5, 8, and GSWA, 2016) only show apparently random uplift of deeper level rocks intruded by initially subhorizontal sills (Fig. 8).

In summary, in previous sections we show that the lithological and temporal relationships, map patterns and scales of deformation and plutonism in East Pilbara are fundamentally similar to equivalents in continental margin arc complexes built on older crust of Phanerozoic accretionary orogens in, for example, the Coast Ranges, Klamaths, and Sierra Nevada mountains of the American Cordillera that were affected by accretionary and slab failure events. These similarities include complex infolding of a basement, intrusions, and associated roof pendants, early deformation involving sub-horizontal thrusting and nappe emplacement with synchronous plutonism, later upright folding associated with additional contraction and strike-slip faulting that formed interference patterns, and to late extensional collapse with doming and more localized pluton emplacement. The similarities are remarkable because in both the Sierra Nevada/Coast Ranges/Cordilleran plutons, and in the Eastern Pilbara plutons, there are raging debates about the
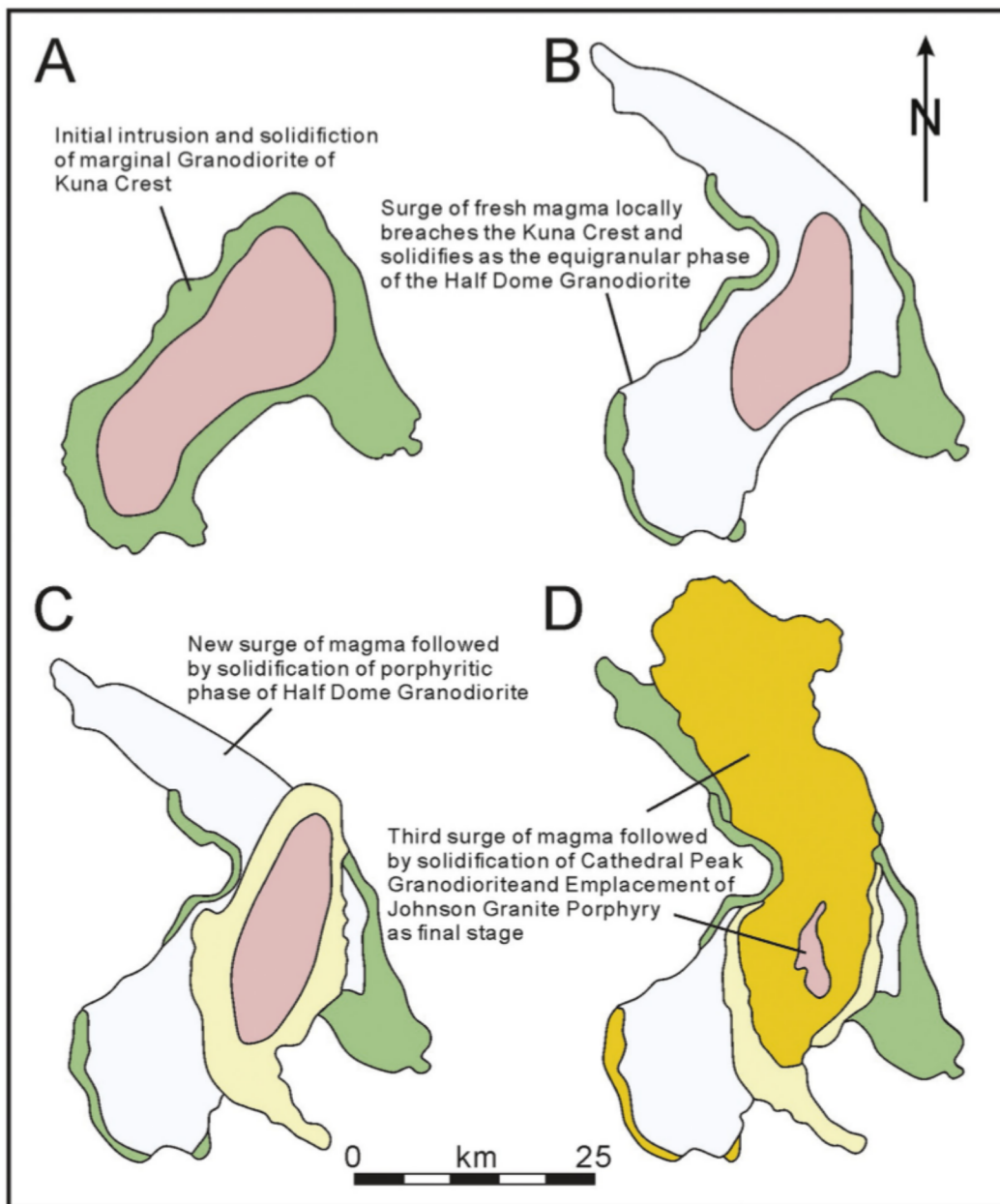
Fig. 16. Maps (modified from Snelling and Gates, 2009) showing the proposed sequential emplacement of the circa 95–85 Ma Tuolomne Intrusive Suite of the Sierra Nevada Batholith, which is part of the Cordilleran-wide Sierra Crest suite (Coleman and Glazner, 1998) to form a set of nested plutons: (a) granodiorite of Kune Crest, (b) (c) Half Dome Granodiorite, and (d) Cathedral Peak Granodiorite and Johnson Granite Porphyry (after Huber et al., 1989). The zones include both distinct chemical and textural zones and lobes within the plutons (Memeti et al., 2010), which represent different pulses of magma that were able to migrate within the pluton, with similar trends along the axis of the batholith with time, related to a massive slab break-off event (Hildebrand and Whalen, 2017). These show similar variations to the circa 3324–3277 Ma Emu Pool and 3274–3223 Ma Cleland Supersuites within the Mount Edgar and other batholithic domes in Eastern Pilbara. These nested plutons are Cretaceous, and show remarkably similar zonations to those of the Eastern Pilbara. However, unlike the nested plutons of the Pilbara and other cratons, the North and South American Cordilleran nested plutons have never been interpreted (as in Hawkesworth et al., 2020) as a response to the start of global plate tectonics.

relative importance and roles of diapirism, ballooning, migmatization or partial melting of older crust, the nature of the oldest crust, the importance of folding of plutons and cover sequences, infolding vs. sinking of roof pendants, source of magmas from arc-type mantle wedge melting, or slab melting during slab failure, and the significance of the magmatism for crustal growth vs. crustal recycling (e.g., Fu et al., 2018; Hildebrand et al., 2018). However, in the case of the Cordilleran batholiths, geologists there are content with the idea that they are working in a specific tectonic environment, i.e., a continental margin arc system, built on older accreted material with an accretionary orogen/intra-

oceanic arc history, and cut by slab failure magmas. Disparagingly, workers concerned with the Pilbara pay little heed to their counterparts, who are familiar with magmatic and tectonic processes in continental margin arc systems and evolved orogens, but rather, prefer to claim that Eastern Pilbara represents a preserved remnant of a period of Earth history that bears little resemblance to any tectonic setting on the modern Earth.
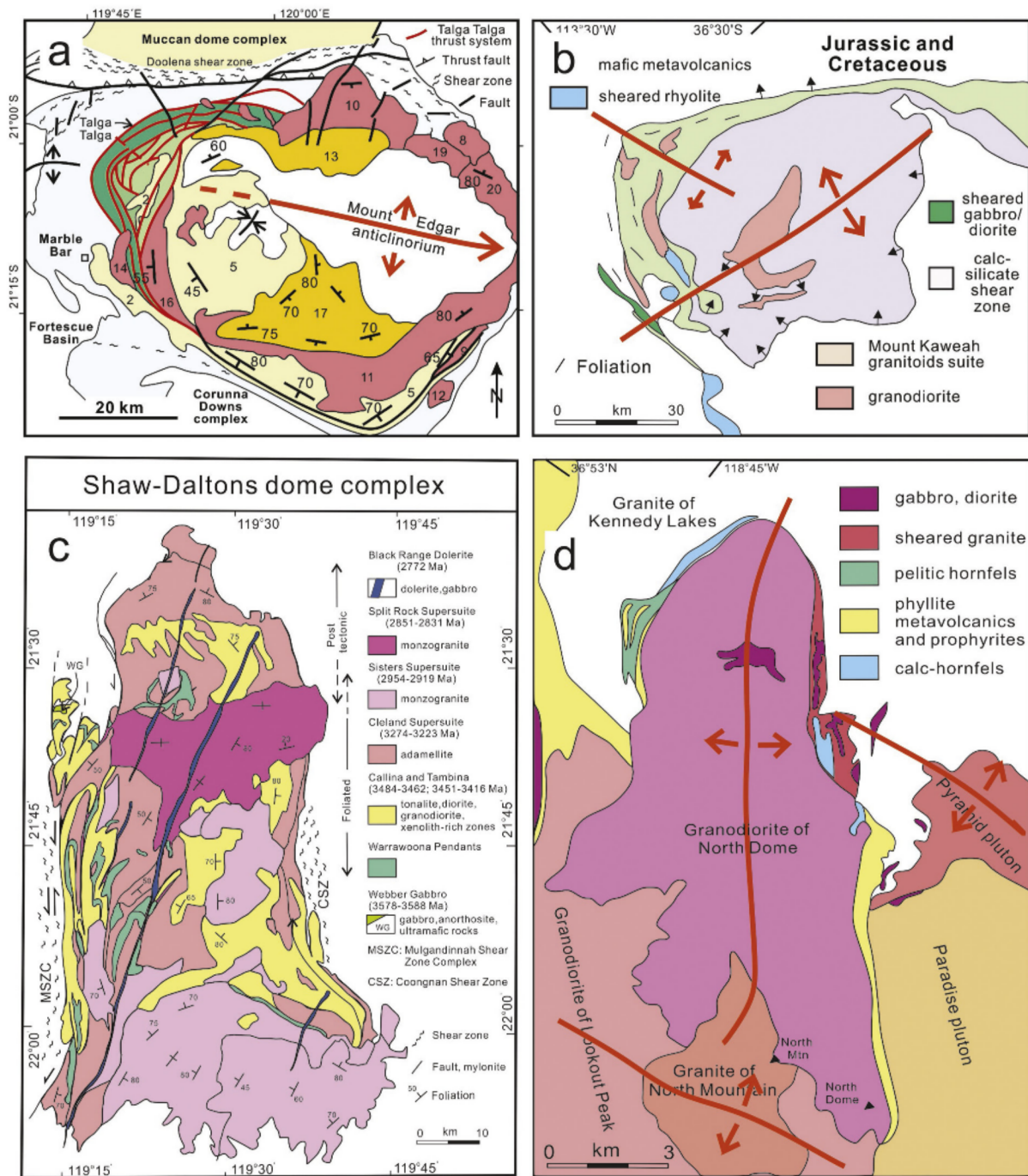
Fig. 17. Comparison of map patterns of Eastern Pilbara with selected plutons of the Sierra Nevada. They are similar to at least 4 orders, including 1) rock types, 2) relationship to surrounding units, 3) scale to an order of magnitude, and 4) temporal duration of magmatism. **(a).** Simplified map of the Mount Edgar dome (from Fig. 6) **(b)** Part of a geological map of the Mount Kaweah granite (purple) and surrounding Jurassic volcano-sedimentary sequences (green and blue) in the Sierra Nevada Batholith (Sequoia National Park area), for comparison. The red granite in the center is the granite of Lion Rock, forming a nested pluton with more K-rich rocks in the center. Map modified from Hildebrand (2013) based on mapping by Moore and Sisson (1987) and Sisson and Moore (1994). Note how the sill-like plutons are folded, and the volcano-sedimentary rocks form steeply dipping folded margins to the plutons, much like the Mount Edgar Dome. **(c)** map of the Shaw dome (North Pole Dome is to the north), simplified as above from Fig. 7. **(d)** map of the North Dome, Sierra Nevada, with the granitoids in red and purple, complexly folded volcanosedimentary sequences on the margin of the pluton, and the elongation of the dome caused by folding and fold interference. Note also the younger pluton intruding the core of the older phases on the margin. Map (d) modified from Hildebrand (2013). (For interpretation of the references to colour in this figure legend, the reader is referred to the web version of this article.)
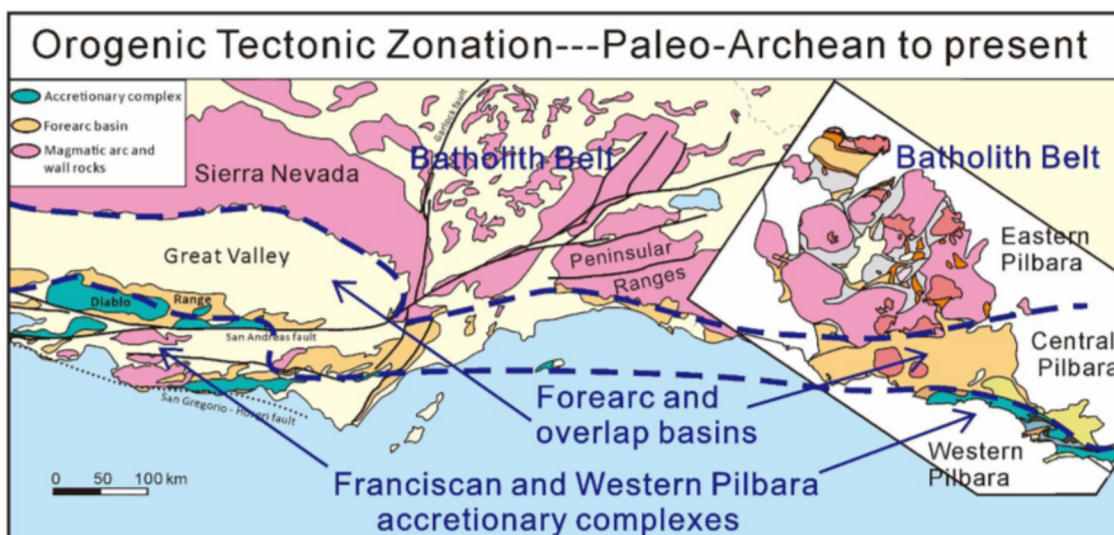
Fig. 18. Comparison of the main litho-tectonic belts of the California segment of the North American Cordillera, with the Pilbara craton, to illustrate their similarity in scale, rock types, and overall geological relationships. Main map is a geological sketch map showing the main belts and terranes of the Franciscan complex, the Great Valley Sequence, and the batholith belt including the Sierra Nevada and Peninsular batholiths. Map is modified from Hildebrand (2013) after Jennings (1977) and Dumitru et al. (2010). Inset is the map of the Pilbara Craton (from Hickman, 2016, simplified from Fig. 5) at same scale and colour-codes as the Cordillera map. Note the striking similarity in rock types, structures, scale, and age relationships between the Eastern Pilbara and the Sierra Nevada Batholith, the Central Tectonic Zone with the Great Central Valley of California, and the Western Pilbara Terrane with the Franciscan Complex.
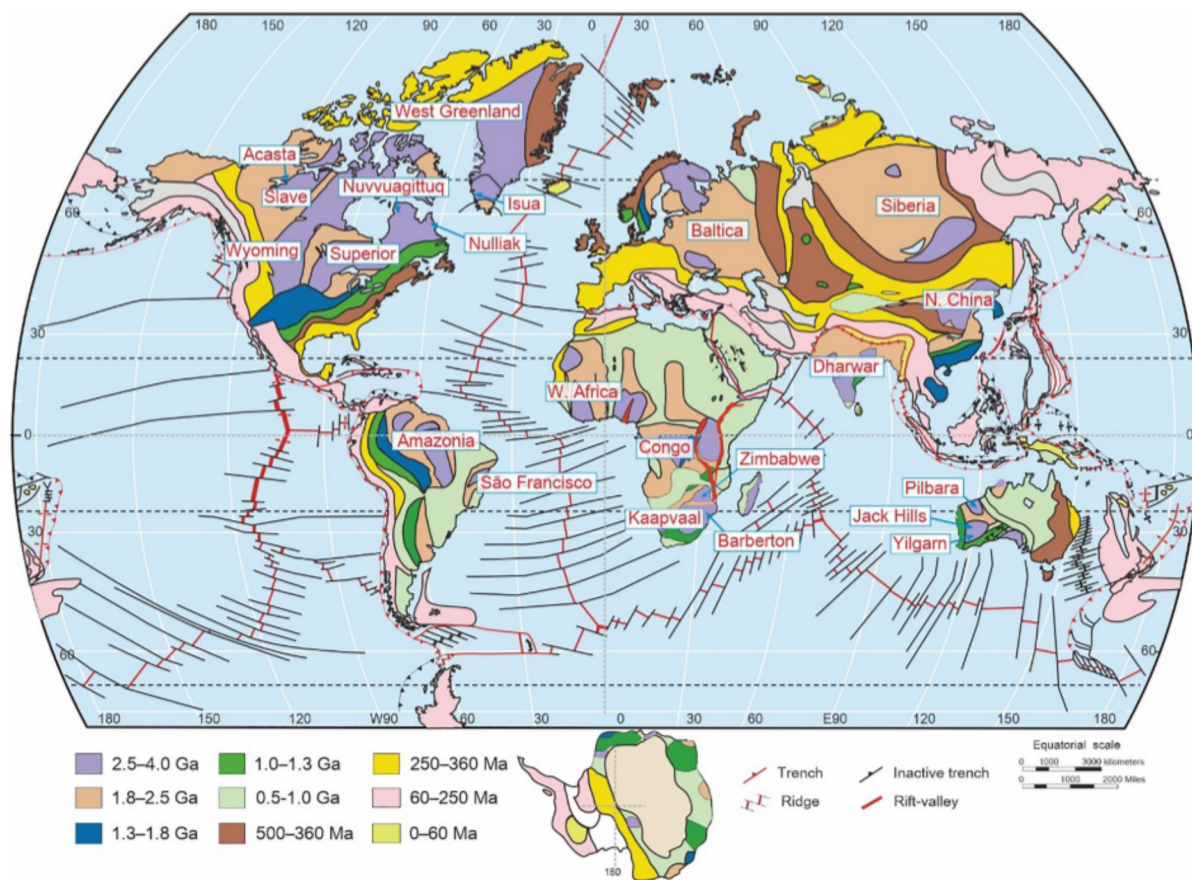

Fig. 19. Simplified geological age map of the world showing distribution of crust of various ages and locations of the main Eoarchean outcrop areas, belts, and cratons. Map compiled from numerous sources, including: (UNESCO, 1976; Liou et al., 1990; Goodwin, 1996; Condie, 1997; Windley, 1995; Maruyama et al., 1996; Kusky and Polat, 1999; Maruyama et al., 2007; Utsunomiya et al., 2007; Sawada et al., 2018; Windley et al., 2021).
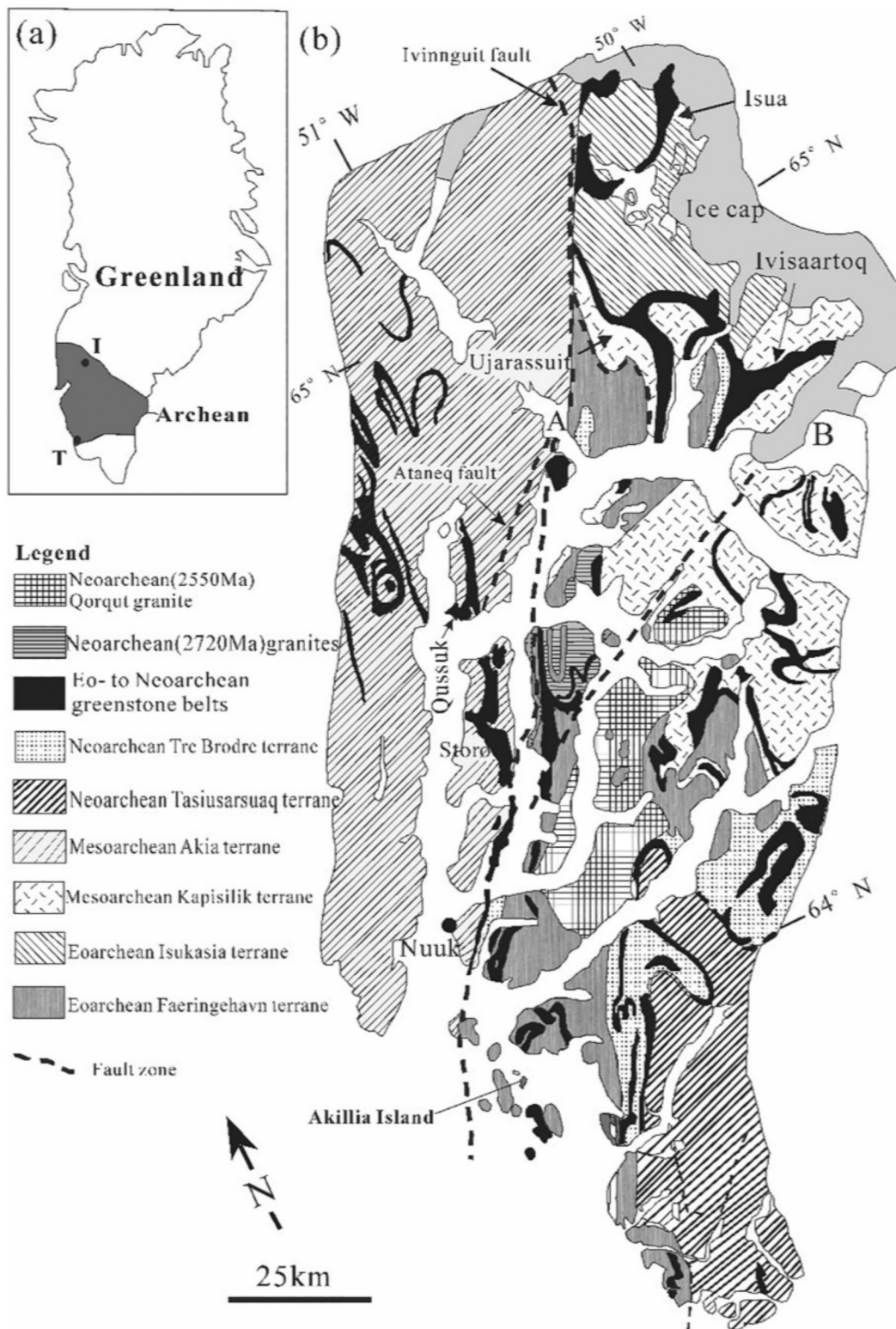
Fig. 20. A simplified geological map of the Itsaq region, showing the Eo- to Neoarchean tectonic terrains with Isua in the far north (see Fig. 21), and Akilia Island in the far south. Modified from Friend and Nutman, 2005a, Nutman and Friend, 2007; Windley et al., 2021). Note the numerous giant refolded nappe structures, throughout the terrain, which are locally form a typical gneiss dome in the north at Isua. Labels in inset I-Isua (Itsak region), T-Tartoq.
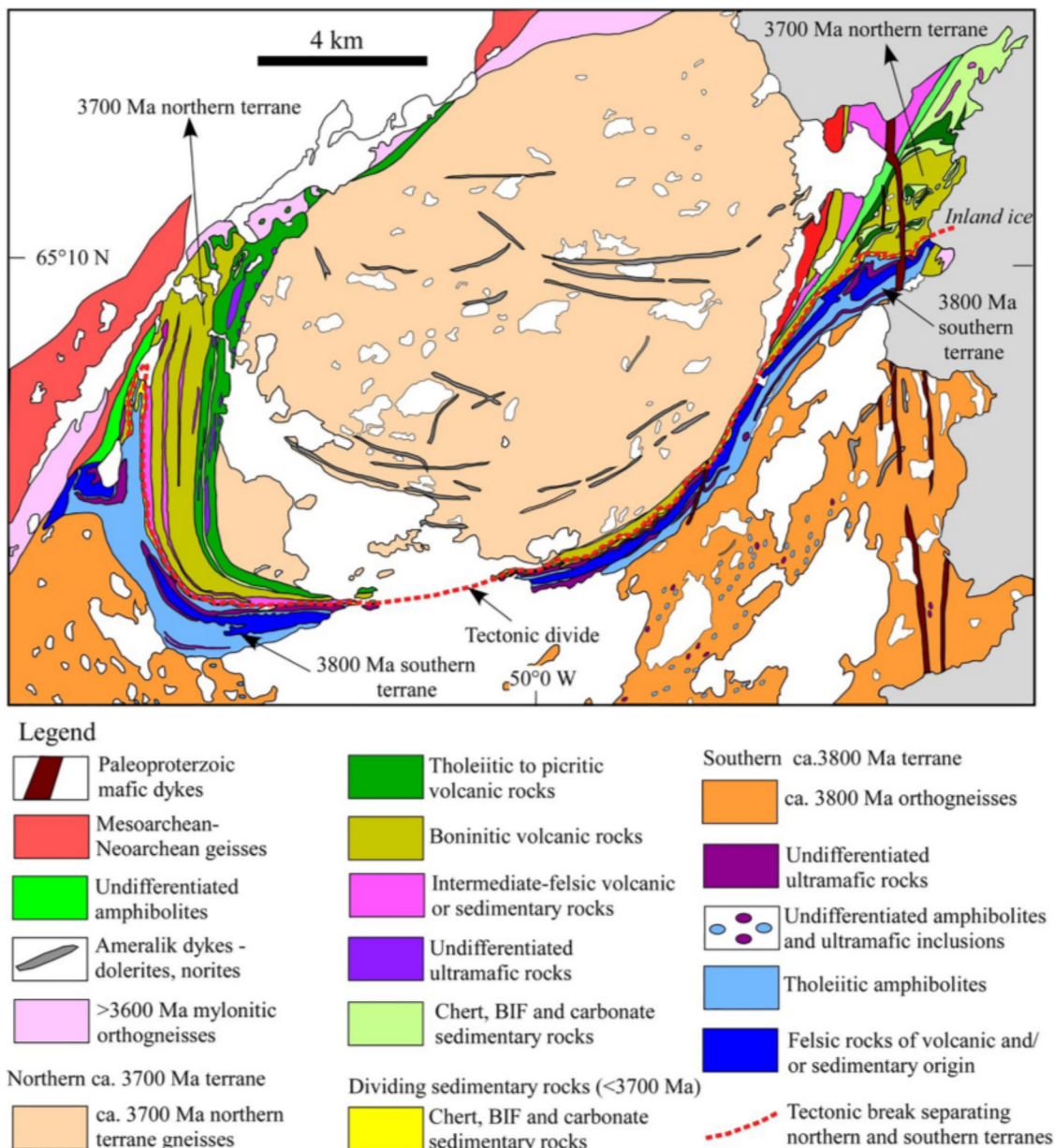
Fig. 21. A geological map of the Isua supracrustal belt showing the ca. 3800 Ma southern and 3700 Ma northern arc terranes, wrapped around a structural dome comprised of 3700 Ma gneissic rocks. See Fig. 20 for location. Note the large-scale structure is that of a gneiss dome, but it formed, as in the Pilbara, by a long sequence of structural imbrication events of oceanic ophirags, OPS, folding, and refolding events, as described in the text. Modified from Nutman and Friend (2009), and Windley et al. (2021).

4. Discussion

4.1. Development of the Eastern Pilbara in the context of accretionary orogens evolving to a continental margin arc intruded by slab-failure magmas during collision

The Pilbara craton is particularly infamous for being the type example of a Paleo-Mesoarchean terrane that exhibits outcrop patterns and relationships that are supposedly unlike those on the planet in Phanerozoic and extant plate mosaics (e.g., Hickman, 2012, 2016; Van Kranendonk et al., 2015; Nijman et al., 2017; Hawkesworth et al., 2020). This is a myth that has been propagated and repropagated without proper assessment using the objective-based and testable null hypothesis. The hypothesis that Eastern Pilbara is different from younger orogens fails the null hypothesis test in every respect. The development of the

Eastern Pilbara can most certainly be readily explained using the current plate tectonic paradigm, allowing for small changes related to the difference in mantle potential temperature (i.e. presence of komatiites). Thus, applying the null hypothesis, and following the scientific method, there is no need to invoke other arbitrary, non-testable or imaginary alternative Earth models to explain the observations and data about the development of the Eastern Pilbara terrane. All one needs is a working understanding of plate tectonics, and a working knowledge of the geology and history of development of orogenic belts of all ages on Earth.

Failure to apply the null hypothesis to understand the development of Eastern Pilbara has led to a plethora of invocations of other mechanisms of heat loss from Earth, such as stagnant lids, vertical drip tectonics, catalytic delamination tectonics, sagduction, and the like (e.g., Choukroune et al., 1995; Van Kranendonk et al., 2004; Bédard, 2006, 2018; Bédard et al., 2013; Debaille et al., 2013; Lin et al., 2013; Johnson
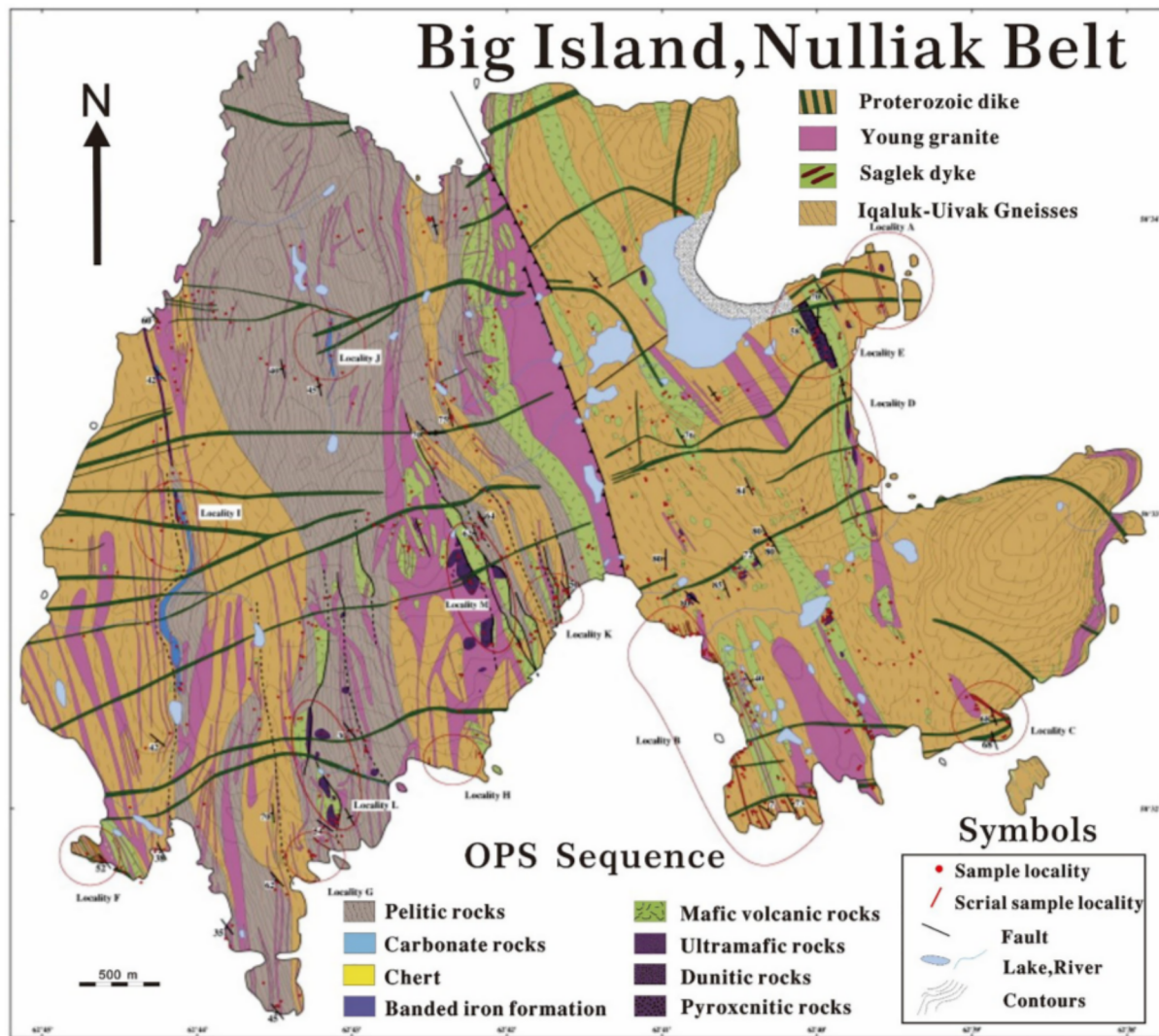
Fig. 22. Geological map of Big Island, Nulliak belt, Saglek Block (modified from Komiya et al., 2015).

et al., 2014; Nebel et al., 2018; Wiemer et al., 2018). These speculations are based on what is often called the "dome-and-keel" structure of granitic gneiss domes, and their relationships to the surrounding volcano-sedimentary sequences, which we show above to be analogous to modern OPS in accretionary orogens intruded by several generations of arc magmas, followed by massive domal intrusions during slab-failure during collision of arcs and/or continental margins. Although there have been a large number of excellent structural studies on the multiple and long-lived events that resulted in the present gneiss dome pattern in Eastern Pilbara (e.g., Koppenburg et al., 2001; Zeegers et al., 1996; Bickle et al., 1980; White et al., 1998; Blewett et al., 2004), these studies are conspicuously not considered in many recent works (e.g. Van Kranendonk et al., 2004, 2006; Van Kranendonk et al., 2007, 2014, 2015; Bédard, 2006, 2018, 2020; Bédard et al., 2013; Wiemer et al., 2018; Hawkesworth et al., 2020). It has alternatively become popular to prefer models in which thick piles of volcanics and sediments accumulate on a stationary lid over a stationary plume for hundreds of millions of years, forming tens of kilometer-thick sections that become so dense that parts spontaneously sink back into the mantle as drips, sink to eclogite facies, partially melt, and generate TTG magmas. Not only do these models not account for the ample structural data from the Pilbara, use unrealistic geological and rheological model inputs (Korenaga, 2021), they also do not consider the geology of Phanerozoic (or Proterozoic, or Archean) orogenic belts, nearly all of which contain zones of gneiss domes rising

through overlying older volcano-sedimentary packages, forming identical structural and temporal relationships (Whitney et al., 2004, 2013; Kusky et al., 2018). To emphasize this point, Fig. 17 shows maps of Cretaceous plutonic suites in the Sierra Nevada batholith, compared with maps of some of the domes in Eastern Pilbara described in this paper. The similarity to at least the fourth degree (rock types, map pattern, structures, relative temporal sequence) is so striking, that we wonder why so many statements about the so-called unique map character of the domes of the Eastern Pilbara have so-far gone unchallenged. We ask instead, with the exception of komatiites produced by a hotter mantle in the Paleoarchean, *"what specifically is unique about the eastern Pilbara that we cannot find it in the geologic record of Phanerozoic plate tectonics, or more specifically, in the convergent margin accretionary orogen batholith belts of the circum-Pacific?"*

In addition to the similarity to the fourth order of the map patterns, the supposed older Eoarchean continental basement upon which these volcanic piles were supposed to have been built has never been found, and yet the oldest rocks in Eastern Pilbara are a dismembered ophiolitic-gabbro complex, temporally correlated with the oldest MORB-type sections of the Warrawoona Group, which forms the structural base to one of Earth's oldest intraoceanic arc and accretionary orogenic systems. Models calling for a dramatically different early Earth based on the geology of Eastern Pilbara are internally inconsistent, and self-contradictory in that they deny significant crustal shortening, yet
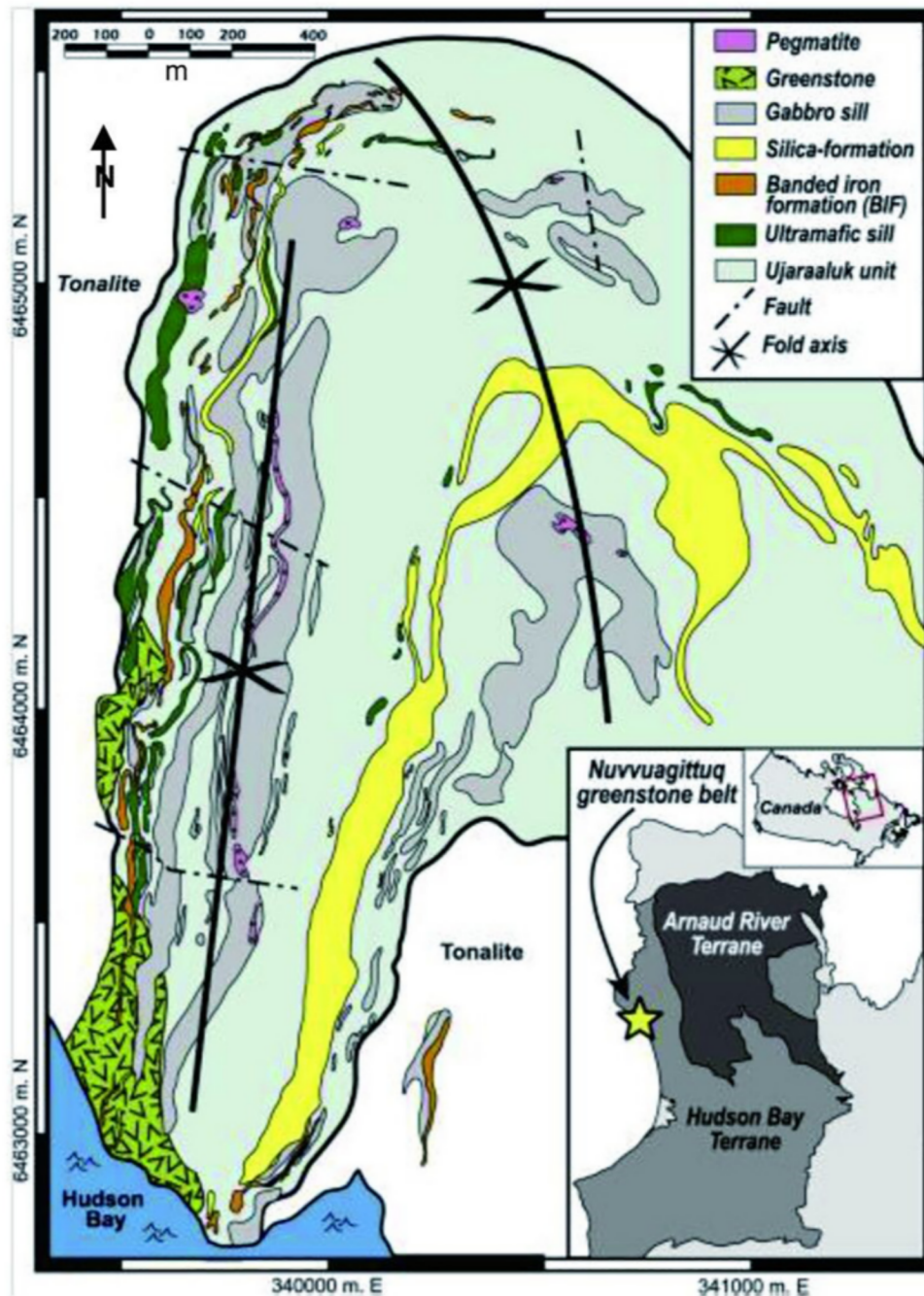
Fig. 23. Simplified geological map of the Eoarchean Nuvvuagittuq belt of the northeastern Superior Craton outlining the distribution of pillow basalts, bedded cherts, banded iron formations and intrusive sills. Modified after O'Neil et al. (2012) and Windley et al. (2021).

require hundreds of kilometers of shortening to form drips that reach to eclogite facies depths (Van Kranendonk et al., 2007, 2015; Nebel et al., 2018), and they ignore the geology of most younger orogens of the planet.

Here we very briefly summarize the tectonic development of Eastern Pilbara that resulted in the formation of the classic dome-and-basin patterns, using the modern plate tectonic framework and examples from Phanerozoic orogens described above.

4.2. Nature of the oldest basement of the Eastern Pilbara

The characteristics of the Webber gabbro suggest to us that it represents part of a dismembered oceanic basement complex that was accreted during early accretion of the Pilbara craton, and thus it represents the basement upon which later successive island and continental margin arcs were built. Interestingly, it is the same age, within error, as the uppermost thrust sheet in the duplexes of the Warrawoona Group at North Pole reported by Kitajima et al. (2008), suggesting that the most ancient ophiolitic crust in Eastern Pilbara may be more widespread than currently recognized. The geochemistry of the Webber gabbro, particularly its low Nb—Ta compared to LREE and Th, is consistent with the model of Polat et al. (2018a, 2018b) for derivation from a mantle source enriched in LREE by recycling oceanic crust (i.e. subduction). The old 3660 Ma basalts in the North Pole duplexes have a MORB-like geochemical signature and they are associated with ocean floor-type metamorphism and sea-floor hydrothermal alteration (Kitajima et al.,
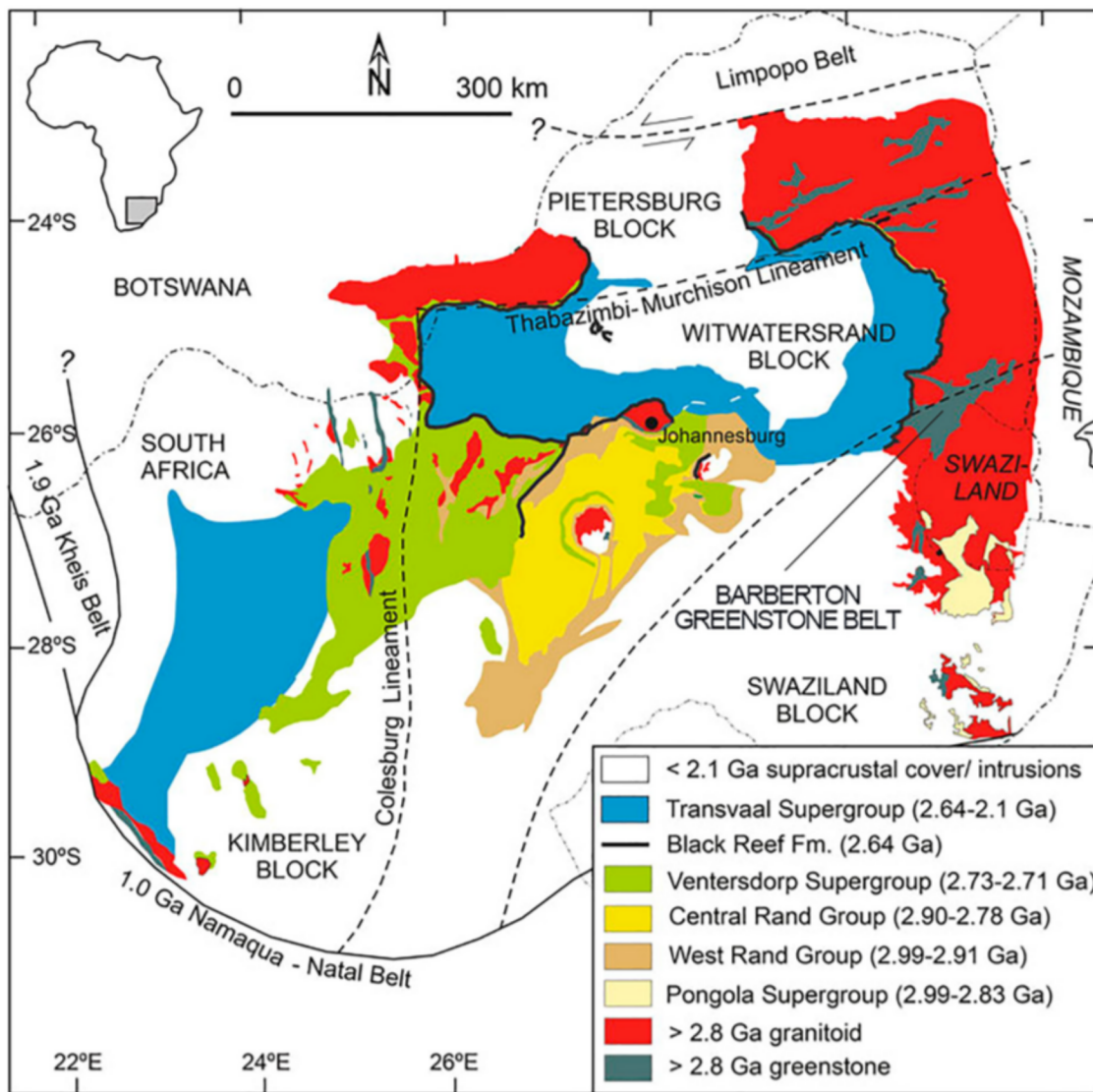
Fig. 24. Main tectonic divisions of the Kaapvaal Craton (modified from Frimmel (2019), Kröner and Hofmann (2019), and Windley et al. (2021)).

2008). As such, the oldest basement in Eastern Pilbara is directly anal-
ogous to the accreted OPS, ophiolitic mélanges, and Trinity, Josephine,
Calaveras and other ophiolites of the Klamaths and Western Sierras
described above in section 2.

Petersson et al. (2019) noted that the plateau-stagnant lid-sagduc-
tion model for the evolution of the Pilbara, and other Archean cratons of
Van Kranendonk et al. (2015) requires a 35 km thick mafic/ultramafic
protocrust (double that of even the 12–15 km stratigraphic models, and
six times that of the demonstrable structural thicknesses) to sink, and
partially melt, to generate the TTG suite, which would then leave a
strongly depleted mantle residue with superchondritic Hf isotopes,
which is exactly the opposite to what is observed. In contrast, the highly
chrondritic $^{176}Hf/^{177}Hf$ signature of the Webber gabbro argues against
these models, and suggests that much less continental material had been
extracted from the Pilbara mantle than estimated by Van Kranendonk
et al. (2015) and Wiemer et al. (2018). In addition, Petersson et al.
(2019) noted that their Lu—Hf and O isotopic data from the Webber
gabbro resemble those from hydrothermal systems or modern mid-
ocean ridges, so we suggest that the Webber gabbro suite may repre-
sent hydrothermally altered circa 3.59–3.58 oceanic crustal basement of
the Eastern Pilbara Terrane.

4.3. Arc magmatism and slab-failure magmatism are responsible for the generation of Archean crust and dome-and-basin structures of all ages

In the sections above, we have shown that multiple orogenic defor-
mation events punctuated by multiple intrusive events lead to complex
map patterns and geological evolution, whether the rocks being
analyzed belong to an evolved continental margin arc, a Phanerozoic
orogen, or one of the planet's oldest Archean cratons. The comparability
in terms of poly-orogenic development from an early accretionary oro-
gen stage (e.g., Windley et al., 2021), to immature to mature island and
continental margin arc stage, followed by intrusion by slab-failure
magmas during a late stage of collision is striking and compulsive, to
multiple degrees of similarity. Many cratons and younger orogens were
in late stages intruded by yet more post-orogenic plutons, often referred
to post-orogenic magmas that in some cases can be related to orogenic
collapse (Kusky, 1993), and in others to a variety of other possible
younger events.

Based on the above detailed analysis, we summarize the main fea-
tures and tectonic affinities of each of the main groups of magmatic
rocks in Eastern Pilbara as follows:

(1) oceanic basement
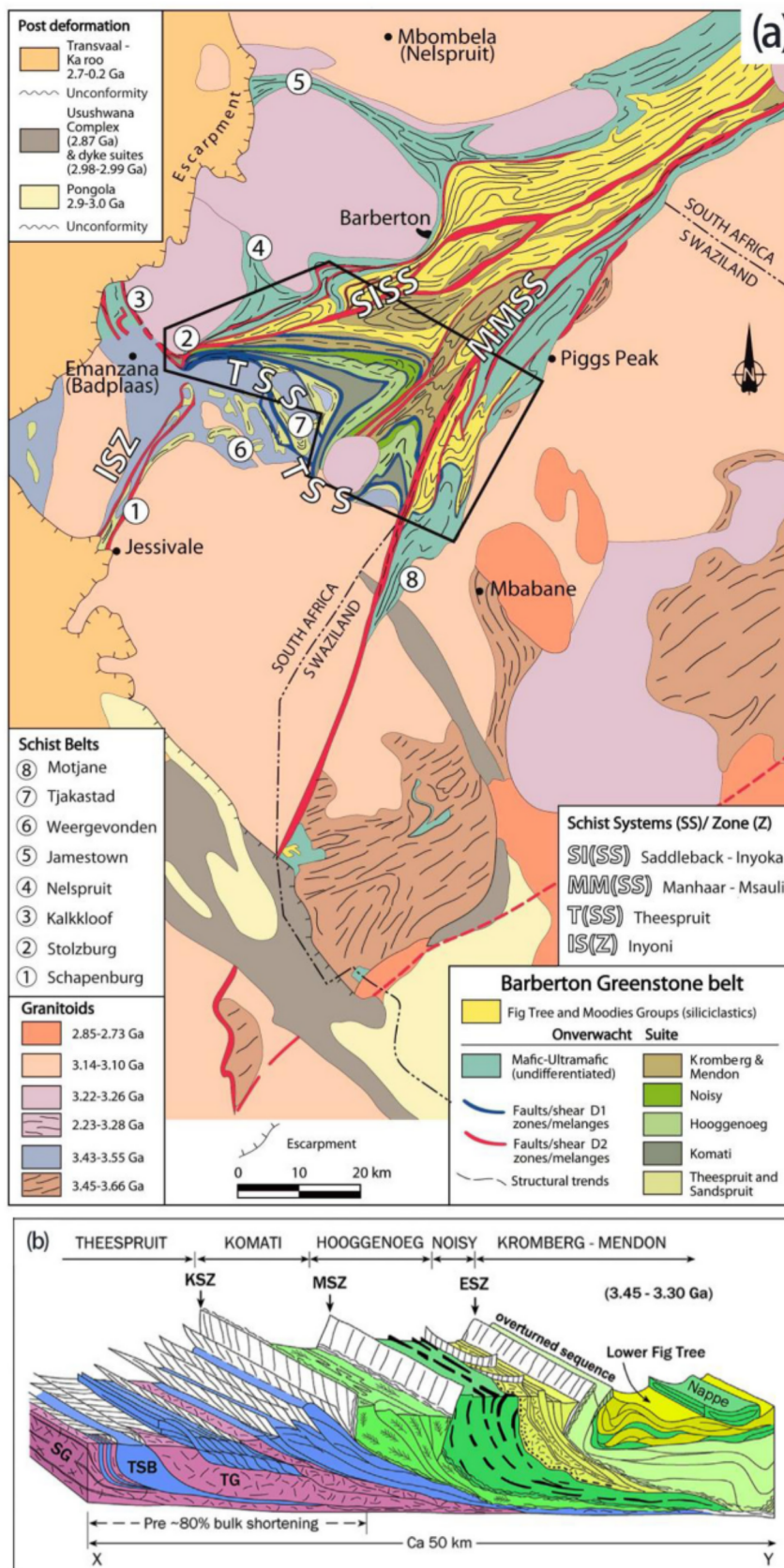**Mount Webber Gabbro/Lower Warrawoona litho-tectonic**

Fig. 25. a. Generalized geologic map of the Makhonjwa Mountains (Barberton greenstone belt), Kaapvaal Craton, and vicinity. Black polygon outlines area of detailed mapping by the late Maarten de Wit and his colleagues and students. Modified after de Wit et al. (2018). **b.** Diagrammatic sketch illustrating the structure of the Onverwacht Group of the Barberton supracrustal belt in the Kaapvaal Craton (see Fig. 24). Modified after de Wit et al. (2018).
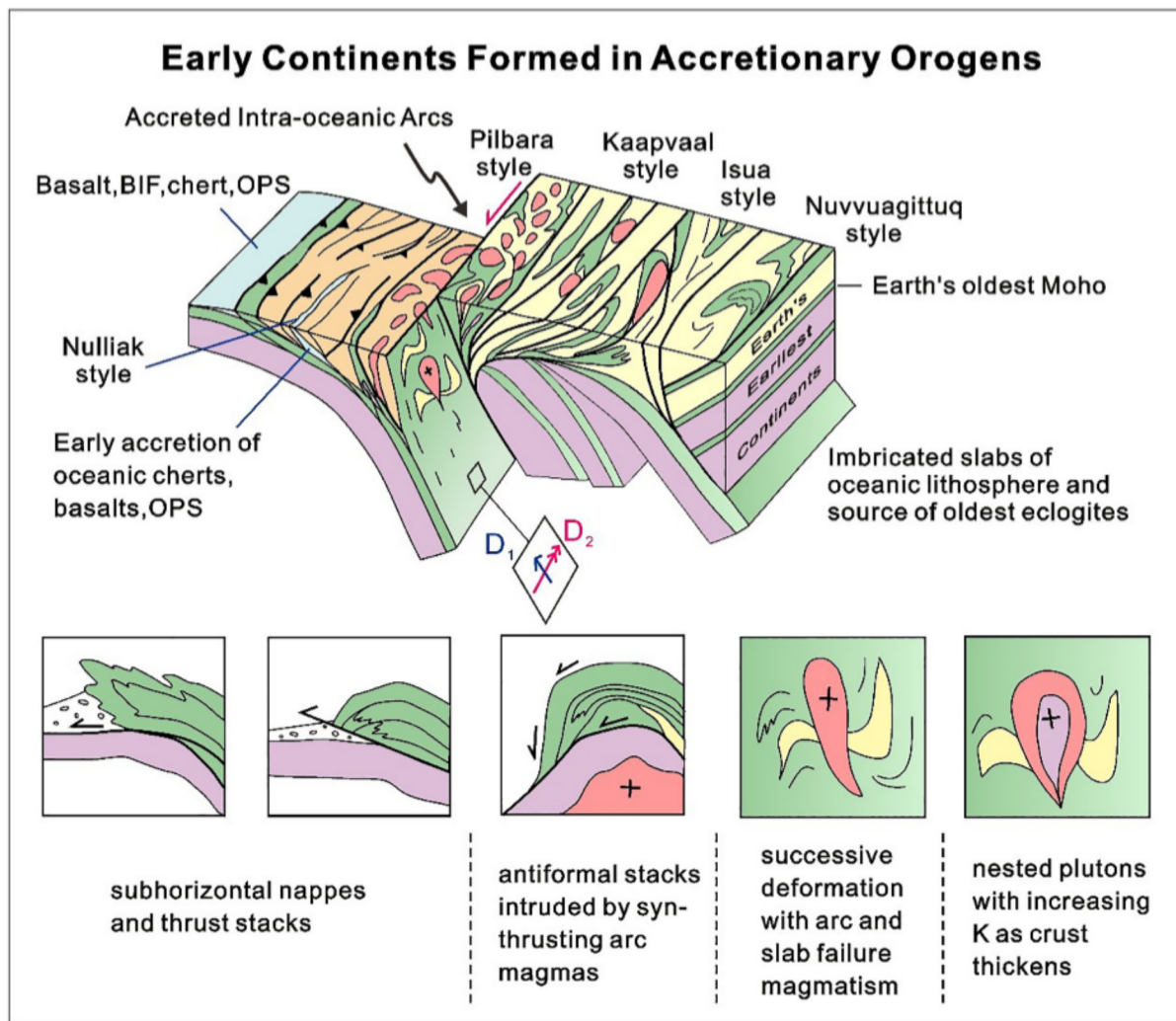
Fig. 26. Conceptual model showing the growth of the Pilbara craton, in the context of other Eo-Mesoarchean terranes discussed in the text. All formed in Earth's oldest accretionary orogens, with initial off-scraping of oceanic basalt, komatiite, chert, gabbro, anorthosite and rare cumulates, and were intruded by successive generations of initially primitive arc magmas, but that changed to more evolved K-rich magma types as the early crust thickened. Panel showing lineations (D_1, D_2) correspond to early layer-parallel thrusting, and later strike-slip shearing. See text for detailed discussion.

assemblage (~3560–3480 Ma), accreted oceanic crust and mantle, with preserved ocean plate stratigraphy OPS including chert, deep marine pelagic sediments, and younger clastic rocks. Basalts from the Warrawoona Group were altered under sea-floor conditions, at abyssal depths of 3800–2500 m similar to that of mid-ocean ridges, and dissimilar to that of thick plateaus which would have shallow surface depths. The Upper Warrawoona and higher units of the Pilbara Supergroup resemble upper plate arc sequences from younger orogens.

(2) arc magmatism

Callina and Tambina Supersuites (3484–3416 Ma). Dioritic to granitic gneiss. We suggest these are arc-related plutons, preserved in only relatively small remnant areas, most are now deformed gneissic sheets folded together with the Warrawoona litho-tectonic assemblage along the borders of some domes (e.g. Shaw dome complex).

(3) slab-failure magmatism

Emu Pool Supersuite (3324–3277). TTG suite. The most voluminous suite in the craton. Field relations show that the protoliths magmas intruded during deformation. Some intruded as layer parallel sills that were folded later into antiforms and synforms with wavelengths of tens of kms.

Cleland Supersuite. 3274–3223 Ma. Monzogranite. Steep cross-cutting plutons in the cores of domes, analogous to the nested plutons

of the Sierra Crest and related Cretaceous plutons along the 15,000 km long length of the American Cordilleras. These are late-stage slab failure magmas with more crustal melting components than the Emu Pool Supersuite.

(4) post-orogenic collapse

Split Rock and Related Suites (2851–2831 Ma). Late discordant, highly-fractionated, Si-rich (>73%) monzogranites, 350 Ma younger than everything above. These rocks may be part of a former belt, which is only preserved as a few plutons in a 200 × 150 km area, making assessment of their affinity and relationships to other features obscure. Their derivation from melted older crust and association with sub-horizontal pegmatite sheets that intruded soon after the North Pilbara Orogeny (circa 2960–2920 Ma; GSWA, 2016) suggests that they may be related to post-orogenic collapse and extension (e.g., Dewey, 1988) as in other cratons (Kusky, 1993), or as hypothesized by Hickman (2012) were related to lower crustal delamination, or movement across a hot spot, or lower crustal melting that preceded Forteqcue rifting.

(5) younger rifting

Black Range dolerite dike swarm (2772 Ma). The last significant Archean igneous event in Eastern Pilbara was intrusion of NE-striking doleritic-gabbroic dikes of the Black Range swarm at circa 2772 Ma. Evans et al. (2017) suggested that the dikes and coeval rocks in the lower
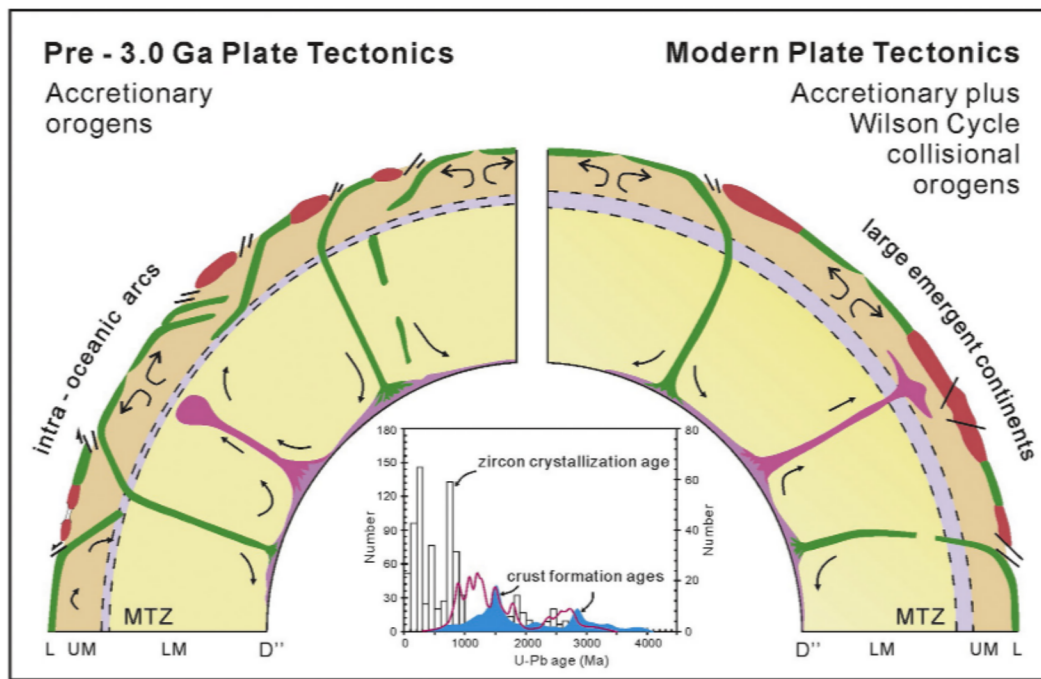
Fig. 27. Conceptual model of Earth planetary processes, from the Eoarchean to present, showing how accretionary orogens have been the locus of continental growth through time. Modified from Windley et al., 2021. Inset in the "core" shows the volume of continental crust preserved through time (from Hawkesworth et al., 2020), illustrating the preserved record of continental growth, but not necessarily the record of any relationship between growth, preservation, and destruction.

Fortescue Group had different paleomagnetic poles that record rapid drift of the Pilbara craton across the polar circle during rifting at 2772 Ma. The swarm may thus be related to the break up of an unknown early continental mass, pre-Kenoraland.

4.4. *The importance of scale in comparative tectonics*

In a recent review Hawkesworth et al. (2020) note the importance of scale when interpreting the ancient geologic record, yet compared the Pilbara and Yilgarn tectonic maps using a greatly enlarged version of Pilbara. We agree with the importance of scale, remembering that the Eastern Pilbara Terrane that forms the basis for so much interpretation and modeling of Paleo-Mesoarchean planetary behavior is only 200 × 200 km in area, and would easily blend in with any map of the batholith belts of the North or South American Cordilleran orogens (Figs. 1, 2), with those of eastern Asia, or with the accreted batholith belts of the Alpine-Himalayan orogen (Kusky et al., 2018; Fu et al., 2018). The importance of scale is further emphasized, by some recent claims that in order to "prove" the operation of plate tectonics in the Archean, one must "prove" that there was a globally linked and distributed network of plate boundaries with deformation concentrated at the boundaries (e.g., Lenardic, 2018a, 2018b; Brown et al., 2020). With the scale of the preserved Eoarchean -Paleoarchean regions being so small, this is an impossible test to test, as with cratons that are only 200 km across, there is no way to prove a globally linked network. Geologists must look instead, at the geological signature of plate tectonics, in the igneous, sedimentological, structural, geochemical, metamorphic histories of the rocks, and use the null hypothsis, to test if plate tectonics can explain these features. If so, applying the null hypothesis, there is no justification to advocate other ad hoc mechanisms.

We have shown above that the geological histories, rock components, structures, processes and map patterns in Eastern Pilbara are remarkably similar to those of juvenile arcs that evolved in early accretionary orogens. We use examples from the Cordillera of the western Americas, predominantly North America.

To emphasize the importance of scale, we have shown Eastern

Pilbara plotted to scale, on maps showing 1) the western North America Cordilleran batholith belt (Fig. 1), and the Sierra Nevada Batholith (Fig. 2) where the entire Pilbara would form only a small part of any of the major batholiths such as the Coast Ranges, Sierra Nevada, or Peninsular Ranges. If extended to the full >15,000 km hemispheric length of batholith belts of the western Americas, which have such similar characteristics to the Pilbara, one wonders why the geological community has accepted such speculations that eastern Pilbara represents a tectonic environment unlike any on Earth.

In this section, we take the comparison of scale one step further. Fig. 18 shows a map of Pilbara (Fig. 5 plotted on its side) at the same scale as the tectonic map of California USA (drawn after Hildebrand, 2013). The eastern Pilbara terrane compares directly with the Sierra Nevada Batholith, to the fourth degree, as described above. The De Gray Superbasin, consisting largely of marine and continental sedimentary deposits with a mafic volcanic substrate, is similar to the Great Central Valley Sequence that consists of marine and continental sedimentary deposits with a mafic volcanic (ophiolitic) substrate. The Western Pilbara accretionary terrane is strikingly like the Franciscan and other accretionary units of eastern California. In this comparison, we are noting simply the juxtaposition of similar types of tectono-magmatic terranes, not necessarily implying the Western Pilbara is the accretionary wedge part of the Eastern Pilbara arc terrane, because the temporal relationships are far more complex. Likewise, while many have simply assumed that the Franciscan and related units represent accreted trench material, and the Great Valley Sequence is a forearc basin that formed atop the Coast Ranges ophiolitic basement, and that the Sierras represent a long-lived arc with continuous east-directed subduction, this relationship is questioned (Hildebrand and Whalen, 2014a, 2014b; Hildebrand, 2013). However, from the map pattern and lithological/structural comparison, if the ages were taken away from the maps, no-one would doubt the similarity in scale and rock types between the Pilbara craton and the tectonic zonation of western North America (Fig. 18).

Note also the similarity of the Sierran roof pendants that are isoclinally infolded, and sink into the sea of surrounding granitoids, in a

present-day mobile lid Earth. We also note the similarity in ages, with older basement in the Sierras (Precambrian, with Jurassic-Cretaceous Batholiths on top), and the similar magmatic flare ups, that lasted for 10–30 Ma, and spaced every 10–100 Ma.

In summary, there is no significant discernable difference in rock types (with the exception of komatiites produced by higher mantle temperatures), map patterns, deformation features, or temporal or spatial scales, between the geology of the Eastern Pilbara craton, or the entire Pilbara, and any modern continental-margin arcs that evolved from an intraoceanic arc accretionary orogen, to a mature thickened Andean arc on the edge of a craton. There is therefore no basis to use the map pattern of domes-and-basins of the East Pilbara Terrane to suggest that the Archean Earth behaved in any way drastically different from the modern Earth. Applying the null hypothesis, if the plate tectonic paradigm can explain the formation of continental margin batholiths built upon older accretionary orogens in a modern plate mosaic, it should also be used to explain the formation of exactly the same relationships that are so well exposed at mid-crustal levels in the ancient Pilbara. It is therefore not incumbent for geologists to prove that plate tectonics existed in the Archean, but rather, it is incumbent upon those who propose other models based on no data proven on Earth. The present-day Earth has a wide variety of tectonic environments, that formed under different conditions such as heat flow, ambient mantle temperature, slab dips, etc., and there is no reason to expect that the Archean Earth did not also have a similar range in conditions as the present Earth.

Perhaps the deep exposures of the Pilbara can be used to help better understand the processes currently on-going in inaccessible regions beneath the active batholith belts of the Cordilleras. For instance, deep levels of arcs are postulated to have thick residues of arclogites and related rocks (e.g., Ducea et al., 2020a, 2020b)- but they are not known to be present in the Pilbara. Why? There are many questions that could be addressed by recognizing a horse as a horse, to understand both different levels of exposure, and how specific processes may have evolved through time with changes in mantle temperature on an evolving planet.

5. Earth's first continents formed in accretionary orogens, through repeated accretion-related deformation and synchronous arc- and collision-related magmatism

The above analysis has shown that the domes-and-basins of the Pilbara are structurally complex constructs consisting of early-accreted oceanic plate materials including basalts, komatiites, gabbroic suites, and serpentinized ultramafic rocks, initially capped by deep-water hydrothermal cherts and less-abundant clastic rocks. These are imbricated in complex thrust structures, intruded by multiple generations of initially primitive magmatic rocks, the character of which gradually changed to more evolved compositions as the thickness of the accreted crust increased. The sequence of structural and magmatic development of the Pilbara is the same as in modern accretionary orogens, where accreted oceanic material is progressively added to a thickening crust, until at some point, it is thick enough to make a proto-continent. At this stage, the orogen becomes a continental-margin accretionary orogen and arc system. To test whether or not the sequence and processes we document in the making of the Pilbara craton applies to other early Archean terranes, we next briefly examine the history of the planet's other well-studied Eo-Paleoarchean cratons (Fig. 19), to test for similarities and differences, and to search for a common theme on the emergence of Earth's first continents.

5.1. Isua, North Atlantic craton, SW Greenland

The North Atlantic craton (Figs. 19, 20) of SW Greenland has long been known to include some of Earth's oldest rocks, where retreating glaciers have created some of the best exposures to test various tectonic, magmatic, and metamorphic processes that operated in the Eoarchean

(e.g., Bridgwater et al., 1975; Friend and Nutman, 1991, 2005a, 2005b; Nutman and Friend, 2009; Windley and Garde, 2009; Kolb et al., 2012; Dziggel et al., 2014; Polat et al., 2015, Polat et al., 2016a, 2016b; Nutman et al., 2020). The Akulleq terrane centered around Godthaab Fjord (Nuup Kangerlua) in SW Greenland includes mainly TTG gneisses, granite intrusions, belts of amphibolitic to granulitic volcano-sedimentary rocks (greenstone belts), and layered anorthosite complexes (Nutman et al., 2004, 2013; Steenfelt et al., 2005; Polat et al., 2009, 2011, 2015; Windley and Garde, 2009; Hoffmann et al., 2014; Dziggel et al., 2014), with greenschist facies rocks locally preserved in the Tartoq greenstone belts (Kisters et al., 2012; Polat et al., 2016a). Boundaries between the TTG gneisses and greenstone sequences are generally marked by 5–20 m-wide mylonitic shear zones (Polat et al., 2015), but in some places TTG plutons intrude the volcano-sedimentary packages. These greenstone belts form several km wide by several to tens of km long poly-deformed and metamorphosed and internally imbricated packages of dominantly mafic volcanic rocks, with subordinate amounts of meta- sedimentary rocks, gabbros, and ultramafic rocks. Remnants of the volcano-sedimentary sequences are also preserved as partly assimilated trains of boudins within the TTG gneisses (Windley and Garde, 2009). Poly-deformed layered anorthosite forms meter-to-km scale conformable layers of anorthosite, gabbro, and ultramafic rocks (Polat et al., 2015).

One of the best-studied greenstone belts in SW Greenland is Isua (Figs. 20, 21), located about 150 km NE of Nuuk in the Akulleq terrane, which is composed of the 3.8–3.66 Ga Amitsoq gneiss and the 2.82 Ga Ikkatoq gneiss. The Amitsoq gneiss contains volcanosedimentary enclaves of the Eoarchean Akilia association, whereas the Ikkatoq gneiss contains enclaves of the Neoarchean Malene supracrustals and anorthosite (Nutman et al., 1999; McGregor, 1993). The circa 2.52 Ga post-orogenic K-rich Qorqut granite intrudes the Akulleq terrane, representing the last significant magmatic event (Moorbath et al., 1981; McGregor, 1993), although the Paleoarchean Ameralik dikes, and a suite of N-striking circa 2.2 Ga high-Mg andesite dikes also cut units with appropriate ages (Nutman et al., 1996). Friend et al. (1987) recognized significant tectonic breaks between these terranes, and proposed that the northern 3.23–2.98 Ga Akia terrane collided with the southern 2.92–2.83 Ga Tasiusarsuaq terrane, with the Akulleq terrane wedged between, at 2.82–2.712 Ga (Fig. 20). While most rocks in SW Greenland are poly-deformed and metamorphosed to amphibolite to granulite facies, the Isua belt located in the NE part of the Akulleq terrane is a less deformed and metamorphosed supracrustal remnant, with ductile shear zone contacts on both sides with the Amitsoq gneisses (Bridgewater et al., 1975). The Isua belt is the largest greenstone belt in the Akulleq terrane, forming an arcuate structure wrapped around 3.7 Ga northern terrane gneisses that form a typical dome structure (Figs. 20, 21). Its southern extension is intruded by the tonalitic Amitsoq gneisses and the supracrustal rocks are preserved as enclaves within the gneiss. The Isua belt is special because of the low-grade Barrovian metamorphism (Boak and Dymek, 1982), it preserves primary structures, which are essential to understand the pre-3.8 Ga history of Earth (Nutman, 1986; Schidlowski, 1988; Nutman et al., 1993, 1996, 1997; Mojzsis et al., 1996; Komiya et al., 1999).

In a detailed structural study of the Isukasia area, Komiya et al. (1999) mapped the northern portion of the Isua belt (Fig. 21), separating five main lithologic units, including from base to top, 1) ultramafic rocks, 2) diabase-gabbro intrusives, 3) basaltic pillow lava, 4) chert and banded iron formation, and 5) dominantly mafic turbidites with minor conglomerate. There is no continental or arc-derived detritus in the basalts or cherts (units 1, 2, and 3), but detrital materials start to appear in the uppermost cherts and are common in the turbidites and conglomerates. Similar relationships are documented in the Warawoona basalts described above, and in younger OPS sequences deposited on oceanic substratum, that where later incorporated in accretionary prisms after their transit across the ocean from a ridge to a subduction zone (Isozaki et al., 1990; Kusky and Young, 1999; Kusky et al., 2013).

Komiya et al. (1999) divided the belt into three main structural units, bounded by low-angle thrust-sense shear zones. The southern unit contains 14 structural horses within a large duplex structure, each with a similar lithostratigraphy grading up from low-K tholeiitic (locally pillowed) basalts, overlain by chert and banded iron formation, in turn overlain by turbidites rich in mafic detritus, then conglomerates. They related this to modern ocean plate stratigraphy, and the structures to modern day accretionary wedges, suggesting therefore that the Isua belt represents the oldest preserved accretionary prism with OPS in the world, and demonstrating the operation of plate tectonics at 3.8 Ga. After accretion of the OPS by 3.71 Ga, they were intruded by arc-like tonalitic plutons at 3.702–3.627 Ga, similar to the Jurassic and Permian OPS remnants in SW Japan, that are now preserved as enclaves within huge Cretaceous TTG batholiths, exactly reminiscent of the Eoarchean of SW Greenland, and similar to the sequence described above for eastern Pilbara. Komiya et al. (1999) use the changing thickness of the chert unit within different duplexes to infer that thin chert units were deposited close to ridges, and thick chert had experienced significant travel from the ridge to accumulate such thick sequences. Using this hypothesis, they suggested that two ridges were subducted during accretion of the Isua OPS, thus explaining the stratigraphic and structural features in the Isua belt. In some places in the Isua belt, Komiya et al. (1999) also recognized accreted seamount rocks, and some arc-type clasts in the upper conglomeratic horizon of the OPS.

Farther south the circa 3.0 Ga Tartoq greenstone belt (Fig. 20) preserves the lowest (greenschist facies) volcano-sedimentary sequences in SW Greenland (Kisters et al., 2012; Szilas et al., 2013; Dziggel et al., 2014), and is part of the Kvanefjord block in the arc-accretionary model of Windley et al., 2021. It is exposed in four main areas, including the Nuuluk, Iterlak, Amitsuarsua, and Bikuben sub-belts, which include metamorphosed basalts, gabbros, serpentinized ultramafic rocks, and sedimentary sequence that resemble OPS, as in the Isua belt. The belt is structurally underlain by primitive TTG gneisses. Kisters et al. (2012) documented four main phases of deformation at greenschist to lower granulite facies, and interpreted the belt as an accretionary complex. The serpentinized ultramafic rocks have compositions of lower arc-cumulates (Szilas et al., 2013). Kisters et al. (2012) divided the Iterlak part of the belt into two units. The upper unit consists of greenstones, metagabbro, serpentinite and thin layers of banded iron formation, and is structurally juxtaposed with the lower unit, which has a greater proportion of metagabbro and serpentinite. The belt is intruded by 2.95 Ga TTG sheets (Kisters et al., 2012) some of which are tectonically imbricated with the metavolcanics (Szilas et al., 2013). Szilas et al. interpreted the belt to represent a dismembered supra-subduction zone ophiolite preserved in an accretionary prism, and the TTG intrusive rocks show geochemical traits that show they were derived from partial melting of the accreted amphibolites (Kisters et al., 2012).

Polat et al. (2016a) have documented a series of tectonically imbricated slices of metabasalts, gabbro, peridotite, felsic mylonites and sedimentary rocks within duplex structures, and also interpreted the belt as a circa 3.0 Ga accretionary complex. Geochemical data supports a supra-subduction zone back-arc ophiolitic zone setting. The felsic mylonites are shown to be high-Si adakites derived from partial melting of the back-arc basalts in response to ridge subduction, and intruded along thrust faults at 3.015–2.990 Ga (Polat et al., 2016a). Polat et al. (2016a) compare the rocks, structures, and compositions of the igneous rocks to younger subduction accretion complex including the Chugach terrane of Alaska, and the Altaids, and document remarkable similarities between the two. Polat et al. (2016a) note that the possible thicker and more buoyant oceanic crust in the Archean (~20 km, as opposed to the modern ~7; Sleep and Windley, 1982) may have led to more offscraping of the upper oceanic crust, as preserved in the Tartoq accretionary complex. Ridge subduction, in SW Greenland at 3.0 Ga was very similar to that of the Eocene documented in southern Alaska (Kusky et al., 2003), and led to partial melting of the subducted accretionary complex, leading to the intrusion of the high-Si adakites in both cases.

The oceanic rock assemblages in the OPS at Isua and Tartoq, intruded by upper-mid crustal TTG and deformed with them are remarkably similar to intra-oceanic arc and accretionary prism systems, with the OPS reflecting the later transport of the (preserved) underlying oceanic crust, overlain by deep-water cherts, then an increasingly proximal clastic sequence reflect the subducting oceanic lithosphere approaching an eroding (and deforming, perhaps colliding) arc system. Notably, also in the Isua belt, Furnes et al., (2007,2020) have identified a section of the greenstone sequence that contains most of the elements of an ophiolite sequence, further supporting this conclusion. Szilas et al. (2013) and Polat et al. (2016a) also interpreted the mafic-ultramafic sections of the Tartoq greenstone belt to be ophiolitic, caught in an accretionary wedge, and intruded by arc-related TTG magmas. The similarities with modern intraoceanic arc systems and accretionary orogens are remarkable, suggesting further that early crustal growth at circa 3.8 Ga included sea-floor spreading and the formation of oceanic lithosphere, the lateral movement of rigid oceanic plates, their subduction to form arcs, which later collided to form an accretionary orogen. The later, Mesoarchean to Neoarchean events are reflected in the six different amalgamated immature and Andean-style arcs in SW Greenland recognized by Windley and Garde (2009).

The numerous field-based structural and metamorphic studies in SW Greenland have generally concluded that the craton formed by a series of accretion of "terranes" or arc segments with intervening accretionary wedges with trapped OPS and ophiolitic fragments (Friend et al., 1987, 1988, 1996; Friend and Nutman, 2001, Friend and Nutman, 2005a; Nutman et al., 2007; Kolb et al., 2012; Dziggel et al., 2014; Polat et al., 2015), with different collisions or convergent events with Eoarchean, Mesoarchean, and Neoarchean ages. The anorthositic complexes are only present in the Mesoarchean terranes, and were assembled in Neoarchean collisions (Nutman et al., 2004, 2007; Friend and Nutman, 2005a; Steenfelt et al., 2005; Polat et al., 2008, Polat et al., 2009; Hoffmann et al., 2012; Szilas et al., 2013), with accompanying magmatism and metamorphism (Friend et al., 1988; Windley and Garde, 2009; Kolb et al., 2012; Dziggel et al., 2014; Nutman et al., 2020). Windley and Garde (2009) proposed a model in which six fault-bounded tectonic wedges show high crustal levels amphibolite facies rocks in the south, and deeper granulite facies assemblages in the north. These various blocks were interpreted by Windley and Garde (2009) as immature oceanic and more-evolved Andean arcs accreted in a series of prolonged tectonothermal events. Thus, SW Greenland contains vestiges of the oldest oceans and IOAS on Earth, that were amalgamated to form more coherent Andean-style archipelagoes, in early stages of the formation of our present continents. All structures, rock types, and relationships in this Eoarchean – Neoarchean terrane are remarkably similar to younger accretionary orogens that are extant around the Pacific in the present plate mosaic (Fig. 19), and not easily explained by other non-uniformitarian models, such as the "sagduction", "heat pipe" and other models (e.g., Webb et al., 2020) with no basis on Earth for comparison, and that do not adequately incorporate the many decades of detailed field, structural, geochemical, and metamorphic work of the pioneers who mapped southeastern Greenland. Ironically, the "heat pipe" concept was, as far as we know, first used by Wegmann (1953) to describe the enhanced metamorphic grades in the dome-like root zones of the Lepontine Alps, suggesting higher heat flow was focused in the vertical sheath-fold tube-like root of the Maggia nappe, which has many structural, lithological, metamorphic and other similarities to the Isua dome structure.

5.2. Nulliak Belt, Saglek Block, Labrador

The Saglek Block of northern Labrador, Canada (Bridgwater and Collerson, 1976; Bridgwater et al., 1990), has been suggested to contain the Earth's oldest known volcano-sedimentary rocks within the Nulliak greenstone belt (Fig. 19), with field-based relationships and geochronological constraints showing that the greenstone belt is intruded by up

to seven generations of tonalitic-trondhjemitic-granodioritic plutons called the Iqaluk–Uivak Gneiss series with ages including 3902 +/− 25 Ma, 3892 +/− 33 Ma, and 3897 +/− 33 Ma (Komiya et al., 2017). However, the rocks in the Saglek block are highly deformed, laterally discontinuous, and some conflicting geochronologic studies suggest that some of the units in the Nulliak belt could be Meoarchean or even Neoarchean (Bridgwater and Schiotte, 1991; Ryan and Martineau, 2012; Whitehouse et al., 2019), a debate which requires further detailed field and geochronologic studies.

The Saglek block forms the westernmost part of the North Atlantic craton, and is correlated with the Akulleq terrane in SW Greenland (Fig. 19). Eoarchean volcano-sedimentary rocks of the Nulliak belt in the Saglek block are included within and tectonically interleaved with these intrusive orthogneisses, showing that they are the oldest-known volcano-sedimentary group known on Earth (Komiya et al., 2015). The Eoarchean rocks are also intruded by the Paleoarchean Saglek dikes (equivalent to the Ameralik dikes in the Itsaq gneiss of SW Greenland, see above), granitic intrusions, and Proterozoic mafic dikes. The Nulliak greenstone belt includes in ascending order a recognizable series of strongly deformed and metamorphosed (amphibolite to granulite facies) ultramafic rocks, mafic volcanic/plutonic rocks, overlain by banded iron formation, chert, carbonates, pelitic rocks, and psammites, forming a classic OPS sequence (Komiya et al., 2015). Detailed structural mapping by Komiya et al. (2015) shows clearly that this OPS sequence is distributed in a series of duplex structures, with floor, roof, and linking thrusts, repeated numerous times (Fig. 22), and there is no discernable difference between the rock types, structures, and intrusive relationships between the world's oldest volcano-sedimentary sequence, and modern accretionary wedges with OPS and the upper part of the subducting oceanic plate scraped off from the subducting plate and accreted to the overriding plate in the modern day circum-Pacific (Komiya et al., 2015; Wakita and Metcalfe, 2005).

The ultramafic rocks in the Nulliak belt have tectonic boundaries at their base where exposed, form tectonic slivers up to 170 m thick, are massive and banded, and include serpentinized harzburgite (with large needles of olivine), CPX-rich peridotite (lherzolite?), wehrlite, and dunite and pyroxenite intrusions (Komiya et al., 2015). On Big Island (Fig. 22) some ultramafic blocks occur within a highly-deformed metapelitic matrix, and resemble younger mélanges. Carbonates include carbonate minerals as well as amphibole, quartz, magnetite and sulfides (Komiya et al., 2015). The first type is associated with BIF, pelite and chert and is up to 10 m thick on Big Island (Fig. 22), whereas a second type is associated with the mafic and ultramafic rocks and is interpreted to be metasomatic, formed by carbonization of the greenstones in the presence of a CO_2 rich fluid, which characterized the Eoarchean atmosphere, oceans, and hydrothermal fluids (e.g., Shibuya et al., 2007). Some have wavy stromatolite-like structures and contain chert nodules and pelitic layers and are probably sedimentary deposits, but others appear to be pseudomorphed ultramafic rocks. Chert includes a pure white or green variety, and white-to -gray variety with dark green nodules. BIF includes chemical sedimentary and metasomatic types. Most of the true sedimentary BIF's are <5 m thick but reach up to 32 m, and show well-developed black and white bands. The black bands consist of magnetite, quartz, OPX, CPX, and minor cummingtonite, hornblende, pyrite and apatite (Komiya et al., 2015). The white bands consist mostly of quartz. Some BIF and carbonate layers are metasomatic in origin, and display branching map patterns that duplicate different units, and thus mark shear zones, much as BIF units in the Belingwe Zimbabwe greenstone belt have been shown to do (Kusky and Winsky, 1995; Hoffman and Kusky, 2004). In between these faults, the basic lithostratigraphy from ultramafic rocks, to mafic, to chert/BIF, carbonates, then pelites to clastic sandstones and conglomerates is repeated numerous times, in various locations around St Johns Harbor that were mapped in detail by Komiya et al. (2015). The whole area is thus interpreted to contain OPS, with an ophiolitic-like basement, repeated numerous times within duplex structures that are part of an Eoarchean

accretionary wedge complex (Komiya et al., 2015, 2017). Metapelites include true metapelites, containing garnet, biotite, quartz, zircon, plagioclase, and graphite, and metasomatic pelitic fringes (with plagioclase and amphibole) in migmatitic rocks adjacent to ultramafic layers. Conglomerates have clasts of quartzite (up to boulder size).

Komiya et al. (2015) suggested a model for the origin of the Nulliak greenstone belt involving shallow-level melting of a subducted slab perhaps during ridge subduction, with carbonates deposited near the elevated ridge, and BIF deposited as exhalative deposits further from the ridge, and some pelitic rocks deposited directly on the oceanic crust, because of a very short distance between the ridge and trench (consistent with small plates in the Eoarchean). As the ridge was subducted, the existing accretionary wedge was uplifted (e.g., Kusky et al., 1997a,b), shedding clastic sediments into the trench, and incorporating slices of the oceanic lithosphere into the accretionary wedge, similar to the Resurrection ophiolite in Alaska (Kusky and Young, 1999). The magmatic history of the Nulliak Belt is similar to the Pilbara, in that the orthogneisses in the Saglek block include multiple generations with multiple origins (e.g., Shimojo et al., 2013, 2016), over a 200 Ma period from 3.902 to ~3.7 Ga (Collerson, 1983; Shimojo et al., 2013, 2016) but with the early TTG series intruded in a short interval of ~10 Ma between 3902 and 3892 (Komiya et al., 2017). The longer duration of ~200 Ma is similar to that in the Japanese arc (Harayama et al., 2000) and other arc complexes, including the Famatinian of the southern Andes (Ducea et al., 2010), whereas the short-duration pulse of TTG intrusion shortly after formation of the volcano-sedimentary sequence is characteristic of intra-oceanic arc systems, intruded by melts derived from either the partially melted subducting slab, or from partial melting of the asthenospheric wedge.

The field, petrographic, structural and geochronological data presented by Komiya et al. (2015, 2017) is positive evidence for the lateral translation of an oceanic plate away from a ridge at a plate accretion boundary at ~3.9 Ga, and for the progressive accumulation of pelagic oceanic sediments, and of the final deposition of clastic, continental- or arc-derived clastic sediments (Kusky et al., 2013). The whole package was partly off-scraped by thrusting in the trench and added to an overriding arc or continental plate at a paleo-convergent plate boundary. Well-documented examples have now been recorded in accretionary orogenic belts of all ages, back to the oldest volcano-sedimentary sequences preserved on Earth at Nulliak, Isua, and the Pilbara, and thus OPS provides first-order evidence of the operation of plate tectonics throughout Earth history.

5.3. Nuvvuagittuq in Québec, Canada

The Eoarchean Nuvvuagittuq belt of the Hudson Bay terrane of the Superior craton of northeastern Quebec, Canada (Figs. 19, 23) is one of at least a dozen km-scale supracrustal enclaves in tonalite-trondhjemite-granodiorite-granite-monzonite gneisses that dominate the region. The belt includes ultramafic and gabbroic units, amphibolites, basaltic pillow lavas, bedded cherts, and banded iron formations (Cates and Mojzsis, 2007; O'Neil et al., 2011, 2012; Mloszewaka et al., 2013) intruded by circa 3.66 Ga tonalites (David et al., 2009), and felsic intrusive with ages near ~3.8 Ga (O'Neil et al., 2012). The preserved part of the Nuvvuagittuq belt is only ~10 km², forming a south-plunging, north-closing synform, engulfed by a sea of younger (circa 2.7 Ga) TTG intrusives (Fig. 24). The refolded western limb of the larger fold structure preserves a tight- to isoclinally-folded, steeply E-plunging synform, revealing that the belt is multiply deformed, and also preserves two metamorphic events at ~3.6 and 2.7 Ga (Cates and Mojzsis, 2009).

The main mafic unit (Ujaraaluk Unit), has a lower section dominated by heterogeneous basalts to basaltic andesites. Since they are metamorphosed, these rocks now consist of cummingtonite-biotite-plagioclase-garnet, and chlorite-epidote-quartz-plagioclase-actinolite schists (Guitreau et al., 2013). The banded iron formation has seawater chemical signatures and heavy Fe isotopes suggestive of

precipitation of Fe from hydrothermal fluids, with positive Eu anomalies in jasper and carbonate BIF consistent with hydrothermal sea-floor activity. The Ujaraaluk Unit is interpreted to represent hydrothermally altered mafic volcanic crust transitional in composition between tholeiitic, boninitic and calc-alkaline magmas, that formed in a submarine volcanic setting (O'Neil et al., 2011). The cherts contain micro-scale haematite tubes and filaments that resemble those of filamentous microbes in modern seafloor hydrothermal vents. Dodd et al. (2017) proposed that these deposits represent an oxidized biomass formed in a submarine, hydrothermal, mid-oceanic vent at >3.77 Ga.

5.4. Kaapvaal Craton: Earth's earliest continent

One of the largest and oldest cratons on Earth, meaning preserving extensive areas of >3.0 Ga crust that has not been significantly changed since then is the circa 4.0–3.0 Ga Kaapvaal craton of southern Africa (Figs. 19, 24), with ages largely overlapping with the Pilbara craton. The Archean history of the Kaapvaal craton saw its most important events in two major periods, the first from 3.7–3.1 Ga, and the second from about 3.1–2.6 Ga (de Wit, 1982; de Wit et al., 1982, 1987, 1992, 2011, 2018; Kröner and Hofmann, 2019). The first main period of the Kaapvaal's evolution witnessed large-scale extraction of melts from the mantle by partial melting, much as occurs at mid ocean ridges and intra-oceanic arcs in the modern plate tectonic regime, although it has been suggested that this occurred in a setting with generally shallower water than today, where the ocean ridge valleys are on average about 2.7 km below sea level (de Wit et al., 1982, 1987, 1992, 2011; de Wit and Furnes, 2016). The 3.48–3.49 Ga ophiolitic relicts contain signatures of sea-floor metamorphism, alteration, hydrations, and oxygen isotope profiles as modern submarine hydrothermal systems along modern ridges (de Wit and Hart, 1993; de Wit et al., 2018). Early oceanic lithosphere may in this case have resembled modern oceanic plateaux with ridges in character, with shallow depths of volcanism, with Iceland being a possible modern analog (Kusky and Kidd, 1992). Some of these ancient relicts of oceanic lithosphere are preserved in the well-studied Barberton and Pietersburg greenstone belts. The second main period of evolution of the Kaapvaal was from 3.1 Ga to 2.6 Ga, and was characterized mainly by subduction-related magmatism and accretion at convergent boundaries (including in accretionary orogens, Humbert et al., 2019), as well as other continental margin and intra-continental processes, including the oldest well-preserved rift (the Pongola, Burke et al., 1985a). Some of the sedimentary sequences in the Limpopo Province that separates the Kaapvaal and Zimbabwe cratons have also been interpreted to be ancient passive margins formed in this interval, but this has recently been challenged (Yin et al., 2020).

The geodynamic setting of the greenstone belts of the Kaapvaal Craton, and their relationship to surrounding granitoids, has been debated for decades (see papers in Kröner and Hofmann, 2019). Most of the field and structural geologists who have worked in the Kaapvaal and specifically the Barberton region, have proposed different accretionary tectonic models for the region. However, more recently some numerical and other models have interpreted parts of the Kaapvaal (esp. Barberton) as "just another drip", in a sagduction setting (e.g., Johnson et al., 2014), where the greenstone sequences were purportedly erupted forming a 45 km thick pile over the "sialic" basement, then sunk between rising granitoid plutons, forming a dome and keel structure as shown in Fig. 25. Since the argument is very similar to that in the Pilbara, we examine the geological evidence.

The Kaapvaal craton covers an area of about 1.2×10^6 km^2, including the high-grade Limpopo Province which separates the Kaapvaal from the Zimbabwe craton to the north (Fig. 24). It is bounded to the south and west by the Proterozoic Namaqua-Natal orogen and Damara Province, and on the east by the Lebombo monocline of Jurassic volcanic rocks, related to Gondwana break-up, and rocks of the Mozambique orogen. It is well-established that the Kaapvaal craton has a very thick lithospheric root reaching about 350 km, and thus is characterized by low heat-flow, seismicity, and an abundance of dia-mondiferous kimberlites that have yielded a wealth of data on the deep structure of the sub-continental lithospheric mantle (SCLM) forming the craton's root (e.g., Boyd et al., 1985; Richardson et al., 2001; Begg et al., 2009; Shirey and Richardson, 2011; Griffin et al., 2003; Aulbach and Viljoen, 2015; Ortiz et al., 2019; Celli et al., 2020).

The craton can be divided into a number of different blocks or sub-domains with different characteristics. Depending on which characteristics are used, the divisions of the craton are different. The simplest division, based largely on chronostratigraphy (Fig. 24, after Kröner and Hofmann, 2019, after Frimmel, 2014) divides the craton into four blocks, the Kimberly in the west, Swaziland in the south, Witwatersrand in the center, and Pietersburg in the north. In this classification the Limpopo orogen is regarded as a younger orogen bounding the craton and separating it from the Zimbabwe craton to the north. In a more detailed division, de Wit et al. (1992) divide the craton into 12 different "terrains" (distinctive from terranes, as to not imply they are far-travelled allochthonous units) or subdomains, based on different age, structural, and geological features. de Wit et al. (1992) show that the oldest subdomains occur in the eastern part of the craton (Frimmel, 2014), and include the Ancient Gneiss Complex of Swaziland, and the southern part of the Barberton terrain or greenstone belt, which de Wit (1982, 1987, 1992, 1997, 2004, 2018) have convincingly shown consists of a number of oceanic back-arc type circa 3.5 Ga ophiolites (de Wit et al., 2018), emplaced onto contemporaneous arc-type crust between 3.46 and 3.43 Ga (Fig. 25b). A second period of major thrusting occurred at 3.3–3.2 Ga affected both the northern and southern Barberton terrains, emplacing additional 3.3–3.2 Ga ophiolite fragments, which were then cut by strike-slip shear zones, then cut by granite sheets of the Mpuluzi suite and Nelspruit granite between 3.15 and 3.07 Ga, showing that this segment of early continental crust stabilized by about 3.1 Ga. This was interpreted by de Wit et al. (1992) to represent the first pre-served emergence of a significant area of continental crust, covering an area of about a half-million (5×10^5) km^2. The lithospheric mantle beneath this oldest continent is sampled by mantle xenoliths, and shown to consist of metamorphosed peridotites and basalts, some now eclogites, consistent with subduction of oceanic lithosphere, now preserved as imbricated slabs forming the SCLM (e.g., Kusky, 1993; Richardson et al., 2001; Shirey and Richardson, 2011). The upper crust, consists largely of TTG plutons, many intruding the slightly older imbricated ocean crust (de Wit et al., 1992, 2017).

South of the Barberton greenstone belt, rocks in the Natal terrain (southern part of the Swaziland block) include 3.4–3.2 Ga greenstones that include boninites and komatiites, but show chemical evidence for interaction with older crust (de Wit et al., 1992). de Wit et al. (1992) first proposed that the greenstones and TTG terranes of the Swaziland block (his South Barberton, Natal, and Southern terrains) are a fragment of Earth's first continent, formed first by extraction of oceanic crust from the mantle, remelting in imbricated slabs and arc settings, then stabilized by a younger generation of plutonism by 3.3 or 3.1 Ga, and that the thick lithospheric root had already formed by that time, helping to stabilize the early continent (Richardson et al., 1984; Kusky, 1993).

de Wit et al. (1992) proposed that the ancient oceanic lithosphere preserved within the Barberton and other 3.5–3.3 Ga greenstone belts of the Kaapvaal craton became pervasively hydrated with a density as low as 2.67 g/cm^2, making it difficult to subduct. They suggested instead that this early oceanic crust became stacked as buoyant hydrated slabs, that partially melted to yield TTG magmas when the imbricated, accretionary-prism like wedges reached thicknesses of >20 km, forming the typical granite-greenstone terrane rock types and relationships. An important difference in their model to younger accretionary wedges, is that in the de Wit et al. (1992) model, the oceanic (and any thin OPS) slabs are stacked with the younger ones over the older ones because of their low density, in effect forming an obduction pile or perhaps giant antiformal stacks of accreted oceanic lithosphere intruded by TTG melts derived from partial melting of the mafic crust at depth (Fig. 25b). These

relationships are similar to those at Marble Bar and North Pole in the Pilbara, described above, except at North Pole in the Pilbara, older-younger thrusting is well documented. Following this early period of formation of the first continent through generation and partial melting of oceanic lithosphere, followed by arc magmatism, the proto-Kaapvaal craton began to accumulate thick sedimentary basin assemblages, marking stabilization of the craton with a thick root. These assemblages include the circa 3.1–2.9 Ga Pongola rift sequence (the world's oldest well-preserved rift; Burke et al., 1985a), the Witwatersrand Basin (a poly-phase retro-arc and collisional foreland basin, Burke et al., 1986; Frimmel, 2019), the Ventersdorp intercontinental rift basins, and the Transvaal carbonate platform/ramp sequence by the end of the Archean.

In their model for the formation of the first large continent, de Wit et al. (1992) divide the late Archean craton (Swaziland and Witwatersrand blocks) development into several stages, the first "mid-Archean shield development" described above, and a later 3.1–2.6 Ga 'late Archean craton development' stage. In this later stage, de Wit et al. (1992) recognize a circa 2.9–2.7 Ga *primary orogenic collage* in which the amalgamated greenstones and TTG terranes were progressively thrust northwards forming an accretionary orogen along the northern margin of the shield, with subduction towards the south and progressive northwards growth of the continent. This northward growth formed orogenic mountains that shed gold-bearing detritus to the south, to be deposited in complex intermountain retro-wedge foreland basins, analogous to some of the flysch basins in Alaska, as opposed to basins like the Witwatersrand being a two-phase retro-arc and collisional foreland basin, as suggested by Burke et al. (1986). The craton next experienced *collisional orogeny with extrusion, and late orogenic collapse*, as documented in late (2.68 Ga) southward thrusting along the southern edge of the Limpopo belt, and exhuming the high-pressure metamorphic rocks in the central zone of the Limpopo, and emplacing granulite-facies klippen up to 50 km south of the main trace of the bounding faults. de Wit et al. (1992) relate the Ventersdorp extension and volcanism to late-orogenic collapse, whereas Burke et al. (1986) relate it to extension from the supposed Kaapvaal – Zimbabwe collision, and Humbert et al. (2019) relate it to rifting of the continent, removal of the western segment, then thermal subsidence in the Transvaal sequence recording the rifting to drifting transition and the first Wilson cycle.

To the north in the Pietersburg block (Figs. 24), the 3.46–3.2 Ga greenstones, intruded by 3.46–3.17 and 3.12–2.85 TTG gneisses, form part of a well-documented accretionary orogen containing ophiolites in the Pietersburg and Giyani belts (Brandl and de Wit, 1997; Zeh and Gerdes, 2012; Laurent et al., 2019). This orogen mantled the north margin of the craton, and grew progressively to the north in a long-lived Paleoarchean accretionary orogen, resulting in significant growth of the Kaapvaal craton before stabilization in the Mesoarchean. The greenstones consist largely of metabasalts and metakomatiites, with rare 2.95–2.84 felsic volcanics intercalated with BIF, chert, and siliciclastics that were deposited at 3.05–2.92 Ga in the Murchison belt, 2.88–2.80 in the Pietersburg belt, and 2.76–2.71 in the Rhenosterkoppies belt and southern margin of the Limpopo Province (Laurent et al., 2019). The greenstones are all affected by Mesoarchean N-S contraction, greenschist-amphibolite facies metamorphism, and in the Murchison Belt, intruded by the 2.97–2.96 Ga Rooiwater Complex, formed by fractionation of mantle-derived melts (Laurent et al., 2019). The overall history of the Pietersburg greenstone belt is thus one of the mafic-ultramafic simatic basement in an oceanic environment from 3.46–> 2.95 Ga, followed by deposition of overlying subaerial molasse in a foreland basin at <2.88 Ga, with major N-S compression and metamorphism at 2.87–2.84 Ga deforming the belt into imbricate thrust-stacks (Zeh and Gerdes, 2012). Similarly, the Giyani greenstone belt consist of a lower dominantly mafic volcanic/plutonic sequence with minor siliciclastics, that experienced NW-vergent thrusting with greenschist to amphibolite facies metamorphism at 2.87–2.80 Ga. The Rhenosterkoppies greenstone belt forms an up to 500 m thick stack of amphibolite and BIF intercalated with ultramafic schist, serpentinite,

quartzose layers, calc-silicates, and Ky-quartz schists (Brandl et al., 2006). The belt is structurally complex, with amphibolite-facies D1 isoclinal folds, D2 north-vergent greenschist facies thrusts and associated 2.76–2.71 Ga shear zones, and D3 large-scale open folds (Passeraub et al., 1999).

The Paleoarchean geodynamic evolution of the Pietersburg block between 3.46 and 3.18 Ga is associated with the formation of minor TTG suites and greenstones, particularly in the Pietersburg and Giyani greenstone belts, which may have formed a coherent microterrane. Chondritic Hf isotope compositions suggest that this terrane was primitive and did not involve older crust (Laurent and Zeh, 2015), and the dominantly mafic and associated TTG suites led Laurent and Zeh (2015) to suggest that this may have been a circa 30 km thick oceanic plateau, or an immature oceanic arc system. From 3.15–2.98 Ga, subduction was initiated beneath the proto-Kaapvaal craton, forming ENE-striking structures, and a progressive northward migration of metamorphism and sediment deposition associated with N-vergent thrusts (Kramers et al., 2014). TTG suites were emplaced from 3.12 to 3.02 Ga, with some being derived from melting at >45 km (Laurent and Zeh, 2015; Zeh et al., 2013), probably in a continental margin arc setting, and shedding detritus to the north in a fore-arc or intra-arc system (Zeh et al., 2013). From 2.97–2.84 Ga, the Pietersburg block witnessed the formation and accretion of an oceanic arc and back-arc system (Fig. 24) located north of the Rooiwater Complex, forming additional TTG plutons formed through high-pressure melting (>50 km) (Jaguin et al., 2012), which were intensely deformed at 2.95–2.92 Ga in a N-S contractional event (Zeh et al., 2013), and progressive southward movement of the arc axis until it collided with the proto-Kaapvaal craton at circa 2.92, closing the intervening back arc basin containing the Rooiwater and Rubbervale complexes, and thrusting the Pietersburg greenstone belt southwards over the proto-Kaapvaal craton (Fig. 24). Subduction then continued to the south, accreting micro-terranes to the growing accretionary orogen (Kramers et al., 2014), with associated with metamorphism, north-directed thrusting, sedimentation, and minor volcanism (Zeh and Gerdes, 2012). This phase was associated with intrusion of voluminous TTG plutons in the accreted fragments from 2.95–2.84 Ga.

Crustal re-working of the Pietersburg block in an Andean-type arc dominated the period from 2.84–2.73 Ga, forming biotite-muscovite granites, (Laurent and Zeh, 2015), and a cessation of TTG magmatism. Crustal thickening caused high-T metamorphism and partial melting, but was still associated with N-S contractional structures (Passeraub et al., 1999). Isotopic data (Laurent et al., 2014a, 2014b, 2014c) suggests that the magmas in this stage had a contribution from partially melted subducted sediments. The final stage of cratonization for the Pietersburg block was at 2.73–2.65 Ga, involving further re-working during continent-continent collision. Rocks in the northernmost part of the Pietersburg block were buried to >30 km and subject to granulite facies metamorphism at 2.71 Ga, in association with N-directed thrusting, and exhumation of granulite facies rocks on a series of S-directed back-thrusts (Kramers et al., 2014). This event is generally attributed to the 2.71–2.67 Ga collision of the Pietersburg block with an exotic terrane in the Central Zone of the Limpopo Province (Kramers et al., 2011; Laurent et al., 2019), which may have included some of the Paleoarchean rocks such as the 3.31–3.28 Ga Sand River TTG gneisses and the Beit Bridge Complex sedimentary sequence, which contains 3.95–3.18 Ga detrital zircons (Laurent et al., 2019). The collision is postulated to be associated with lithospheric delamination, causing upwelling of the hot asthenosphere, and formation of the Banderlierkop granulites (Laurent et al., 2014a, 2019). This model is consistent with the early granulite-facies deformation at 2.72–2.69 Ga in the Limpopo Province (Van Reenen et al., 2019), but the causes of two vastly different (circa 2.72 Limpopo orogeny, and 2.0 Ga events) episodes of deformation and high-grade metamorphism in the Limpopo Province have led to many controversial models for its origin, including a N-S. collision between the Kaapvaal and Zimbabwe cratons (Light, 1982, Burke et al., 1985b, 1986), collision with the Pietersburg accretionary orogen on the

northern margin of the amalgamated Kaapvaal craton (Laurent et al., 2019), or some combination including late intracontinental emplacement of hot nappes by diapiric processes (Van Reenen et al., 2019). In a starkly different interpretation, Yin et al. (2020) suggested that the Central Zone of the Limpopo Province is an allochthonous terrane, thrust 600 km from the east over the Zimbabwe and Kaapvaal cratons at circa 2.0 Ga, and later folded into its present synformal geometry by N-S compression.

In summary, the early models for the growth of the first continent in the Kaapvaal craton by de Wit et al. (1992, 2018), in which the first continent grew and stabilized over a period of 1 billion years, the first stage starting at 3.7 Ga and continuing to 3.1 Ga, with large-scale intra-oceanic thrusting of serpentinized slabs of thin (?) oceanic crust and lithosphere, with partially melted when the thrust stacks became thick enough generating the TTG suite, and differentiating the early crust by two melting events. This primitive form of accretionary thrust-stacking would have emerged when the ocean spreading centers first became subaqueous, which de Wit et al. (1992) suggest happened by 4.0 Ga. This style of tectonic thrust stacking of oceanic material formed at spreading centers may be analogous in some ways to the accretion of oceanic plateaus as they collide with oceanic arcs, such as the ongoing Ontong Java/Solomon Islands collision. It is interesting that the Ontong Java plateau, like most cratons, has a fairly thick lithospheric keel and kimberlite-like (alnoite) intrusions contain garnet lherzolite xenoliths, derived from underlying depleted oceanic slabs from depths of ~135 km (Nixon and Neal, 1987). From 3.1–2.6 Ga, the core of the craton in the Swaziland and Witwatersrand blocks was dominated by continental margin arc magmatic processes, and the gradual emergence and stability of intra-continental processes ranging from the Pongola rift at 3.1 Ga (Luskin et al., 2019), to the Neoarchean Witwatersrand (Frimmel, 2019), Ventersdorp, and Transvaal (Burke et al., 1985a, 1985b, 1986; Humbert et al., 2019) basins. At the same time, a large Pacific-style accretionary orogen was growing in the Pietersburg block on the northern margin of the proto-Kaapvaal craton.

In the Pietersburg block, the Paleoarchean interval from 3.46–3.18 Ga was marked by formation of microterranes consisting of island arc and oceanic plateau rocks, then in the Meso-Neoarchean the 3.15–2.65 Ga the block grew above a major south-dipping subduction system as an accretionary orogen (Laurent et al., 2019). This was terminated, and the Pietersburg block of the craton stabilized at 2.73–2.65 Ga through a continent/continent collision with a different block to the north, possibly preserved in the Central Zone of the Limpopo Province (Laurent et al., 2019). This collision is marked by intrusion of hornblende-biotite-(Cpx) sanukitoids, and biotite-epidote granites derived by melting of enriched sub-continental lithospheric mantle, with crustal assimilation (Laurent et al., 2019).

Earth's oldest continents were thus born and raised.

In the early Archean, as shown by the Pilbara, and examples from Isua and Nuvvuagittuq described elsewhere (Windley et al., 2021), it appears that the proto-continental crusts were not exceptionally thick, as in the modern Andes, but somewhere between modern oceanic and average continental margin arcs. All of Earth's well-preserved Eoarchean terranes show similar characteristics (Fig. 26), of being formed from accreted oceanic material, similar to the Klamaths, being deformed during progressive intrusive events, causing the early sheet-like, structurally controlled intrusions to become folded into domes. Similar domes are found in orogens of all ages, throughout Earth history, and reflect a normal stage of orogenesis, in specific parts of orogens, and do not reflect any secular change in planetary behavior.

5.5. Early continents formed in accretionary orogens. Synthesis of the global geological data set

The detailed analysis presented above has shown a consistent pattern in the development of Earth's oldest continents, first growing by accretion of oceanic crust and overlying OPS, followed by continued intrusion by arc-related magmas, deformation, and thickening until the continents gradually became thick and large enough to emerge, as shown especially well by the Kaapvaal and Pilbara examples. However, the geological record is incomplete, and likely shows a preservational bias (Morgan, 1985; Kusky et al., 2018; Harrison, 2020; Korenaga, 2021). What is preserved shows remnants of small, not overly-thick proto-continents, with structures and rocks derived from accretion from the early oceans, intruded by magmas derived by subduction from the early subduction zones, to make the early continents. The preserved rock record also shows, that what is preserved, is readily interpreted in terms of some form of plate tectonics, perhaps operating with slightly higher mantle temperatures, different plate sizes and thicknesses, a different biota and atmospheric/ocean chemistry, but still plate tectonics. Based on the scale- the size of the preserved fragments of the Eo-Paleoarchean terranes, the scientific community must use the geological record (and associated geochemical, isotopic, geochronological, etc., records) to assess the question of the operation and style of tectonics in early Earth history. Many of the proposed tests in recent literature call for "proof" of a globally linked network of plate boundaries, or claim that even excellent documentation of subduction does not mean plate tectonics, but the tests proposed are untestable. With early remnants of Earth's crust only measuring 200 × 200 km as for Pilbara, and only 10 km^2 for Nuvvuagittuq, there is no way to test a globally linked plate network. The rock record bears the imprints of the processes from which they formed.

While the record may be incomplete, and we only see a small part of what was there, there is apparently no record of large continents emerging until near the end of the Archean locally around 3.1 Ga, and more extensively at 2.7–2.5 Ga (Windley et al., 2021). This time represents the time of the first well-preserved regional-scale passive margin sequences, trans-continental mafic dike swarms like the 2772 Ma Black Range dolerites of the Pilbara described above. Thus, as described in Windley et al. (2021), we offer that accretionary-orogen style plate tectonics (Fig. 27), with lateral motion of plates above a convecting mantle with recycling from subduction, formed the first continents. When the continents grew large enough, they could rift on a continental-scale, then collide, starting Wilson-Cycle style tectonics (operating together with accretionary tectonics), and the supercontinent cycle. Throughout the preserved geological record, every geological terrain can be explained using the current mode of plate tectonics, without a need for alternative Earth models, but with a gradual change from a planet dominated by juvenile accretionary orogens with multiple small oceans, to one where continents and supercontinents emerged to co-exist with the still-ongoing accretionary orogen mode. As the Earth gradually cools, the prescient models of stagnant lids and a gradually slowing, cooling Earth will come into effect, as the planet dies tectonically over the next 2 billion years (Sleep, 2000; Kusky et al., 2018; Harrison, 2020; Windley et al., 2021; Korenaga, 2021).

6. Conclusions

Archean dome-and-basin provinces exemplified by Eastern Pilbara are characterized by a complex series of deformation events related to the early accretion of oceanic materials including ophiorags (ophiolitic fragments), dominated by basalt/chert and rare gabbro with ultramafics, and clastic sedimentary rocks. These were intruded by suites of dioritic to TTG magmas in intraoceanic arc-type settings. They typically form sheet-like bodies that are folded with the accreted tectonostratigraphy, then were repeatedly deformed and intruded by additional magmas during arc-arc accretion events, until they formed parts of Andean margin complexes, with folded sheets contorted into domes with intervening basins of roof-pendant material. In these settings, the accretionary orogens were intruded again by pulses of intermediate plutons, identical to the TTGD suite exposed in the deep levels of Phanerozoic arcs, and intruded once again by voluminous TTG - granitoid magmas during slab failure events during and after collisions.

These plutons are typically steep-walled, some have zoned or nested structures with contacts parallel to roof pendants that were strongly deformed and metamorphosed during various accretion events within a mid-arc crust. Deep cumulates and residues are rarely preserved, but are known in a few arcs and Archean dome-and-basin terranes.

Late stages of arc evolution see the most massive volumes of plutonism with melts generated during slab-failure intruding an upper plate containing an arc, and a lower plate, if it rebounds after slab break-off. Late stage plutons are typically mixtures of melted mantle and crustal material, which evolve to more K-rich varieties with time, have cross-cutting relationships with their wall rocks, and are often associated with extension, which in turn may be caused by slab break-off, slab roll-back, or extensional collapse of orogens after significant crustal thickening. Many of these plutons intrude the cores of older plutons causing them to dome upward forming the nested plutons with more mafic TTG series on the outside, and more K-rich varieties in the cores of the plutons. Since nested plutons that show a similar progression from mafic through TTG magmas to K-rich granites are common in Precambrian, Paleozoic, Mesozoic, and Cenozoic orogens, their age in the Eastern Pilbara craton cannot be used to mark the onset of global plate tectonics at 3.0–3.2 Ga as has recently been suggested (Hawkesworth et al., 2020). The best example is the late Cretaceous hemispherical subduction polarity flip recorded in the western Americas, and resultant slab-failure magmatic event related to the accretion of the Cordilleran ribbon continent against the Americas at circa 100 Ma, with nested plutons such as the Sierra Crest suite that formed along the entire >15,000 km length of the North and South American Cordillera (Hildebrand and Whalen, 2014a, 2014b). Thus, calls that nested plutons in Archean cratons can be used to indicate the start of modern-style plate tectonics on Earth (Hawkesworth et al., 2020) are misguided.

The mid-crust in Andean arcs is dominated by zones complexly folded plutons intruded by TTG domal plutons that cut and are deformed with previously accreted volcano-sedimentary sequences (Saleeby, 1983; Ducea, 2015a, b), often during deformation, with concomitant downward flow of their host sequences (Fig. 3), so producing identical outcrop patterns as those in the Paleo-Mesoarchean Eastern Pilbara (and similar) granite greenstone terranes (Fig. 5). The dome-and-basin character is completed in cases of slab break-off which forms suites of distinctive TTG magmatism, deformed further in late stages of collision. The duration of different, even un-related stages of magmatic activity in Andean arcs can be hundreds of millions of years as in the Pampean (Cambrian) and Famatinian (Ordovician) (Otamendi et al., 2012) arcs in the Central and Southern Andes, which were later affected by Permian to Mesozoic intrusives of the Peruvian coastal batholith (Demouy et al., 2012). These arcs were active magmatically off and on since the Cambrian and Ordovician, and their loci of magmatism has migrated back and forth, depending on slab dip, and many other factors, by hundreds of kilometers (Mamani et al., 2010). The episodic repetition of magmatic activity over hundreds of millions of years, each characterized by shorter pulses or flare ups separated by magmatic lulls, had the same duration as in the Pilbara and other Archean cratons.

Most arcs that are no longer active have collided with other arcs or continents leading to slab break-off with concomitant slab-failure magmatism, with the arc sequences forming the upper plate in these collisions. If the lower plate had a continental margin attached to subducted oceanic lithosphere, this would typically rebound isostatically under the upper plate after slab detachment, causing rapid uplift and erosion of the upper plate as the slab-failure magmas intrude the lower and upper plates. Therefore, much of the upper crust of former arcs is eroded leaving predominantly deeper levels, which tend to be dominated by domal plutons in the mid-crust of the arcs, and were intruded by suites of slab failure magmas in nested domal plutons that are more K-rich in their cores. Examples include the Ordovician Oliverian gneiss domes in the Applachians that formed by slab-failure in the waning stages of the Taconic collision, and the Cretaceous Sierra Crest magmatic suite in the North American Cordillera (Hildebrand and Whalen, 2017,

2020).

The scale of plutonic activity, and associated tectonic belts such as accretionary wedges and fore-arc basins, is the same in the Pilbara, and the North and South American Cordilleran Belts, with no discernable changes in pluton shape or dimensions, internal relationships between phases, across or along strike-lengths of belts, depths of intrusion, mechanisms of intrusion, relationships with surrounding country rocks, or style of deformation. Archean dome-and-basin provinces thus represent ancient deeply eroded remnants of Earth's oldest continental arcs and their accretionary-to-collisional orogens that are infested with slab-failure magmas, each with their own prior history.

Gneiss domes similar in some aspects to those in the Pilbara can also be produced during the formation of metamorphic core complexes, such as the Suhshwap dome in British Columbia, the Menderes massif of western Anatolia, and many others (Vanderhaeghe and Teyssier, 1997; Vanderhaeghe et al., 1999; Whitney et al., 2004, 2013; Lamont et al., 2019). These are typically generated during late-orogenic collapse, slab break-off, or slab roll-back effects in the upper plate of a subduction system. However, these differ in that they are typically cored by metamorphic basement with decompression-driven migmatization, and melts derived from partial melting of pre-existing crust.

Based on these outstanding similarities, there can be no valid claims that the map patterns of the Pilbara, or other Eo- to Neoarchean cratons with domes-and-basins, represent a unique or different style of tectonics on Earth from that of the present. Domes-and-basins indicate specific tectonic environments, not a temporal evolution of planet Earth.

We therefore reject any claims that the tectonic style represented by Eastern Pilbara is any different from the tectonic style in the modern Earth. What is special about the Pilbara, however, is that the mid-crust of the arc and collisional orogen is deeply eroded to a relatively flat surface, providing a spectacular view into the magmatic and tectonic processes of a convergent margin that evolved on Earth more than 3 billion years ago.

Geological relationships of the Pilbara can be readily explained using a plate tectonic paradigm, in a consistent model that is no more complex than that of a typical Phanerozoic orogen such as the Appalachians or North American Cordillera, which have not yet experienced their final collisions. Thus, the Archean geology passes the uniformitarian null hypothesis test that the present paradigm readily explains all observations from the past, and therefore there is no justification to invoke other alternative worlds that have no testable objective data.

Plate tectonics has been extant on Earth from the very beginning, *ab ovo*.

Funding

Author contributions

TK conceptualized, designed and performed the structural analysis and comparative tectonic analysis and led the project. BFW and AP helped conceptualize and formulate the hypotheses tested in the paper. The first draft of the paper was written by TK, with significant writing by BFW and AP. The figures were designed and initially drafted by TK, and the final text and figures were written, corrected, and drafted by all

authors, with contributions to specific hypotheses by BH, WBN, and YTZ. All authors contributed to the final submission.

Declaration of Competing Interest

The authors declare that they have no known competing financial interests or personal relationships that could have appeared to influence the work reported in this paper.

Acknowledgements

References

Allen, C.M., Barnes, C.G., 2006. Ages and some cryptic sources of Mesozoic plutonic rocks in the Klamath Mountains, California and Oregon. In: Snoke, A.W., Barnes, C. G. (Eds.), Geological Studies in the Klamath Mountains Province, California and Oregon: A Volume in Honor of William P. Irwin. Geological Society of America Special Paper, 410, pp. 223 245. https://doi.org/10.1130/2006.2410(11).

Amelin, Y., Lee, D.-C., Halliday, A.N., 2000. Early-middle Archaean crustal evolution deduced from La–Hf and U–Pb isotopic studies of single zircon grains. Geochim. Cosmochim. Acta 64, 4205–4225.

Arculus, R.J., 2003. Use and abuse of the terms calcalkaline and calcalkalic. J. Petrol. 44, 929 935.

Arevalo, R., McDonough, W.F., Luong, M., 2009. The K/U ratio of the silicate Earth: insights into mantle composition, structure and thermal evolution. Earth Planet. Sci. Lett. 278, 361–369.

Argand, E., 1924. La tectonique de l'Asie. Int. Geol. Congr. 13, 171–372.

Aulbach, S., Viljoen, K., 2015. Eclogite xenoliths from the Lace kimberlite, Kaapvaal craton: from convecting mantle source to paleo-ocean floor and back. Earth Planet. Sci. Lett. 431, 274–286.

Bagas, L., Farrell, T.R., Nelson, D.R., 2005. The Age and Provenance of the Mosquito Creek Formation, Annual Review. Geological Survey of Western Australia, pp. 62–70.

Barley, M.E., 1993. Volcanic, sedimentary and tectonostratigraphic environments of the ~3.46 Ga Warrawoona megasequence: a review. Precambrian Res. 60, 47–67.

Barley, M.E., Pickard, A.L., 1999. An extensive, crustally derived, 3325 to 3310 Ma silicic volcanoplutonic suite in the eastern Pilbara Craton: evidence from the Kelly Belt, McPhee Dome and Corunna Downs Batholith. Precambrian Res. 96, 41–62.

Barnes, C.G., Snoke, A.W., Harper, G.D., Frost, C.D., McFadden, R.R., Bushey, J.C., Barnes, M.A.W., 2006. Arc plutonism following regional thrusting: petrology and geochemistry of syn- and post-Nevadan plutons in the Siskiyou Mountains, Klamath Mountains province, California. In: Snoke, A.W., Barnes, C.G. (Eds.), Geological Studies in the Klamath Mountains Province, California and Oregon: A Volume in Honor of William P. Irwin. Geological Society of America Special Paper 410, pp. 357–376. https://doi.org/10.1130/2006.2410(17.

Bateman, P.C., 1992. Plutonism in the Central Part of the Sierra Nevada Batholith. U.S.G. S. Professional Paper 1483, 186 pp.

Bateman, P.C., Wahrhaftig, C., 1966. Geology of the Sierra Nevada. In: Baily, E.H. (Ed.), Geology of Northern California: California Division of Mines and Geology Bulletin, 190, pp. 107–172.

Bédard, J.H., 2006. A catalytic delamination-driven model for coupled genesis of Archean crust and sub-continental lithospheric mantle. Geochim. Cosmochim. Acta 70, 1188–1214.

Bédard, J.H., 2018. Stagnant lids and mantle overturns: Implications for Archaean tectonics, magmagenesis, crustal growth, mantle evolution, and the start of plate tectonics. Geosci. Front. 9, 19 49.

Bédard, J., 2020. From the LIPS of a serial killer: Endogenic retardation of biological evolution on unstable stagnant lid planets. Planet. Space Sci. https://doi.org/10.1016/j.pss.2020.105068.

Bédard, J.H., Harris, L.B., Thurston, P.C., 2013. The hunting of the snArc. Precambrian Res. 229, 20 48. https://doi.org/10.1016/j.precamres.2012.04.001.

Begg, G.C., Griffin, W.L., Natapov, L.M., O'Reilly, S.Y., Grand, S.P., O'Neill, C.J., 2009. The lithospheric architecture of Africa: Seismic tomography, mantle petrology, and tectonic evolution. Geosphere 5 (1), 23–50. https://doi.org/10.1130/GES00179.1.

Bickle, M.J., Bettenay, L.F., Boultier, C.A., Groves, D.I., Morant, P., 1980. Horizontal tectonic interaction of an Archean gneiss belt and greenstones, Pilbara block, Western Australia. Geology 8, 525–529.

Bickle, M.J., Bettenay, L.F., Barley, M.E., Chapman, H.J., Groves, D.I., Campbell, I.H., de Laeter, J.R., 1983. A 3500 Ma plutonic and volcanic calc-alkaline province in the Archaean East Pilbara Block. Contrib. Mineral. Petrol. 84, 25–35. https://doi.org/10.1007/BF01132327.

Bickle, M.J., Morant, P., Bettenay, L.F., Boulter, C.A., Blake, T.S., Groves, D.I., 1985. Archean tectonics of the Shaw Batholith, Pilbara Block, Western Australia: structural and metamorphic tests of the batholith concept. In: Ayres, L.D., Thurston, P.C., Card, K.D., Weber, W. (Eds.), Evolution of Archean Supracrustal Sequences, Geological Association of Canada Special Paper, 28, pp. 325–341.

Blewett, R.S., 2000a. North Pilbara 'Virtual' structural field trip. Geoscience Australia Records 2000/45. http://www.ga.gov.au/rural/projects/pilbara/.

Blewett, R.S., 2000b. North Pilbara 'Virtual' structural field trip. Geoscience Australia Records 2000/45. http://www.ga.gov.au/rural/projects/pilbara/.

Blewett, R.S., 2002. Archaean tectonic processes: a case for horizontal shortening in the North Pilbara granite greenstone terrane, Western Australia. Precambrian Res. 113, 87–120.

Blewett, R.S., Shevchenko, S., Bell, B., 2004. The North Pole dome: a non-diapiric dome in the Archean Pilbara craton, Western Australia. Precambrian Res. 133, 105–120.

Boak, J.L., Dymek, R.F., 1982. Metamorphism of the ca. 3800 Ma supracrustal rocks at Isua, West Greenland: implications from early Archean crustal evolution. Earth Planet. Sci. Lett. 59, 155–176.

Bonner, H., Kroner, A., Jacob, D.E., Che, X.C., Wong, J., Xie, H., 2020. Cold avalanche, "super subduction", mantle overturn, followed by buoyant subduction of an oceanic plateau and the formation of TTG's during the Eocene in Vitu Levu, Fiji Islands. Preceambrian Res.. https://doi.org/10.1016/j.precamres.2020.105971.

Boulter, C.A., Bickle, M.J., Gibson, B., Wright, R.K., 1987. Horizontal tectonics pre-dating upper Gorge Creek Group sedimentation Pilbara block, Western Australia. Precambrian Res. 36, 241–258.

Boyd, F.R., Gurney, J.J., Richardson, S.H., 1985. Evidence for a 150–200-km thick Archaean lithosphere from diamond inclusion thermobarometry. Nature 315, 387–389.

Boyer, S.E., Elliot, D., 1982. Thrust systems. Am. Assoc. Pet. Geol. Bull. 66, 1196–1230.

Brandl, G., de Wit, M.J., 1997. The Kaapvaal Craton. In: De Wit, M.J., Ashwal, L.D. (Eds.), Greenstone Belts. Oxford University Press, Oxford, pp. 581–607.

Brandl, G., Cloete, M., Anhaeusser, C.R., 2006. Archean greenstone belts. In: Johnson, M. R., Anhausser, C.R., Thomas, R.J. (Eds.), The Geology of South Africa. Geological Society of South Africa, Johannesburg/ Council for Geoscience, Pretoria, pp. 9–56.

Brenner, A.R., Fu, R.R., Evans, D.A.D., Smirnov, A.V., Trubko, R., Rose, I.R., 2020. Paleomagnetic evidence for modern-like plate motion velocities at 3.2 Ga. Sci. Adv. 6 https://doi.org/10.1126/sciadv.aaz8670 eaaz8670.

Bridgwater, D., Collerson, K.D., 1976. The major petrological and geochemical characters of the 3,600 m.y. Uivak gneisses from Labrador. Contrib. Mineral. Petrol. 54, 43–59.

Bridgwater, D., Schiotte, L., 1991. The Archaean gneiss complex of northern Labrador, a review of current results, ideas and problems. Bull. Geol. Soc. Den. 39, 153 166.

Bridgwater, D., Collerson, K.D., Hurst, R.W., Jesseau, C.W., 1975. Field characteristics of the early Precambrian rocks from Saglek, coast of Labrador. In: Report of Activities, Part A., Geological Survey of Canada, Paper 75-1A, pp. 287–296.

Bridgwater, D., Mengel, F., Schiøtte, L., Winter, J., 1990. Research on the Archean rocks of Northern Labrador, progress report 1989. Current Research (1990) Newfoundland Department of Mines and Energy. Geological Survey Branch, Report 90-1, pp. 227–236.

Brown, E.H., McClelland, W.C., 2000. Pluton emplacement by sheeting and vertical ballooning in part of the southeast Coast Plutonic complex, British Columbia. Geol. Soc. Am. Bull. 112, 708–719. https://doi.org/10.1130/00167606(2000)112<708: PEBSAV>2.0.CO;2.

Brown, E.H., Talbot, J.L., McClelland, W.C., Feltman, J.A., Lapen, T.J., Bennett, J.D., Hettinga, M.A., Troost, M.L., Alvarez, K.M., Calvert, A.T., 2000. Interplay of plutonism and regional deformation in an obliquely convergent arc, southern Coast Belt, British Columbia. Tectonics 19, 493–511.

Brown, M., Johnson, T., Gardiner, N.J., 2020. Plate tectonics and the Archean Earth. Annu. Rev. Earth Planet. Sci. 48, 12. https://doi.org/10.1146/annurev-earth-081619-052705.

Buick, R., Thornett, J.R., McNaughton, N.J., Smith, J.B., Barley, M.E., Savage, M., 1995. Record of emergent continental crust~ 3.5 billion years ago in the Pilbara Craton of Australia. Nature 375, 574–577.

Burchfiel, B.C., Davis, G.A., 1975. Nature and controls of Cordilleran orogenesis, western United States: extension of an earlier synthesis. Am. J. Sci. 275, 363 396.

Burke, K., Kidd, W.S.F., Kusky, T.M., 1985a. The Pongola Structure of southeastern Africa: the world's oldest recognized well-preserved rift? J. Geodyn. 2, 35–50.

Burke, K., Kidd, W.S.F., Kusky, T.M., 1985b. Is the Ventersdorp rift system of southern Africa related to a continental collision between the Kaapvaal and Zimbabwe cratons at 2.64 Ga ago? Tectonophysics 11, 1 24. https://doi.org/10.1016/0040-1951(85) 90096-4.

Burke, K., Kidd, W.S.F., Kusky, T.M., 1986. Archean foreland basin tectonics in the Witwatersrand, South Africa. Tectonics 5, 439–456. https://doi.org/10.1029/ TC005i003p00439.

Calkins, F.C., 1930. The granitic rocks of the Yosemite region. In: Matthes, F.E. (Ed.), Geologic History of the Yosemite Valley. U.S. Geological Survey Paper 160, pp. 120–129.

Cates, N.L., Mojzsis, S.J., 2007. Pre-3750 Ma supracrustal rocks from the Nuvvuagittuq supracrustal belt, northern Québec. Earth Planet. Sci. Lett. 255, 9–21. https://doi. org/10.1016/j.epsl.2006.11.034.

Cates, N.L., Mojzsis, S.J., 2009. Metamorphic zircon, trace elements and Neoarchean metamorphism in the 3.75 Ga Nuvvuagittuq supracrustal belt, Quebec (Canada). Chem. Geol. 261, 98–113.

Celli, N.L., Lebedev, S., Schaeffer, A.J., et al., 2020. African cratonic lithosphere carved by mantle plumes. Nat. Commun. 11, 92. https://doi.org/10.1038/s41467-019-13871-2.

Champion, D.C., Smithies, R.H., 2001. The geochemistry of the Yule granitoid complex, East Pilbara - Granite- Greenstone Terrane: evidence for early felsic crust. Geological Survey of Western Australi Annual Review 1999-2000, 42–48.

Champion, D.C., Smithies, R.H., 2007. Chapter 4.3. Geochemistry of Paleoarchean granites of the East Pilbara Terrane, Pilbara Craton, Western Australia. In: Implications for Early Archean Crustal Growth. Developments in Precambrian Geology 15. Elsevier, pp. 369–409.

Chapman, A.D., Saleeby, J.B., Wood, D.J., Piasecki, A., Kidder, S., Ducea, M., Farley, K., 2012. Late cretaceous gravitational collapse of the southern Sierra Nevada batholith, California. Geosphere 8, 214–341. https://doi.org/10.1130/GES00740.

Chemenda, A.I., Yang, R.K., Hsieh, C.H., 1997. Evolutionary model for the Taiwan collision based on physical modeling. Tectonophysics 274, 253–274. https://doi.org/10.1016/S0040-1951(97)00025-5.

Choukroune, P., Bouhallier, H., Arndt, N.T., 1995. Soft lithosphere during periods of Archean crustal growth or crustal reworking. In: Coward, M.P., Ries, A.C. (Eds.), Early Precambrian Processes, Geological Society of London Special Publication, 95, pp. 67–86.

Clift, P.D., Schouten, H., Draut, A.E., 2003. A General Model of Arc-Continent Collision and Subduction Polarity Reversal from Taiwan and the Irish Caledonides. Geological Society of London Special Publication, 219, pp. 81–98. https://doi.org/10.1144/GSL.SP.2003.219.01.04.

Coleman, D.S.A., Glazner, F., 1997. The Sierra Crest magmatic event: rapid formation of juvenile crust during the late cretaceous in California. Int. Geol. Rev. 39, 768–787. https://doi.org/10.1080/00206819709465302.

Coleman, D.S., Glazner, A.F., 1998. The Sierra Crest magmatic event: rapid formation of juvenile crust during the Late Cretaceous in California. In: Ernst, W.G., Nelson, C.A. (Eds.), Integrated Earth and Environmental Evolution of the Southwestern United States: The Clarence A. Hall Jr. Volume. Bellwether Publishing for the Geological Society of America, Columbia, Maryland, pp. 253–272.

Collerson, K.D., 1983. Ion microprobe zircon geochronology of the Uivak Gneisses: implications for the evolution of early terrestrial crust in the North Atlantic Craton. In: Ashwal, L.D., Card, K.D. (Eds.), Abstracts for Early Crustal Genesis Field Workshop, Lunar and Planetary Institute, Houston, TX, Technical Report, 83-03, pp. 28–33.

Collet, L.W., 1927. The Structure of the Alps, 2nd edition. E. Arnold, London, p. 304.

Collins, W.J., 1989. Polydiapirism of the Archaean Mount Edgar Batholith, Pilbara, Western Australia. Precambrian Res. 43, 41–62.

Collins, W.J. Van Kranendonk, M.J., 1999. Model for the development of kyanite during partial convective overturn of Archean granite–greenstone terranes: the Pilbara Craton, Australia. J. Metamorph. Geol. 17, 145–156.

Collins, W.J., Van Kranendonk, M.J., Teyssier, C., 1998. Partial convective overturn of Archaean crust in the east Pilbara Craton, Western Australia: driving mechanisms and tectonic implications. J. Struct. Geol. 20, 1405–1424.

Condie, K.C., 1981. Archean Greenstone Belts, vol. 3. Elsevier, ISBN 9780080869025, 433 pp.

Condie, K.C., 1997. Plate Tectonics and Crustal Evolution, 4th ed. Butterworth-Heinemann, Oxford.

Cooper, J.A., James, P.R., Rutland, R.W.R., 1982. Isotopic dating and structural relationships of granitoids and greenstones in the East Pilbara, Western Australia. Precambrian Res. 18, 199–236.

Coward, M.P., 1983. Thrust tectonics, thin-skinned or thick-skinned and the continuation of thrusts to deep in the crust. J. Struct. Geol. 5, 113–125.

Coward, M.P., Lintern, B.C., Wright, L.I., 1976. The pre-cleavage deformation of the sediments and gneisses of the northern part of the Limpopo belt. In: Windley, B.F. (Ed.), The Early History of the Earth. Wiley, London, pp. 323–330.

Crawford, M.L., Hollister, L.S., Woodsworth, G.J., 1987. Crustal deformation and regional metamorphism across a terrane boundary, Coast Plutonic Complex, British Columbia. Tectonics 6, 343–361. https://doi.org/10.1029/TC006i003p00343.

Crawford, M.L., Klepeis, K.A., Gehrels, G., Isachsen, C., 1999. Batholith emplacement at mid-crustal levels and its exhumation within an obliquely convergent margin. Tectonophysics 312, 57–78. https://doi.org/10.1016/S0040-1951(99)00170-5.

Daczko, N.R., Piazolo, S., Meek, U., Stuart, C.A., Elliott, V., 2016. Hornblendite delineates zones of mass transfer through the lower crust. Sci. Rep. 6, 31369. https://doi.org/10.1038/srep31369.

Dai, J.G., Wang, C.S., Stern, R.J., Yang, K., Shen, J., 2020. Forearc magmatic evolution during subduction initiation: insights from an Early Cretaceous Tibetan ophiolite and comparison with the Izu-Bonin-Mariana forearc. Geol. Soc. Am. Bull. https://doi.org/10.1130/B35644.1.

David, J., Godin, L., Stevenson, R., O'Neil, J., Francis, D., 2009. U-Pb ages (3.8-2/7 Ga) and Nd isotope data from the newly identified Eoarchean Nuvvuagittuq supracrustal belt, Superior Craton, Canada. Geol. Soc. Am. Bull. 121, 150–163. https://doi.org/10.1130/B26369.1.

Davids, C., Wijbrans, J., White, S.J., 1997. ^{40}Ar/^{39}Ar ages of metamorphic hornblendes from the Coongan Belt, Pilbara, Western Australia. Precambrian Res. 83, 221 242.

Day, H.W., Bickford, M.E., 2004. Tectonic setting of the Jurassic Smartville and Slate Creek complexes, northern Sierra Nevada, California. Geol. Soc. Am. Bull. 116, 1515–1528. https://doi.org/10.1130/B25416.1.

Day, H.W., Moores, E.M., Tuminas, A.C., 1985. Structure and tectonics of the northern Sierra Nevada. Geol. Soc. Am. Bull. 96, 436–450, doi:10.1130/0016-7606(1985)96<436:SATOTN>2.0 .CO;2.

de Wit, M.J., 1982. Gliding and overthrust nappe tectonics in the Barberton Greenstone Belt. J. Struct. Geol. 4, 117–136.

de Wit, M.J., Furnes, H., 2016. 3.5 Ga Hydrothermal fields and diamictites in the Barberton Greenstone Belt – Paleo-Archean crust in cool environments. Sci. Adv. 2 e1500368.

de Wit, M.J., Hart, R.A., 1993. Earth's earliest continental lithosphere, hydrothermal flux and crustal recycling. Lithos 30, 309–335.

de Wit, M.J., Hart, R., Martin, A., Abbot, P., 1982. Archean abiogenic and probable biogenic structures associated with mineralised hydrothermal systems and regional metasomatism, with implications for greenstone belt studies. Econ. Geol. 77, 1783 1801.

de Wit, M.J., Armstrong, R., Hart, R.J., Wilson, A.H., 1987. Felsic igneous rocks within the 3.3- to 3.5-Ga Barberton Greenstone Belt: high crustal level equivalents of the surrounding Tonalite- Trondhjemite Terrain, emplaced during thrusting. Tectonics 6, 529–549.

de Wit, M.J., Roering, C., Hart, R.J., Armstrong, R.A., de Ronde, C.E.J., Green, R.W.E., Tredoux, M., Peberdy, E., Hart, R.A., 1992. Formation of an Archean continent. Nature 357, 553–562.

de Wit, M.J., Furnes, H., Robins, B., 2011. Geology and tectonostratigraphy of the Onverwacht Suite, Barberton Greenstone Belt, South Africa. Precambrian Res. 186, 1 27.

de Wit, M., Furnes, H., MacLennan, S., Doucouré, M., Schoene, B., Weckmann, U., Martinez, U., Bowring, S., 2017. Paleoarchean bedrock lithologies across the Makhonjwa Mountains of South Africa and Swaziland linked to geochemical, magnetic and tectonic data reveal early plate tectonic genes flanking subduction margins. Geoscience Frontiers. https://doi.org/10.1016/j.gsf.2017.10.005.

de Wit, M., Furnes, H., MacLennan, S., Doucouré, M., Schoene, B., Weckmann, U., Martinez, U., Bowring, S., 2018. Paleoarchean bedrock lithologies across the Makhonjwa Mountains of South Africa and Swaziland linked to geochemical, magnetic and tectonic data reveal early plate tectonic genes flanking subduction margins. Geosci. Front. 9, 603 665. https://doi.org/10.1016/j.gsf.2017.10.005.

Debaille, V., O'Neill, C., Brandon, A.D., Haemecour, P., Yin, Q.Z., Mattielli, N., Treiman, A., 2013. Stagnant-lid tectonics in early Earth revealed by ^{142}Nd variations in late Archean rocks. Earth Planet. Sci. Lett. 373, 83–92. https://doi.org/10.1016/j.epsl.2013.04.016.

Demouy, S., Paquette, J.L., de Saint Blanquat, M., Benoit, M., Belousova, E.A., et al., 2012. Spatial and temporal evolution of Liassic to Paleocene arc activity in southern Peru unraveled by zircon U-Pb and Hf in-situ data on plutonic rocks. Lithos 155, 183–200.

Dewey, J.F., 1977. Suture zone complexities: a review. Tectonophysics 40, 53–67.

Dewey, J.F., 1988. Extensional collapse of orogens. Tectonics 7, 1123–1139.

Dilek, Y., 1989. Tectonic significance of post-accretion rifting of a Mesozoic island-arc terrane in the northern Sierra Nevada, California. J. Geol. 97, 503–518. https://doi.org/10.1086/629325.

Dodd, M.S., Papineau, D., Grenne, T., Slack, J.F., Rittner, M., Pirajno, F., O'Neill, J., Little, C.T.S., 2017. Evidence for early life in Earth's oldest hydrothermal vent precipitates. Nature 543, 60–64. https://doi.org/10.1038/nature21377.

Dolan, J.F., Mann, P., 1998. Active strike-slip and collisional tectonics of the northern Caribbean Plate Boundary Zone. Geological Society of America Special Paper 326, 174 pp.

Draper, G., Gutiérrez, G., Lewis, J.F., 1996. Thrust emplacement of the Hispaniola peridotite belt: Orogenic expression of the mid-Cretaceous Caribbean arc polarity reversal? Geology 24, 1143–1146. https://doi.org/10.1130/0091-7613(1996)024<1143:TEOTHP>2.3.CO;2.

Ducea, M.N., Otamendi, J.E., Bergantz, G., Stair, K.M., Valencia, V.A., Gehrels, G.E., 2010. Timing constraints on building an intermediate plutonic arc crustal section: U-Pb zircon geochronology of the Sierra Valle Fertil-La Huerta, Famatinian arc, Argentina. Tectonics 29 article TC4002.

Ducea, M.N., Saleeby, J.B., Bergantz, G., 2015a. The architecture, chemistry, and evolution of continental magmatic arcs. Annu. Rev. Earth Planet. Sci. 43, 299–331. https://doi.org/10.1146/annurev-earth-060614-105049.

Ducea, M.N., Paterson, S.R., DeCelles, P.G., 2015b. High-volume magmatic events in subduction systems. Elements 11, 99–104.

Ducea, M.N., Bowman, E., Chapman, A.D., Balica, C., 2020a. Arclogites and their role in continental evolution; part 1: Background, locations, petrography, geochemistry, chronology and thermobarometry. Earth-Sci. Rev. https://doi.org/10.1016/j.earscirev.2020.103375.

Ducea, M.N., Bowman, E., Chapman, A.D., Balica, C., 2020b. Arclogites and their Role in Continental Evolution; Part 2: Relationship to Batholiths and Volcanoes, Density and Foundering, Remelting and Long-Term Storage in the Mantle (in review).

Dumitru, T.A., Wakabayashi, J., Wright, J.E., Wooden, J.L., 2010. Early Cretaceous transition from nonaccretionary behavior to strongly accretionary behavior within the Franciscan subduction complex. Tectonics 29. https://doi.org/10.1029/2009TC002542.

Dunne, G.C., Gulliver, R.M., Sylvester, A.G., 1978. Mesozoic evolution of rocks of the White, Inyo, Argus and Slate ranges, eastern California. In: Howell, D.G., McDougall, K.A. (Eds.), Mesozoic Paleogeography of the Western United States, Society of Economic Paleontologists and Mineralogists, Pacific Section, Pacific Coast Paleogeography Symposium, 2, pp. 189 207.

Dziggel, A., Diener, J.F.A., Kolb, J., Kokfelt, T.F., 2014. Metamorphic record of accretionary processes during the Neoarchean: the Nuuk region, Southern West Greenland. Precambrian Res. 242, 22–38.

Eriksson, K.A., 1981. Archean platform to trough sedimentation in the east Pilbara Block, Australia. In: Glover, J.E., Groves, D.I. (Eds.), Archean Geology, pp. 236–244, 2nd Archean International Symposium, Perth, W.A., Geological Survey of Western Australia Special Publications 7.

Eskola, P., 1949. The problem of mantled gneiss domes. Geol. Soc. Lond. Quatern. J. 104, 461–476.

Evans, D.A., Smirnov, A.V., Gumsley, A.P., 2017. Paleomagnetism and U-Pb geochronology of the Black Range Dykes, Pilbara Craton, Western Australia: a

Neoarchean crossing of the polar circle. Aust. J. Earth Sci. 64, 225–237. https://doi.org/10.1080/08120099.2017.1289981.

Evenchick, C.A., McMechan, M.E., McNicoll, V.J., Carr, S.D., 2007. A synthesis of the Jurassic–Cretaceous tectonic evolution of the central and southeastern Canadian Cordillera: Exploring links across the orogen. In: Sears, J.W., Harms, T.A., Evenchick, C.A. (Eds.), Whence the Mountains?: Inquiries into the Evolution of Orogenic Systems: A Volume in Honor of Raymond A, Price: Geological Society of America Special Paper, 433, pp. 117–145. https://doi.org/10.1130/2007.2433(06).

Fagan, T.J., Day, H.W., Hacker, B.R., 2001. Timing of arc construction and metamorphism in the Slate Creek Complex, northern Sierra Nevada, California. Geol. Soc. Am. Bull. 113, 1105 1118. https://doi.org/10.1130/00167606(2001) 113<1105:TOACAM>2.0.CO;2.

Fiske, R.S., Tobisch, O.T., 1994. Middle Cretaceous ash-flow tuff and caldera- collapse deposit in the Minarets Caldera, east-central Sierra Nevada, California. Geol. Soc. Am. Bull. 106, 582–593. https://doi.org/10.1130/00167606(1994)106<0582: MCAFTA>2.3.CO;2.

Fossen, H., Cavalcante, G.C.C., Pinheiro, R., Archanjo, C., 2019. Deformation - progressive or multiphase? J. Struct. Geol. 125, 82–99.

Friend, C.R.L., Nutman, A.P., 1991. Refolded nappes during late Archean terrane assembly, Godthåbsfjord, southern West Greenland. J. Geol. Soc. Lond. 148, 507 519.

Friend, C.R.L., Nutman, A.P., 2001. U–Pb zircon study of tectonically-bound blocks of 2940-2840 Ma crust with different metamorphic histories, Paamiut region, South-West Greenland: Implications for the tectonic assembly of the North Atlantic craton. Precambrian Research 105, 143–164.

Friend, C.R.L., Nutman, A.P., 2005a. New pieces to the Archean jigsaw puzzle in the Nuuk region, southern West Greenland: steps in transforming a simple insight into a complex regional tectonothermal model. J. Geol. Soc. Lond. 162, 147–162. https://doi.org/10.1144/0016-764903-161.

Friend, C.R.L., Nutman, A.P., 2005b. Complex 3670-3500 Ma orogenic episodes superimposed on juvenile crust accreted between 3850-3690 Ma, Itsaq Gneiss Complex, southern West Greenland. J. Geol. 113, 375–397. https://doi.org/10.1086/430239.

Friend, C.R.L., Nutman, A.P., McGregor, V.R., 1987. Late-Archaean tectonics in the Færingehavn–Tre Brødre area, south of Buksefjorden, southern West Greenland. J. Geol. Soc. Lond. 144, 369–376.

Friend, C.R.L., Nutman, A.P., McGregor, V.R., 1988. Late Archean terrane accretion in the Godthåb region, southern West Greenland. Nature 335, 535–538.

Friend, C.R.L., Nutman, A.P., Baadsgaard, Kinney, McGregor, V.R., 1996. Timing of late Archean terrane assembly, crustal thickening and granite emplacement in the Nuuk region, southern West Greenland. Earth and Planetary Science Letters 142, 353 365.

Frimmel, H.E., 2014. A giant mesoarchean crustal gold-enrichment episode: possible causes and consequences for exploration. In: Kelley, K., Golden, H.C. (Eds.), Building Exploration Capability for the 21st Century, Society of Economic Geologists, Special Publication, 18, pp. 209–234.

Frimmel, H., 2019. The Witwatersrand Basin and its gold deposits. In: Kröner, A., Hofmann, A. (Eds.), The Archaean Geology of the Kaapvaal Craton, Southern Africa, Regional Geology Reviews, pp. 255–275. https://doi.org/10.1007/978-3-319-78652-0_4.

Fu, D., Kusky, T.M., Wilde, S.A., Polat, A, Huang, B., Zhou, Z.P., 2018. Early Paleozoic collisional-related magmatism in the eastern North Qilian orogen, northeastern Tibet: a linkeage between accretionary and collisional orogenesis. Geol. Soc. Am. Bull. 131, 1031–1056. https://doi.org/10.1130/B35009.1.

Fu, D., Kusky, T.M., Wilde, S.A., Windley, B.F., Polat, A., Huang, B., Zhou, Z.P., 2020. Structural anatomy of the early Paleozoic Laohushan ophiolite and subduction complex: implications for accretionary tectonics of the North Qilian orogenic belt. Geol. Soc. Am. Bull. https://doi.org/10.1130/B35442.1.

Furnes, H., de Wit, M., Staudigel, H., Rosing, M., Muehlenbachs, K., 2007. A vestige of Earth's oldest ophiolite. Science 315, 1704 1707 https://doi.org/10.1126/science.1139170.

Furnes, H., Dilek, Y., Zhao, G.C., Safonova, I., Santosh, M., 2020. Geochemical characterization of ophiolites in the Alpine-Himalayan Orogenic Belt: Magmatically and tectonically diverse evolution of the Mesozoic Neotethyan oceanic crust. Earth Sci. Rev. 208, 103258. https://doi.org/10.1016/j.earscirev.2020.103258.

Gardiner, N.J., Hickman, A., Kirkland, C.L., Lu, Y., Johnson, T., Zhao, J.X., 2017. Processes of crust formation in the early Earth imaged through Hf isotopes from the East Pilbara Terrane. Precambrian Res. 297, 56–76. https://doi.org/10.1016/j.precamres.2017.05.004.

Gehrels, G., Rusmore, M., Woodsworth, G., Crawford, M., Andonicos, C., Hollister, L., Patchett, J., Ducea, M., Butler, R., Klepeis, K., Davidson, C., Friedman, R., Haggart, J., Mahoney, B., Crawfors, W., Pearson, D., Girardi, J., 2009. U-Th-Pb geochronology of the Coast Mountains batholith in north-central British Columbia: constraints on age and tectonic evolution. Geol. Soc. Am. Bull. 121, 1341–1361. https://doi.org/10.1130/B26404.1.

Glikson, A.Y., 1979. Early Precambrian tonalite–trondhjemite sialic nuclei. Earth Sci. Rev. 15, 1–73.

Goodwin, A.M., 1996. Principles of Precambrian Geology. Academic Press, London, 327 pp. ISBN: O-12-28970-2.

Green, M.G., Sylvester, P.J., Buick, R., 2000. Growth and recycling of early Archaean continental crust: geochemical evidence from the Coonterunah and Warrawoona groups, Pilbara Craton, Australia. Tectonophysics 322, 69–88.

Griffin, W., O'Reilly, S., Natapov, L., Ryan, C., 2003. The evolution of lithospheric mantle beneath the Kalahari Craton and its margins. Lithos 71, 215–241. https://doi.org/10.1016/j.lithos.2003.07.006.

GSWA (Geological Survey of Western Australia), 1990. Geology and Mineral Resources of Western Australia Memoir 3, 827 pp.

GSWA (Geological Survey of Western Australia), 2016. Geological Survey of Western Australia, Interpreted bedrock geology of the East Pilbara Craton, Report 143, scale 1:250,000.

Guitreau, M., Blichert-Toft, J., Mojzsis, S.J., Roth, A.S.G., Bourdon, B., 2013. A legacy of Hadean silicate differentiation from Hf isotopes in Eoarchean rocks of the Nuvvuagittuq supracrustal belt (Québec, Canada). Earth Planet. Sci. Lett. 362, 171–181. https://doi.org/10.1016/j.epsl.2012.11.055.

Hacker, B.R., 1993. Evolution of the northern Sierra Nevada metamorphic belt: Petrological, structural, and Ar/Ar constraints. Geol. Soc. Am. Bull. 105, 637–656. https://doi.org/10.1130/0016-7606(1993)105<0637:EOTNSN>2.3.CO;2.

Hacker, B.R., Peacock, S.M., 1990. Comparison of the Central Metamorphic Belt and Trinity terrane of the Klamath Mountains and the Feather River terrane of the Sierra Nevada. In: Harwood, D.S., Miller, M.M. (Eds.), Late Paleozoic and Early Mesozoic Paleogeographic Relations: Klamath Mountains, Sierra Nevada, and Related Rocks: Geological Society of America Special Paper, 255, pp. 75–92.

Hanson, R.E., Saleeby, J.B., Schweickert, R.A., 1988. Composite Devonian island-arc batholith in the northern Sierra Nevada, California. Geol. Soc. Am. Bull. 100, 446–457. doi:https://doi.org/10.1130/0016-7606 (1988)100<0446:CDIABI>2.3.CO;2.

Harayama, S., Takahashi, Y., Nakano, S., Kariya, Y., Komazawa, M., 2000. Geology of the Tateyama District, Quadrangle Series 1:50,000. Geological Survey of Japan.

Harrison, T.M., 2020. Hadean Earth. Springer. https://doi.org/10.1007/978-3-030-46687-9 ebook. 291 pp.

Hawkesworth, C.J., Cawood, P.A., Dhuime, B., 2020. The evolution of the continental crust and the onset of plate tectonics. Front. Earth Sci. https://doi.org/10.3389/feart.2020.00326.

Heritsch, F., 1929. The nappe theory in the Alps (translated by P.G.A. Boswell), 228 p. Methuen, London.

Hickman, A.H., 1983. Geology of the Pilbara Block and its environs. Western Australia Geol. Surv. Bull. 127, 268.

Hickman, A.H., 2012. Review of the Pilbara Craton and Fortescue Basin, Western Australia: crustal evolution providing environments for early life. Island Arc 21, 1–31.

Hickman, A.H., 2016. Northwest Pilbara Craton: A Record of 450 Million Years in the Growth of Archean Continental Crust Report. Geological Survey of Western Australia, p. 104.

Hickman, A.H., Van Kranendonk, M.J., 2004. Diapiric processes in the formation of Archaean continental crust, East Pilbara Granite-Greenstone Terrane, Australia. In: Eriksson, P.G., Altermann, W., Nelson, D.R., Mueller, W.U., Catuneau, O. (Eds.), The Precambrian Earth: Tempos and Events. Elsevier, pp. 54–75.

Hickman, A.H., Van Kranendonk, M.J., 2012. Early Earth evolution: Evidence from the 3.5-1.8 Ga geological history of the Pilbara region of Western Australia. Episodes 35, 283–297. https://doi.org/10.18814/epiiugs/2012/v35i1/028.

Hildebrand, R.S., 2009. Did Westward Subduction Cause Cretaceous–Tertiary Orogeny in the North American Cordillera? Geological Society of America Special Paper 457, 71 pp. https://doi.org/10.1130/2009.2457.

Hildebrand, R.S., 2013. Mesozoic Assembly of the North American Cordillera, Geological Society of America Special Paper 495, 179 pp.

Hildebrand, R.S., Whalen, J.B., 2014a. Arc and slab-failure magmatism in Cordilleran batholiths I—the cretaceous Coastal batholith of Peru and its role in South American orogenesis and hemispheric subduction flip. Paul Hoffman Volume. Geosci. Can. 41, 255–282. https://doi.org/10.12789/geocanj.2014.41.047.

Hildebrand, R.S., Whalen, J.B., 2014b. Arc and slab-failure magmatism in Cordilleran batholiths II the Cretaceous Peninsular Ranges batholith of Southern and Baja California. Paul Hoffman Volume. Geoscience Canada 41, pp. 399–458. https://doi.org/10.12789/geocanj.2014.41.059.

Hildebrand, R.S., Whalen, J.B., 2017. The tectonic setting and origin of Cretaceous batholiths within the North American Cordillera: the case for slab failure magmatism and its significance for crustal growth. Geological Society of America Special Paper 532. https://doi.org/10.1130/2017.2532, 113 pp.

Hildebrand, R.S., Whalen, J.B., 2020. Arc and slab-failure magmatism of the Taconic orogeny, western New England, USA. In: Murphy, J.B., Strachan, R.A., Quesada, C. (Eds.), Pannotia to Pangaea: Neoproterozoic and Paleozoic Orogenic Cycles in the Circum-Atlantic Region. https://doi.org/10.1144/SP503-2019-247. Geological Society London, Special Publications, 503.

Hildebrand, R.S., Whalen, J.B., Bowring, S.A., 2018. Resolving the crustal composition paradox by 3.8 billion years of slab failure magmatism and collisional recycling of continental crust. Tectonophysics 734–735. https://doi.org/10.1016/j.tecto.2018.04.001.

Hoffman, A., Kusky, T.M., 2004. The Belingwe greenstone belt: ensialic or oceanic? Chapter 15. In: Kusky, T.M. (Ed.), Precambrian Ophiolites and Related Rocks, Elsevier, Developments in Precambrian Geology 13, pp. 487–537. https://doi.org/10.1016/S0166-2635(04)13015-6.

Hoffmann, J.E., Svahnberg, H., Piazolo, S., Scherstén, A., Münker, C., 2012. The geodynamic evolution of Mesoarchean anorthosite complexes inferred from the Naajat Kuuat Complex, southern West Greenland. Precambrian Research 196–197, 149–170.

Hoffmann, J.E., Nagel, T.J., Münker, C., Næraa, T., Rosing, M.T., 2014. Constraining the process of Eoarchean TTG formation in the Itsaq Gneiss Complex, southern West Greenland. Earth Planet. Sci. Lett. 388, 374–386.

Hollister, L.S., Diebold, J., Triparna, D., 2008. Whole crustal response to Late Tertiary extension near Prince Rupert, British Columbia. Geosphere 4, 360–374. https://doi.org/10.1130/GES000144.1.

Huber, N.K., Bateman, P.C., Wahrhaftig, C., 1989. Geologic map of Yosemite National Park and vicinity, California, U.S. Geological Survey Miscellaneous Investigations Series Map I-1874, 1 sheet scale 1:125,000.

Humbert, F., de Kock, M., Lenhardt, N., Altermann, W., 2019. Neoarchean to early Paleoproterozoic within-plate volcanism of the Kaapvaal craton: comparing the Ventersdorp Supergroup and the Ongeluk and Hekpoort Formations (Transvaal Supergroup). In: Kröner, A., Hofmann, A. (Eds.), The Archaean Geology of the Kaapvaal Craton, Southern Africa, Regional Geology Reviews, pp. 277–302. https://doi.org/10.1007/978-3-319-78652-0_4.

Irwin, W.P., 1972. Terranes of the western Paleozoic and Triassic belt in the southern Klamath Mountains, California: U.S. Geol. Surv. Prof. Pap. 800-C, C103–C111.

Irwin, W.P., 2003. Correlation of the Klamath Mountains and Sierra Nevada: U.S. Geological Survey Open-File Report 02–490, 2 sheets.

Irwin, W.P., Wooden, J.L., 2001. Maps showing plutons and accreted terranes of the Sierra Nevada, California, with a tabulation of U/Pb isotopic ages. U.S. Geological Survey Open-File Report 01–299, 1 sheet.

Isozaki, Y., Maruyama, Sh., Fukuoka, F., 1990. Accreted oceanic materials in Japan. Tectonophysics 181, 179–205.

Jagoutz, O., Kelemen, P., 2016. Role of arc processes in the formation of continental crust. Annu. Rev. Earth Planet. Sci. 43, 363–404.

Jaguin, J., Gapais, D., Poujol, M., Boulvais, P., Moyen, J.-F., 2012. The Murchison greenstone belt (South Africa): a general tectonic framework. South Afr. J. Geol. 115, 65–76.

Jennings, C.W., 1977. Geologic map of California. Sacramento, California Division of Mines and Geology, scale 1:750,000.

Johnson, T.E., Brown, M., Kaus, B., Van Tongeren, J.A., 2014. Delamination and recycling of Archaean crust caused by gravitational instabilities. Nat. Geosci. 7, 47–52. https://doi.org/10.1038/ngeo2019.

Johnson, T.E., Kirkland, C.L., Gardiner, N.J., Brown, M., Smithies, R.H., Santosh, M., 2019. Secular change in TTG compositions: Implications for the evolution of Archaean geodynamics. Earth Planet. Sci. Lett. 505, 65–75. https://doi.org/10.1016/j.epsl.2018.10.022.

Kato, Y., Ohta, I., Tsunematsu, T., Watanabe, Y., Isozaki, Y., Maruyama, S., Imai, N., 1998. Rare earth element variations in mid-Archean banded iron formations: implications for the chemistry of ocean and continent and plate tectonics. Geochim. Cosmochim. Acta 62, 3475–3497. https://doi.org/10.1016/S0016-7037(98)00253-1.

Kelemen, P.B., Hanghoj, K., Greene, A.R., 2003. One view of the geochemistry of subduction-related magmatic arcs, with an emphasis on primitive andesite and lower crust. In: Rudnick, R.L., Turekian, K.K. (Eds.), Treatise of Geochemistry, 3. Elsevier, Amsterdam, pp. 593–659.

Kemp, A., Vervoort, J.D., Bjorkman, K., Iaccheri, L., 2017. Hafnium isotope characteristics of Paleoarchean zircon OG1/OGC from the Owens Gulley Diorite, Pilbara Craton, Western Australia. Geostandards Analyt. Res. 41, 659 673. https://doi.org/10.1111/ggr.12182.

Key, R.M., Litherland, M., Hepworth, J.V., 1976. The evolution of the Archaean crust of Northeast Botswana. Precambrian Res. 3, 375–413.

Kisters, A.F.M., van Hinsberg, V.J., Szilas, K., 2012. Geology of an Archaean accretionary complex the structural record of burial and return flow in the Tàrtoq Group of South West Greenland. Precambrian Res. 220-221, 107–122. https://doi.org/10.1016/j.precamres.2012.07.008.

Kitajima, K., Maruyama, S., Utsunomiya, S., Liou, J.G., 2001a. Seafloor hydrothermal alteration at an Archaean mid-ocean ridge. J. Metamorph. Geol. 19, 583–599.

Kitajima, K., Utsunomiya, S., Maruyama, S., 2001b. Physico-chemical environment of an Archean mid-ocean ridge: estimate of seawater depth and hydrothermal fluid composition. In: Nakashima, S., Maruyama, S., Brack, A., Windley, B.F. (Eds.), Geochemistry and the Origin of Life. Universal Academy Press, Tokyo, pp. 179 202.

Kitajima, K., Hirata, T., Maruyama, S., Yamanashi, T., Sano, Y., Liou, J.G., 2008. U-Pb zircon geochronology using LA-ICP-MS in the North Pole Dome, Pilbara Craton, Western Australia: a new tectonic growth model for the Archean chert/greenstone succession. Int. Geol. Rev. 50, 1–14. https://doi.org/10.2747/0020-6814.50.1.1.

Kloppenberg, A., White, S., Zegers, T., 2001. Structural evolution of the Warrawoona Greenstone Belt and adjoining granitoid complxes, Pilbara Craton, Australia: implications for Archean tectonic processes. Precambrian Res. 112, 107–147.

Kloppenburg, A., 2003. Structural Evolution of the Marble Bar Domain, Pilbara Granite-Greenstone Terrain, Australia: The Role of Archaean Mid- Crustal Detachments. Utrecht University, Utrecht.

Kolb, J., Kokfelt, T.F., Dziggel, A., 2012. Geodynamic setting and deformation history of an Archaean terrane at mid-crustal level: the Tasiusarsuaq terrane of southern West Greenland. Precambrian Res. 212–213, 34–56.

Komatsu, M., Osanai, Y., Toyoshima, T., Miyashita, S., 1989. Evolution of the Hidaka metamorphic belt, northern Japan. In: Daly, J.S., Cliff, R.A., Yardley, B.W.D. (Eds.), Evolution of Metamorphic Belts, Geological Society of London, Special Publications, 43, pp. 487–493.

Komiya, T., Maruyama, S., Masuda, T., Nohda, S., Hayashi, M., Okamoto, K., 1999. Plate tectonics at 3.8-3.7 Ga: field evidence from the Isua accretionary complex, southern West Greenland. J. Geol. 107, 515 554.

Komiya, T., Yamamoto, S., Aoki, S., Sawaki, Y., Ishikawa, A., Tashiro, T., Koshida, K., Shimojo, M., Aski, K., Collerson, K.D., 2015. Geology of the Eoarchean >3.95 Ga, Nulliak supracrustal rocks in the Saglek Block, northern Labrador, Canada: the oldest geological evidence for plate tectonics. Tectonophysics 662, 40–66.

Komiya, T., Yamamoto, S., Aoki, S., Koshida, K., Shimojo, M., Sawaki, Y., Aoki, K., Sakata, S., Yokoyama, T., Maki, K., Ishikawa, A., Hirata, T., Collerson, K., 2017. A prolonged granitoid formation in Saglek Block, Labrador: Zonal growth and crustal reworking of continental crust in the Eoarchean. Geosci. Front. 8, 355–385. https://doi.org/10.1016/j.gsf.2016.06.013.

Korenaga, J., 2018. Crustal evolution and mantle dynamics through Earth history. Philos. Trans. R. Soc. Lond. A376 https://doi.org/10.1098/rsta.2017.0408, 20170408.

Korenaga, J., 2021. Hadean geodynamics and the nature of early continental crust. Precambrian Res. 359, 106178. https://doi.org/10.1016/j.precamres.2021.106178.

Kramers, J.D., McCourt, S., Roering, C., Smit, C.A., van Reenen, D.D., 2011. Tectonic models proposed for the Limpopo complex: mutual compatibilities and constraints. In: van Reenen, D.D., Kramers, J., McCourt, S., Perchuk, L.L. (Eds.), Origin and Evolution of Precambrian High Grade Gneiss Terranes, with Special Emphasis on the Limpopo Complex of Southern Africa, Geological Society of America Memoir, 207, pp. 311–324.

Kramers, J.D., Henzen, M., Steidl, E.L., 2014. Greenstone belts at the northernmost edge of the Kaapvaal Craton: timing of tectonic events and a possible crustal fluid source. Precambrian Res. 253, 96 113.

Krapez, B., 1993. Sequence stratigraphy of the Archean supracrustal belts of the Pilbara block, western Australia. Precambrian Res. 60, 1–45.

Krapez, B., Eisenlohr, B., 1998. Tectonic setting of Archaean (3325-2775 Ma) crustal-supracrustal belts in the West Pilbara Block. Precambrian Res. 88, 173–205.

Krapez, B., 1984. Sedimentation in a Small, Fault-Bounded Basin: The Lalla Rookh Sandstone East Pilbara Block, vol. 9. Geol. Dept. & Univ. Extensions, University of Western Australia, pp. 89–110.

Krapez, B., Barley, M.E., 1987. Archaean strike–slip faulting and related ensialic basins: evidence from the Pilbara Block, Australia. Geol. Mag. 124, 555–567.

Kröner, A., 1984. Evolution, growth and stabilization of the Precambrian lithosphere. In: Pollack, H.N., Rama Murthy, V. (Eds.), Structure and Evolution of the Continental Lithosphere. Physics and Chemistry of the Earth, 15, pp. 69–106. https://doi.org/10.1016/0079-1946(84)90005-3.

Kröner, A., Hofmann, A., 2019. The Archean Geology of the Kaapvaal Craton, Southern Africa. Regional Geology Reviews. Springer, 302 pp.

Kusky, T.M., 1989. Accretion of the Archean Slave Province. Geology 17, 63–67. https://doi.org/10.1130/0091-7613(1989)017<0063:AOTASP>2.3.CO;2.

Kusky, T.M., 1991. Structural development of an Archean orogen, western Point Lake, Northwest Territories. Tectonics 10, 820–841. https://doi.org/10.1029/91TC00805.

Kusky, T.M., 1992. Relative timing of deformation and metamorphism at mid- to upper-crustal levels in the Point Lake Orogen, Slave Province, Canada. In: Glover, J.E., Ho, S.E. (Eds.), **The Archaean: Terranes, Processes and Metallogeny,** Geology Department (Key Centre) & University Extension, The University of Western Australia, Publication number 22, pp. 59–71.

Kusky, T.M., 1993. Collapse of Archean orogens and the generation of late-to post-kinematic granitoids. Geology 21, 925–928.

Kusky, T.M., 1998. Tectonic setting and terrane accretion of the Archean Zimbabwe craton. Geology 26, 163–166.

Kusky, T.M., 2011. Geophysical and geological tests of tectonic models of the North China Craton. Gondwana Res. 20, 26 35. https://doi.org/10.1016/j.gr.2011.01.004.

Kusky, T.M., Bradley, D.C., 1999. Kinematics of mélange fabrics: examples and applications from the McHugh Complex, Kenai Peninsula, Alaska. J. Struct. Geol. 21, 1773–1796. https://doi.org/10.1016/S0191-8141(99)00105-4.

Kusky, T.M., Kidd, W.S.F., 1992. Remnants of an Archean oceanic plateau, Belingwe greenstone belt, Zimbabwe. Geology 20, 43 46. https://doi.org/10.1130/0091-7613(1992)020<0043:ROAAOP>2.3.CO;2.

Kusky, T.M., Polat, A., 1999. Growth of Granite-Greenstone Terranes at Convergent margins and Stabilization of Archean Cratons. Tectonophysics 305, 43–73. https://doi.org/10.1016/S0040-1951(99)00014-1.

Kusky, T.M., Vearncombe, J., 1997. Structure of archean greenstone belts. In: de Wit, M. J., Ashwal, L.D. (Eds.), Tectonic Evolution of Greenstone Belts, Oxford Monograph on Geology and Geophysics, pp. 95–128. ISBN: 0198540566; 978019540564.

Kusky, T.M., Winsky, P.A., 1995. Structural relationships along a greenstone/ shallow water shelf contact, Belingwe greenstone belt, Zimbabwe. Tectonics 14, 448–471. https://doi.org/10.1029/94TC03086.

Kusky, T., Young, C., 1999. Emplacement of the Resurrection Peninsula ophiolite in the southern Alaska Forearc during a Ridge-Trench Encounter. J. Geophys. Res. 104 (B12), 29,025 29,054. https://doi.org/10.1029/1999JB900265.

Kusky, T.M., Bradley, D.C., Haeussler, P., Karl, S., 1997a. Controls on accretion of flysch and mélange belts at convergent margins: evidence from The Chugach Bay thrust and Iceworm mélange, Chugach Terrane, Alaska. Tectonics 16 (6), 855–878 https://doi.org/10.1029/97TC02780 2.

Kusky, T.M., Bradley, D.C. Haeussler, Haeussler, 1997b. Progressive deformation of the Chugach accretionary complex, Alaska, during a Paleogene ridge-trench encounter. J. Struct. Geol. 19, 139–157. https://doi.org/10.1016/S0191-8141(96)00084-3.

Kusky, T.M., Bradley, D.C., Donley, D.T., Rowley, D., Haeussler, P., 2003. Controls on intrusion of near-trench magmas of the Sanak-Baranof belt, Alaska, during Paleogene ridge subduction, and consequences for forearc evolution. In: Sisson, V.B., Roeske, S., Pavlis, T.L. (Eds.), Geology of a Transpressional Orogen Developed During a Ridge - Trench Interaction Along the North Pacific Margin, Geological Society of America Special Paper 371, pp. 269–292. https://doi.org/10.1130/0-8137-2371-X.269.

Kusky, T.M., Windley, B.F., Safonova, I., Wakita, K., Wakabashi, J., Polat, A., Santosh, M., 2013. Recognition of Ocean plate stratigraphy in accretionary orogens through Earth history: a record of 3.8 billion years of sea floor spreading, subduction, and accretion, GR Focus review paper. In: Kusky, T.M., Stern, R.J., Dewey, J.F. (Eds.), Secular Changes in Geologic and Tectonic Processes, Special Issue of Gondwana Research, v. 42, pp. 501–547. https://doi.org/10.1016/j.gr.2013.01.004.

Kusky, T.M., Polat, A., Windley, B.F., Burke, K.C., Dewey, J.F., Kidd, W.S.F., Maruyama, S., Wang, J.P., Deng, H., Wang, Z.S., Wang, C., Fu, D., Li, X.W., Peng, H. T., 2016. Insights into the tectonic evolution of the North China Craton through comparative tectonic analysis: A record of outward growth of Precambrian continents. Earth Science Reviews 162, 387–432. https://doi.org/10.1016/j.earscirev.2016.09.002.

Kusky, T.M., Windley, B.F., Polat, A., 2018. Geological evidence for the operation of plate tectonics throughout the Archean: records from Archean paleo-plate boundaries. J. Earth Sci. 29, 1291–1303. https://doi.org/10.1007/s12583-018-0999-6.

Kusky, T.M., Wang, J.P., Wang, L., Huang, B., Ning, W.B., Fu, D., Peng, H.T., Deng, H., Polat, A., Zhong, Y.T., Shi, G.Z., 2020. Mélanges through time: life cycle of the world's largest Archean mélange compared with Mesozoic and Paleozoic subduction-accretion-collision mélanges. Earth-Sci. Rev. https://doi.org/10.1016/j.earscirev.2020.103303.

Lackey, J.S., Valley, J.W., Chen, J.H., Stockli, D.F., 2008. Dynamic magma systems, crustal recycling, and alteration in the Central Sierra Nevada Batholith: the oxygen isotope record. J. Petrol. 49, 1397–1426. https://doi.org/10.1093/petrology/egn030.

Lamont, T.N., Searle, M.P., Waters, D.J., Roberts, N., Palin, R., Smye, A., Dyck, B., Gopon, P., Weller, O., St-Onge, M.R., 2019. Compressional origin of the Naxos metamorphic core complex, Greece: Structure, petrography, and thermobarometry. Geol. Soc. Am. Bull. 132, 149–197. https://doi.org/10.1130/B31978.1.

Laurent, O., Zeh, A., 2015. A linear Hf isotope-age array despite different granitoid sources and complex Archean geodynamics: example from the Pietersburg block (South Africa). Earth Planet. Sci. Lett. 430, 326–338.

Laurent, O., Martin, H., Moyen, J.-F., Doucelance, R., 2014a. The diversity and evolution of late-Archean granitoids: evidence for the onset of "modern-style" plate tectonics between 3.0 and 2.5 Ga. Lithos 205, 208–235.

Laurent, O., Nicoli, G., Zeh, A., Stevens, G., Moyen, J.-F., Vezinet, A., 2014b. Comment on "Ultrahigh temperature granulites and magnesian charnockites: evidence for the Neoarchean accretion along the northern margin of the Kaapvaal craton". Precambrian Res. 255, 455–458.

Laurent, O., Rapopo, M., Stevens, G., Moyen, J.-F., Martin, H., Doucelance, R., Bosq, C., 2014c. Contrasting petrogenesis of Mg–K and Fe–K granitoids and implications for post-collisional magmatism: case study from the late-Archean Matok pluton (Pietersburg block, South Africa). Lithos 196, 131–149.

Laurent, O., Zeh, A., Brandl, G., Vezinet, A., Wilson, A., 2019. In: Kröner, A., Hofmann, A. (Eds.), The Archaean Geology of the Kaapvaal Craton, Southern Africa, Regional Geology Reviews. https://doi.org/10.1007/978-3-319-78652-0_4.

Lee, C.-T.A., Morton, D.M., Kistler, R.W., Baird, A.K., 2007. Petrology and tectonics of Phanerozoic continent formation: from island arcs to accretion and continental arc magmatism. Earth Planet. Sci. Lett. 263, 370–387. https://doi.org/10.1016/j.epsl.2007.09.025.

Lenardic, A., 2018a. In: Deeg, H.J., Belmonte, J.A. (Eds.), Volcanic-tectonic modes and planetary life potential. Springer, Handbook of Exoplanets, pp. 1–20. https://doi.org/10.1007/978-3-319-30648-3_65-1.

Lenardic, A., 2018b. The diversity of tectonic modes and thoughts about transitions between them. Phil. Trans. R. Soc. A 376, 20170416. https://doi.org/10.1098/rsta.2017.0416.

Leo, G.W., 1991. Oliverian Domes, Related Plutonic Rocks, and Mantling Ammonoosuc Volcanics of the Bronson Hill Anticlinorium, New England Appalachians. United States Geological Survey Professional Paper 1516.

Light, M.P.R., 1982. The Limpopo Belt, Southern Africa: a result of continental collision. Tectonics 1, 325–342.

Lin, S., Parks, J., Heaman, L.M., Simonetti, A., Corkery, M.T., 2013. Diapirism and sagduction as a mechanism for deposition of "Timiskaming-type" sedimentary sequences, Superior Province: evidence from detrital zircon geochronology and implications for the Borden Lake conglomerate exposed middle to lower crust in the Kapuskasing Uplift. Precambrian Res. 238, 148 157.

Liou, J.G., Maruyama, S., Wang, X., Graham, S., 1990. Precambrian blueschist terranes of the world. Tectonophysics 181, 97–111. https://doi.org/10.1016/0040-1951(90)90010-6.

Luskin, C., Wilson, A., Gold, D., Hofmann, A., 2019. The Pongola Supergroup: Mesoarchean deposition following Kaapvaal craton stabilization. In: Kröner, A., Hofmann, A. (Eds.), The Archaean Geology of the Kaapvaal Craton, Southern Africa. https://doi.org/10.1007/978-3-319-78652-0_9. p. 225-254. Regional Geology Reviews.

MacGregor, A.M., 1947. An outline of the geological history of Southern Rhodesia. Southern Rhodesia Geol. Surv. Bull. 38.

Macgregor, A.M., 1951. Some milestones in the Precambrian of Southern Rhodesia. Geol. Surv. Southern Rhodesia, Proc. 38, 229–245.

Mamani, M., Worner, G., Sempere, T., 2010. Geochemical variations in igneous rocks of the central Andean orocline (13 S to 18 S): tracing crustal thickening and magma generation through time and space. Geol. Soc. Am. Bull. 122, 162 182. doi.org/10.1130/B26538.1.

Marschall, H.R., Schumacher, J.C., 2012. Arc magmas sourced from mélange diapirs in subduction zones. Nat. Geosci. 5 (12), 862–867.

Maruyama, S., Liou, J.G., Terabayashi, M., 1996. Blueschists and eclogites of the world and their exhumation. Int. Geol. Rev. 38, 490 596. https://doi.org/10.1080/00206819709465347.

Maruyama, S., Yuen, D.A., Windley, B.F., 2007. Dynamics of plumes and superplumes through time. In: Yuen, D.A., Maruyama, S., Karato, S.-H., Windley, B.F. (Eds.), Superplumes: Beyond Plate Tectonics. Springer, Netherlands, pp. 441–502.

Maunder, B., Prytulak, J., Goes, S., Reagan, M., 2020. Rapid subduction initiation and magmatism in the Western Pacific driven by internal vertical forces. Nat. Commun. 11, 1874. https://doi.org/10.1038/s41467-020-15737-4.

McClay, K.R., 1992. Thrust Tectonics. Chapman & Hall, London.

McGregor, V.R., 1993. Descriptive text to 1 : 100000 geological map of Greenland Qôrqut 64 V.1 Syd. Copenhagen, Geological Survey of Greenland, 40 p.

McNaughton, N.J., Compston, W., Barley, M.E., 1993. Constraints on the age of the Warrawoona Group, Eastern Pilbara, Western Australia. Precambrian Res. 60, 69–98.

Memeti, V., Paterson, S., Matzel, J., Mundil, R., Okaya, D., 2010. Magmatic lobes as "snapshots" of magma chamber growth and evolution in large, composite batholiths: an example from the Tuolumne intrusion, Sierra Nevada, California. Geol. Soc. Am. Bull. 122, 1912–1931. https://doi.org/10.1130/B30004.1.

Miller, J., Miller, R., Wooden, J., Harper, G., 2003. Geochronologic links between the Ingalls ophiolite, North Cascades, Washington and the Josephine ophiolite, Klamath Mountains, Oregon and California. Geological Society of America Abstracts with Programs 35, no. 6, p. 113.

Mloszewaka, A.M., Mojzsis, S.J., Pecoits, E., Papineau, D., Dauphas, N., Konhauser, K.O., 2013. Chemical sedimentary protoliths in the <3.75 Ga Nuvvuagittuq supracrustal belt (Québec, Canada). Gondwana Res. 23, 574–594. https://doi.org/10.1016/j.gr.2012.11.005.

Mojzsis, S., Arrhenius, G., McKeegan, K.D., Harrison, T.M., Nutman, A.P., Friend, C.R.L., 1996. Evidence for life on Earth before 3,800 million years ago. Nature 385, 55–59.

Moorbath, S., Taylor, P.N., Goodwin, R., 1981. Origin of granitic magma by crustal remobilisation: Rb-Sr and Pb/Pb geochronology and isotope geochemistry of the late Archean Qôrqut Granite complex of southern West Greenland. Geochim. Cosmochim. Acta 45, 1051 1060.

Moore, J.G., Sisson, T.W., 1987. Geologic map of the Triple Divide Peak quadrangle, Tulare County, California. U.S. Geological Survey Geological Quadrangle Map GQ-1636 scale 1:62,500.

Morgan, P., 1985. Crustal radiogenic heat production and the selective survival of ancient continental crust. Proceedings of the Lunar and Planetary Science Conference, Journal of Geophysical Research, Supplement 90, C561–C570. https://doi.org/10.1029/JB090iS02p0C561.

Nadin, E.S., Saleeby, J.B., 2008. Disruption of regional primary structure of the Sierra Nevada batholith by the Kern Canyon fault system, California. In: Wright, J.E., Shervais, J.W. (Eds.), Ophiolites, Arcs, and Batholiths: A Tribute to Cliff Hopson, Geological Society of America Special Paper, 438, pp. 429–454. https://doi.org/10.1130/2008.2438(15).

National Academies of Sciences, Engineering, and Medicine, 2020. A Vision for NSF Earth Sciences 2020–2030. Earth in Time. The National Academies Press, Washington, D.C. https://doi.org/10.17226/2576.

Nebel, O., Capitanio, F.A., Moyen, J.-F., Weinberg, R.F., Clos, F., Nebel-Jacobsen, Y.J., Cawood, P.A., 2018. When crust comes of age: on the chemical evolution of Archaean, felsic continental crust by crustal drip tectonics. Phil. Trans. R. Soc. A 376, 20180103. https://doi.org/10.1098/rsta.2018.0103.

Nelson, D.R., 1999. Banded biotite tonalite gneiss, 6 Mile Well (No. 345) Geochronology Record Geological Survey of Western Australia.

Nijman, W., de Bruijne, K.C.H., Valkering, M.E., 1998. Growth fault control of early Archaean cherts, barite mounds, and chert-barite veins, North Pole Dome, eastern Pilbara, western Australia. Precambrian Res. 88, 25–52. https://doi.org/10.1016/S0301-9268(97)00062-4.

Nijman, W., Kloppenburg, A., de Vries, S.T., 2017. Archean basin margin geology and crustal evolution: an East Pilbara traverse. J. Geol. Soc. Lond. 174, 1090–1112. https://doi.org/10.1144/jgs2016-127.

Ning, W.B., Kusky, T., Wang, J.P., Wang, L., Deng, H., Polat, A., Huang, B., Peng, H.T., Feng, P., 2020. From subduction initiation to arc-polarity reversal: Life cycle of an Archean subduction zone from the Zunhua ophiolitic mélange, North China Craton. Precambrian Res. 350, 105868. https://doi.org/10.1016/j.precamres.2020.105868.

Nixon, P.H., Neal, C.R., 1987. in Mantle Xenoliths (edited by P.H. Nixon). Wiley, Chichester, pp. 335–345.

Nutman, A.P., 1986. The early Archaean to Proterozoic history of the Isukasia area, southern West Greenland. Grønlands Geol. Unders. Bull. 154, 80 p.

Nutman, A.P., Friend, C.R.L., 2007. Adjacent terranes with ca. 2715 and 2650 Ma high pressure metamorphic assemblages in the Nuuk region of the North Atlantic Craton, southern West Greenland: complexities of Neoarchaean collisional orogeny. Precambrian Res. 155, 159–203.

Nutman, A.P., Friend, C.R.L., 2009. New 1:20,000 scale geological maps, synthesis and history of investigation of the Isua supracrustal belt and adjacent orthogneisses, southern West Greenland: a glimpse of Eoarchean crust formation and orogeny. Precambrian Res. 172, 189–211.

Nutman, A.P., Friend, C.R.L., Kinny, P.D., McGregor, V.R., 1993. Anatomy of an early Archean gneiss complex: 3900 to 3600 Ma crustal evolution in southern West Greenland. Geology 21, 415–418.

Nutman, A.P., McGregor, V.R., Friend, C.R.L., Bennett, V.C., Kinney, P.D., 1996. The Itsaq Gneiss Complex of southwest Greenland: the world's most extensive record of early crustal evolution (3900-3600 Ma). Precambrian Res. 78, 1–39. https://doi.org/10.1016/0301-9268(95)00066-6.

Nutman, A.P., Bennett, V.C., Friend, C.R.L., Rosing, M.T., 1997. 3710 and 3790 Ma volcanic sequences in the Isua (Greenland) supracrustal belt; structural and Nd isotope implications. Chem. Geol. 141, 271–287.

Nutman, A.P., Bennett, V.C., Friend, C.R.L., Norman, M.D., 1999. Meta-igneous (non-gneissic) tonalites and quartz-diorites from an extensive ca. 3800 Ma terrain south of the Isua supracrustal belt, southern West Greenland: constraints on early crust formation. Contrib. Mineral. Petrol. 137, 364 388. https://doi.org/10.1007/s004100050556.

Nutman, A.P., Friend, C.R.L., Barker, S.L.L., McGregor, V.R., 2004. Inventory and assessment of Palaeoarchaean gneiss terrains and detrital zircons in southern West Greenland. Precambrian Res. 135 https://doi.org/10.1016/j.precamres.2004.09.002, 281–31.

Nutman, A.P., Christiansen, O., Friend, C.R.L., 2007. 2635 Ma amphibolite facies gold mineralisation near a terrane boundary (suture?) on Storø, Nuuk region, southern West Greenland. Precambrian Research 159, 19–32.

Nutman, A., Bennett, V.C., Friend, C.R.L., Hikada, H., Yi, K., Lee, S.R., Kamachi, T., 2013. The Itsaq Gneiss Complex of Greenland: Episodic 3900 to 3660 Ma juvenile crust formation and recycling in the 3660 3600 Ma Isukasian orogeny. Am. J. Sci. 313, 877–911.

Nutman, A.P., Bennett, V.C., Friend, C.R.L., Yi, K., 2020. Eoarchean contrasting ultra-high-pressure to low-pressure metamorphisms (< 250 to > 1000 °C/GPa) explained by tectonic plate convergence in deep time. Precambrian Res. 344, 105770. https://doi.org/10.1016/j.precamres.2020.105770.

Ohta, H., Maruyama, S., Takahashi, E., Watanabe, Y., Kato, Y., 1996. Field occurrence, geochemistry and petrogenesis of the Archean Mid-Oceanic Ridge basalts (AMORBs) of the Cleaverville area, Pilbara Craton, Western Australia. Lithos 37, 199–221. https://doi.org/10.1016/0024-4937(95)00037-2.

O'Neil, J., Francis, D., Carlson, R.W., 2011. Implications of the Nuvvuagittuq greenstone belt for the formation of Earth's early crust. J. Petrol. 52, 985–1009. https://doi.org/10.1093/petrology/egr014.

O'Neil, J., Carlson, R.W., Paquette, J.-L., Francis, D., 2012. Formation age and metamorphic history of the Nuvvuagittuq greenstone belt. Precambrian Res. 220-221, 23 44. https://doi.org/10.1016/j.precamres.2012.07.009.

Ortiz, K., Nyblade, A., van der Meijde, M., Paulssen, H., Kwadiba, M., Ntibinyane, O., 2019. Upper mantle P and S wave velocity structure of the Kalahari Craton and surrounding Proterozoic terranes, southern Africa. Geophys. Res. Lett. 46, 9509–9518. https://doi.org/10.1029/2019GL084053.

Otamendi, J.E., Ducea, M.N., Tibldi, A.M., Bergantz, G.W., de la Rosa, J., Vujovich, G., 2009. Generation of tonalitic and dioritic magmas by coupled partial melting of gabbroic and metasedimentary rocks with the deep crust of the Famatinian magmatic arc, Argentina. J. Petrol. 50, 841–873. https://doi.org/10.1093/petrology/egp022.

Otamendi, J.E., Ducea, M.N., Bergantz, G.W., 2012. Geological, Petrological and Geochemical evidence for Progressive Construction of an Arc Crustal Section, Sierra de Valle Fertil, Famatinian Arc, Argentina. J. Petrol. 53, 761–800.

Passeraub, M., Wüst, T., Kreissig, K., Smit, C.A., Kramers, J.D., 1999. Structure, metamorphism and geochronology of the Rhenosterkoppies greenstone belt, Northern Province, South Africa. S. Afr. J. Geol. 102, 323–334.

Paterson, S.R., Farris, D.W., 2008. Downward host rock transport and the formation of rim monoclines during emplacement of Cordilleran batholiths. Trans. R. Soc. Edinb. Earth Sci. 97, 397–413.

Paterson, S.R., Okaya, D., Memeti, V., Economos, R., Miller, R.B., 2011. Magma addition and flux calculations of incrementally constructed magma chambers in continental margin arcs: combined field, geochronologic, and thermal modeling studies. Geosphere 7, 1439–1468.

Pavlis, T.L., Amato, J.A., Trop, J.M., Ridgeway, K.D., Roeske, S.M., Gehrils, G.E., 2019. Subduction polarity in ancient arcs: a call to integrate geology and geophysics to decipher the Mesozoic tectonic history of the Northern Cordillera of North America. GSA Today 29. https://doi.org/10.1130/GSATG402A.1.

Pearce, J.A., Stern, R.J., 2006. The origin of back-arc basin magmas: Trace element and isotope perspectives. In: Christie, D.M., Fisher, C.R., Lee, S.-M., Givens, S. (Eds.), Back-Arc Spreading Systems: Geological, Biological, Chemical and Physical Interactions, American Geophysical Union, Geophysical Monograph, 166, pp. 63–86.

Petersson, A., Kemp, A., Hickman, A.H., Whitehouse, M., Martin, L., Gray, C., 2019. A new 3.59 Ga magmatic suite and a chondritic source to the east Pilbara Craton. Chem. Geol. 511, 51 70. https://doi.org/10.1016/j.chemgeo.2019.01.021.

Pfiffner, O.A., Gonzalez, L., 2013. Mesozoic-Cenozoic evolution of the western margin of South America: Case study of the Peruvian Andes. Geosciences 3, 262–310. https://doi.org/10.3390/geosciences3020262.

Pitcher, W.S., 1993. The Nature and Origin of Granite. Blackie Academic & Professional, London. https://doi.org/10.1007/978-94-017-3393-9, 321 p.

Poblet, J., Lisle, R.J., 2011. Kinematic evolution and structural styles of fold-and-thrust belts. In: Poblet, J., Lisle, R.J. (Eds.), Kinematic Evolution and Structural Styles of Fold-and-Thrust Belts, Geological Society, London, Special Publications, 349, pp. 1–24. https://doi.org/10.1144/SP349.1.

Polat, A., Frei, R., Apple, P.W.U., Dilek, Y., Fryer, B., Ordóñez-Calderon, J.C., Yang, Z., 2008. The origin and compositions of Mesoarchean oceanic crust: evidence from the 3075 Ma Ivisaartoq greenstone belt, SW Greenland. Lithos 100, 293–321.

Polat, A., Appel, P.W.U., Fryer, B., Windley, B., Frei, R., Samson, I.M., Huang, H., 2009. Trace element systematics of the Neoarchean Fiskenæsset anorthosite complex and associated meta-volcanic rocks, SW Greenland: evidence for a magmatic arc origin. Precambrian Res. 175, 87–115. https://doi.org/10.1016/j.precamres.2009.09.002.

Polat, A., Fryer, B., Appel, P.W.U., Kalvig, P., Kerrich, R., Dilek, Y., Yang, Z., 2011. Geochemistry of anorthositic differentiated sills in the Archean (~2970 Ma) Fiskenæsset Complex, SW Greenland: Implications for parental magma compositions, geodynamic setting, and secular heat flow in arcs. Lithos 123, 50 72. https://doi.org/10.1016/j.lithos.2010.12.003.

Polat, A., Wang, L., Appel, P.W.U., 2015. A review of structural patterns and melting processes in the Archean craton of West Greenland: evidence for crustal growth at convergent plate margins as opposed to non-uniformitarian models. Tectonophysics 662, 67–94. https://doi.org/10.1016/j.tecto.2015.04.006.

Polat, A., Kokfelt, T., Burke, K.C., Kusky, T.M., Bradley, D., Dziggel, A., Kolb, J., 2016a. Lithological, structural, and geochemical characteristics of the Mesoarchean Tartoq Greenstone Belt, Southwestern Greenland: Evidence for Uniformitarian processes in the Archean. Can. J. Earth Sci. https://doi.org/10.1139/cjes-2016-0023.

Polat, A., Kokfelt, T., Burke, K.C., Kusky, T.M., Bradley, D., Dziggel, A., Kolb, J., 2016b. Lithological, structural, and geochemical characteristics of the Mesoarchean Tartoq Greenstone Belt, southern West Greenland, and the Chugach-Prince William

accretionary complex, southern Alaska: evidence for uniformitarian plate-tectonic processes. Can. J. Earth Sci. 53, 1336–1371.

Polat, A., Frei, R., Longstaffe, F.J., Woods, R., 2018a. Petrogenetic and geodynamic origin of the Neoarchean Doré Lake Complex, Abitibi subprovince, Superior Province, Canada. Int. J. Earth Sci. 107, 811–843. https://doi.org/10.1007/s00531-017-1498-1.

Polat, A., Longstaffe, F.J., Frei, R., 2018b. An overview of anorthosite-bearing layered intrusions in the Archaean craton of southern West Greenland and the Superior Province of Canada: implications for Archaean tectonics and the origin of megacrystic plagioclase. Geodin. Acta 30, 84–99. https://doi.org/10.1080/09853111.2018.1427408.

Pubellier, M., Bader, A.G., Rangin, C., Deffontaines, B., Quebran, R., 1999. Upper plate deformation induced by subduction of a volcanic arc: the Snellius Plateau (Molucca Sea, Indonesia and Mindanao, Philippines). Tectonophysics 304 (4), 345–368. https://doi.org/10.1016/s0040-1951(98)00300-x.

Ramberg, H., 1967. Gravity, Deformation and the Earth's Crust. Academic Press, London, 214p.

Ramsay, J.G., Huber, M.I., 1987. The Techniques of Modern Structural Geology. Volume 2. Folds and Fractures. Academic Press, London. https://doi.org/10.1017/S0016756800010384, 391 pp.

Reagan, M.K., Ishizuka, O., Stern, R.J., Kelley, K.A., Ohara, Y., Blichert-Toft, J., Bloomer, S.H., Cash, J., Fryer, P., Hanan, B.B., Hickey-Vargas, R., Ishii, T., Kimura, J. I., Peate, D.W., Rowe, M.C., Woods, M., 2010. Forearc basalts and subduction initiation in the Izu–Bonin–Mariana system. Geochem. Geophys. Geosyst. 11 (3), 1–17. https://doi.org/10.1029/2009GC002871.

Reagan, M.K., McClelland, W.C., Girard, G., Goff, K.R., Peate, D.W., Ohara, Y., Stern, R. J., 2013. The geology of the southern Mariana fore–arc crust: implications for the scale of Eocene volcanism in the western Pacific. Earth Planet. Sci. Lett. 380, 41–51. https://doi.org/10.1016/j.epsl.2013.08.013.

Reagan, M.K., Pearce, J.A., Petronotis, K., Almeev, R.R., Avery, A.J., Carvallo, C., Chapman, T., Christeson, G.L., Ferre, E.C., Godard, M., Heaton, D.E., Kirchenbaur, M., Kurz, W., Kutterolf, S., Li, H., Li, Y., Michibayashi, K., Morgan, S., Nelson, W.R., Prytulak, J., Python, M., Robertson, A.H.F., Ryan, J.G., Sager, W.W., Sakuyama, T., Shervais, J.W., Shimizu, K., Whattam, S.A., 2017. Subduction initiation and ophiolite crust: new insights from IODP drilling. Int. Geol. Rev. 59 (11), 1439–1450. https://doi.org/10.1080/00206814.2016.1276482.

Richardson, S.H., Gurney, J.J., Erlank, A.J., Harris, J.W., 1984. Origin of diamonds in old enriched mantle. Nature 30, 198–200.

Richardson, S.H., Shirey, S.B., Harris, J.W., Carlson, R.W., 2001. Archean subduction recorded by Re-Os isotopes in eclogitic sulfide inclusion in Kimberly diamonds. Earth Planet. Sci. Lett. 191, 257 266.

Roberts, N.M., 2020. Internal Fabrics and Marginal Deformation of the Paleoarchean Mt Edgar Dome, East Pilbara Terrane, Western Australia: Structural constraints on crustal flow in the early Earth. Ph.D. Dissertation. University of Wisconsin-Madison.

Roberts, N.M., Tikoff, B., 2021. Internal structure of the Paleoarchean Mt Edgar dome, Pilbara Craton, Western Australia. Precambrian Res. 358, 106163. https://doi.org/10.1016/j.precamres.2021.106163.

Robinson, P., Thompson, P.J., Elbert, D.C., 1991. The nappe theory in the Connecticut Valley region: Thirty five years since Jim Thompson's first proposal. Am. Mineral. 76, 689–712.

Ross, D.C., 1989. The Metamorphic and Plutonic Rocks of the Southernmost Sierra Nevada, California, and Their Tectonic Framework. U.S. Geological Survey Professional Paper 1381, 159 p.

Ryan, B., Martineau, Y., 2012. Revised and coloured edition of 1992 map showing the Geology of the Saglek Fiord – Hebron Fiord area, Labrador (NTS 14L/2,3,6,7). Scale: 1:100 000, Government of Newfoundland and Labrador, Department of Natural Resources, Geological Survey, pp. Map 2012–2015, Open File 2014L/0091 (Update of map originally released as Newfoundland Department of Mines and Energy, Geological Survey Branch, Map 92-18B and Geological Survey of Canada, Open File 2466).

Saleeby, J.B., 1983. Accretionary tectonics of the North American Cordillera. Annual Reviews if Earth and Planetary Science 15, 45–73.

Saleeby, J.B., 1990. Progress in tectonic and petrogenetic studies in an exposed cross section of young (~100 Ma) continental crust, southern Sierra Nevada, California. In: Salisbury, M.H. (Ed.), Exposed Cross Sections of the Continental Crust. D. Reidel, Dordrecht, Neth, pp. 132–158.

Saleeby, J.B., 1999. On some aspects of the geology of the Sierra Nevada. In: Moores, E. M., Sloan, D., Stout, D.L. (Eds.), Classic Cordilleran Concepts: A View from California: Geological Society of America Special Paper, 338, pp. 173 184.

Saleeby, J.B., Busby-Spera, C., 1993. Paleogeographic and tectonic setting of axial and western metamorphic framework rocks of the southern Sierra Nevada, California. In: Dunne, G., McDougall, K. (Eds.), Mesozoic Paleogeography of the Western United States—II: Pacific Section, Society of Economic Paleontologists and Mineralogists, Book, 71, pp. 197 226.

Saleeby, J.B., Goodin, S.E., Sharp, W.D., Busby, C.J., 1978. Early Mesozoic paleotectonic-paleogeographic reconstruction of the southern Sierra Nevada region. In: Howell, D. G., McDougall, K.A. (Eds.), Mesozoic Paleogeography of the Western United States: Society of Economic Paleontologists and Mineralogists, Pacific Section, Pacific Coast Paleogeography Symposium, 2, pp. 311–336.

Saleeby, J.B., Shaw, H.F., Niemeyer, S., Moores, E.M., Edelman, S.H., 1989. U/Pb, Sm/Nd and Rb/Sr geochronological and isotopic study of northern Sierra Nevada ophiolitic assemblages, California. Contrib. Mineral. Petrol. 102, 205–220. https://doi.org/10.1007/BF00375341.

Saleeby, J.B., Ducea, M.N., Clemens-Knott, D., 2003. Production and loss of high-density batholithic roots. Tectonics 22, TC001374.

Saleeby, J.B., Ducea, M.N., Busby, C.J., Nadin, E.S., Wetmore, P.H., 2008. Chronology of pluton emplacement and regional deformation in the southern Sierra Nevada batholith, California. In: Wright, J.E., Shervais, J.W. (Eds.), Ophiolites, Arcs, and Batholiths: A Tribute to Cliff Hopson, Geological Society of America Special Paper, 438, pp. 397–427. https://doi.org/10.1130/2008.2438(14).

Sawada, H., Isozaki, Y., Sakata, S., Hirata, T., Maruyama, 2018. Change in lifetime of granitic crust and the continental growth: a new view from detrital zircon ages of sandstones. Geosci. Front. 9, 1099–1115. https://doi.org/10.1016/j.gsf.2016.11.0101674-9871.

Sawada, H., Sawaki, Y., Sakata, S., Ishikawa, A., Muteta, B., Isozaki, Y., Maruyama, S., 2020. New geochronological constraints on the middle Archean Shurugwi greenstone belt; toward an understanding of the crustal evolution of the Zimbabwe craton. J. Afr. Earth Sci. https://doi.org/10.1016/j.jafrearsci.2020.104021.

Schidlowski, M., 1988. A 3,800-million-year isotopic record of life from carbon in sedimentary rocks. Nature 333, 313–318.

Schweickert, R.A., Bogen, N.L., 1983. Tectonic Transect of Sierran Paleozoic through Jurassic Accreted Belts (Field Guide). Society of Economic Petrologists and Mineralogists, Pacific Section, Los Angeles, 22 p.

Şengör, A.M.C., Natal'in, B.A., 1996a. Turkic-type orogeny and its role in the making of the continental crust. Annu. Rev. Earth Planet. Sci. 24, 263–337. https://doi.org/10.1146/annurev.earth.24.1.263.

Şengör, A.M.C., Natal'in, B.A., 1996b. Paleotectonics of Asia: fragments of a synthesis. In: Yin, A., Harrison, T.M. (Eds.), The Tectonic Evolution of Asia. Cambridge University Press, Cambridge, pp. 486–640.

Şengör, A.M.C., Natal'in, B.A., Burtman, V.S., 1993. Evolution of the Altaid tectonic collage and Palaeozoic crustal growth in Eurasia. Nature 364, 299 307. https://doi.org/10.1038/364299a0.

Shepard, S., Krapez, B., Zi, J.W., Rasmussen, B., Fletcher, I., 2017. SHRIMP U-Pb zircon geochronology establishes that banded iron formations are not chronostratigraphic markers across Archean greenstone belts of the Pilbara craton. Precambrian Res. 292, 290–304. https://doi.org/10.1016/j.precamres.2017.02.004.

Shibuya, T., Kitajima, K., Komiya, T., Terabayashi, M., Maruyama, S., 2007. Middle Archean ocean ridge hydrothermal metamorphism and alteration recorded in the Cleaverville area, Pilbara Craton,Western Australia. J. Metamorph. Geol. 25, 751–767. https://doi.org/10.1111/j.1525-1314.2007.00725.x.

Shibuya, T., Komiya, T., Nakamura, K., Takai, K., Maruyama, S., 2010. Highly alkaline, high-temperature hydrothermal fluids in the early Archean Ocean. Precambrian Res. 182, 230–238. https://doi.org/10.1016/j.precamres.2010.08.011.

Shimojo, M., Yamamoto, S., Aoki, S., Sakata, S., Maki, K., Koshida, K., Ishikawa, A., Hirata, T., Collerson, K.D., Komiya, T., 2013. Occurrence of >3.9 Ga "Nanok" Gneiss from Saglek Block, Northern Labrador. Mineral. Mag. 77 (5), 2202.

Shimojo, M., Yamamoto, S., Sakata, S., et al., 2016. Occurrence and geochronology of the Eoarchean, ~3.9 Ga, Iqaluk Gneiss in the Saglek Block, northern Labrador, Canada: evidence for the oldest supracrustal rocks in the world. Precambrian Res. 278, 218–243. https://doi.org/10.1016/j.precamres.2016.03.018.

Shirey, S.B., Richardson, S.H., 2011. Start of the Wilson Cycle at 3 Ga shown by diamonds from subcontinental mantle. Science 333, 434–436.

Sisson, T.W., Moore, J.G., 1994. Geologic map of the Giant Forest quadrangle, Tulare County, California. U.S. Geological Survey Geologic Quadrangle Map GQ-1751 (scale 1:62,500).

Sizova, E., Gerya, T., Stüwe, K., Brown, M., 2015. Generation of felsic crust in the Archean:a geodynamic modeling perspective. Precambrian Res. 271, 198–224. https://doi.org/10.1016/j.precamres.2015.10.005.

Sleep, N.H., 2000. Evolution of the mode of convection within terrestrial planets. J. Geophys. Res. 105, 17563–17578. https://doi.org/10.1029/2000JE001240.

Sleep, N.H., Windley, B.F., 1982. Archean plate tectonics: Constraints and inferences. J. Geol. 90, 363–379.

Smart, C.M., Wakabayashi, J., 2009. Hot and deep: Rock record of subduction initiation and exhumation of high-temperature, high-pressure metamorphic rocks, Feather River ultramafic belt, California. Lithos 113, 292–305. https://doi.org/10.1016/j.lithos.2009.06.012.

Smith, J.B., Barley, M.E., Groves, D., Krapez, B., McNaughton, N.J., Bickle, M.J., Chapman, H.J., 1998. The Sholl Shear Zone, Western Pilbara: evidence for a domain boundary structure from integrated tectonic analyses, SHRIMP UPb dating and isotopic and geochemical data of granitoids. Precambrian Res. 88, 143–171. https://doi.org/10.1016/S0301-9268(97)00067-3.

Smithies, R.H., 2002. Archaean boninite-like rocks in an intracratonic setting. Earth Planet. Sci. Lett. 197, 19–34.

Smithies, R.H., Nelson, D.R., Pike, G., 2001. Development of the Archaean Mallina Basin, Pilbara Craton, northwestern Australia; a study of detrital and inherited zircon ages. Sediment. Geol. 141-142, 79–94.

Smithies, R.H., Champion, D.C., Sun, S.S., 2004. Evidence for early LREE-enriched mantle source regions: diverse magmas from the c. 3.0 Ga Mallina Basin, Pilbara Craton, NW Australia. J. Petrol. 45, 1515 1537.

Smithies, R.H., Lu, Y., Kirkland, C.L., Johnson, T.E., Mole, D.R., Champion, D.C., Martin, L., Jeon, H., Wingate, M., Johnson, S., 2021. Oxygen isotopes trace the origins of Earth's earliest continental crust. Nature 592, 70–75 (2021). https://doi.org/10.1038/s41586-021-03337-1.

Snelling, A.A., Gates, D., 2009. Implications of Polonium radiohalides in nested plutons of the Tuolumne Intrusive Suite, Yosemite, California. Answers Res. J. 2, 53–77.

Snoke, A.W., Barnes, C.G., 2006. The development of tectonic concepts for the Klamath Mountains province, California and Oregon. In: Snoke, A.W., Barnes, C.G. (Eds.), Geological Studies in the Klamath Mountains Province, California and Oregon: A Volume in Honor of William P. Irwin. Geological Society of America Special Paper, 410, pp. 1–29. https://doi.org/10.1130/2006.2410(01).

Steenfelt, A., Garde, A.A., Moyen, J.-F., 2005. Mantle wedge involvement in the petrogenesis of Archaean grey gneisses in West Greenland. Lithos 79, 207–228.

Stern, R.J., 2010. The anatomy and ontogeny of modern intra-oceanic arc systems. In: Kusky, T.M., Zhai, M.-G., Xiao, W. (Eds.), The Evolving Continents: Understanding Processes of Continental Growth. Geological Society, London, Special Publications, 338, pp. 7 34.

Stille, H., 1924. Grundfragen der vergleichenden Tektonik. GebruderBorntrager, Berlin.

Stowe, C.W., 1968. Geology of the country south and west of Selukwe. Bull. Geol. Surv. Rhodesia 59, 209.

Stowe, C.W., 1971. Summary of the tectonic development of the Rhodesian Archaean craton. Geological Society of Australia Special Publication 3, 377 383.

Stowe, C.W., 1974. Alpine-type structures in the Rhodesian basement complex at Selukwe. J. Geol. Soc. 130, 411–425. https://doi.org/10.1144/gsjgs.130.5.0411.

Stuart, C.A., Piazolo, S., Daczko, N.R., 2016. Mass transfer in the lower crust: evidence for incipient melt assisted flow along grain boundaries in the deep arc granulites of Fiordland, New Zealand. Geochem. Geophys. Geosyst. 17, 3733 3753.

Stuart, C.A., Meek, U., Dacko, N.R., Piazolo, S., Huang, J.X., 2018. Chemical signatures of melt-rock interaction in the root of a magmatic arc. J. Petrol. 59, 321–340. https://doi.org/10.1093/petrology/egy029.

Suess, E., 1875. Die Entstehung der Alpen. WilhelmBraumuller.

Szilas, K., Van Hinsberg, V.J., Kisters, A.F.M., Hoffmann, J.E., Windley, B.F., Kokfelt, T. F., Scherstén, A., Frei, R., Rosing, M.T., Münker, C., 2013. Remnants of arc-related Mesoarchaean oceanic crust in the Tartoq Group of SW Greenland. Gondwana Res. 23, 436–451.

Taira, A., 2001. Tectonic evolution of the Japanese island arc system. Annu. Rev. Earth Planet. Sci. 29, 109 134.

Teng, L.S., Lee, C.T., Tsai, Y.B., Hsiao, L.Y., 2000. Slab break off as a mechanism for flipping subduction polarity in Taiwan. Geology 28 (2). https://doi.org/10.1130/00917613(2000)28<155:SBAAMF>2.0.CO;2.

Terabayashi, M., Masafa, Y., Ozawa, H., 2003. Archean ocean-floor metamorphism in the North Pole area, Pilbara Craton, western Australia. Precambrian Res. 127, 167–180. https://doi.org/10.1016/S0301-9268(03)00186-4.

Tessalina, S.G., Bourdon, B., Van Kranendonk, M., Birck, J.-L., Philippot, P., 2010. Influence of Hadean crust evident in basalts and cherts from the Pilbara Craton. Nat. Geosci. 3, 214–217.

Teyssier, C., Whitney, D.L., 2002. Gneiss domes and orogeny. Geology 30, 1139–1142. https://doi.org/10.1130/0091-7613(2002)030<1139:GDAO>2.0.CO;2.

Thorpe, R.I., Hickman, A.H., Davis, D.W., Mortensen, J.K., Trendall, A.F., 1992. U/Pb zircon geochronology of Archaean felsic units in the Marble Bar region, Pilbara Craton, Western Australia. Precambrian Res. 56, 169–189.

Tobish, O., 1966. Large-scale Basin-and-Dome pattern resulting from the interference of major folds. Geol. Soc. Am. Bull. 77, 393–408.

Turner, S., Wilde, S., Wörner, G., Schaefer, B., Lai, Y.J., 2020. An andesitic source for Jack Hills zircon supports onset of plate tectonics in the Hadean. Nat. Commun. 11, 1241. https://doi.org/10.1038/s41467-020-14857-1.

UNESCO, 1976. Geological World Atlas, 1:10,000,000. Unesco and Commission for the Geological Map of the World, Paris.

Utsunomiya, A., Ota, T., Windley, B.F., Suzuki, N., Uchio, Y., Munekata, K., Maruyama, S., 2007. History of the Pacific superplume: implications for Pacific paleogeography since the Late Proterozoic. In: Superplumes: Beyond Plate Tectonics. Springer, Dordrecht, pp. 363–408.

Van Haaften, W.M., White, S.H., 1998. Evidence for multiphase deformation in the Archean basal Warrawoona Group in the Marble Bar area, East Pilbara, Western Australia. Precambrian Research 88, 53 66.

Van Kranendonk, M.J., 2006. Volcanic degassing, hydrothermal circulation and the flourishing of early life on Earth: a review of the evidence from c. 3490-3240 Ma rocks of the Pilbara Supergroup, Pilbara Craton, Western Australia. Earth Sci. Rev. 74, 197–240.

Van Kranendonk, M.J., Hickman, A.H., Smithies, R.H., Nelson, D., Pike, G., 2002. Geology and Tectonic Evolution of the Archaean North Pilbara Terrain, Pilbara Craton. Western Australia. Econ. Geol. 97, 695–732.

Van Kranendonk, M.J., Collins, M.J., Hickman, A.H., Pawley, M.J., 2004. Critical tests of vertical vs horizontal tectonic models for the Archaean East Pilbara granite-greenstone terrane, Pilbara Craton, Western Australia. Precambrian Research 131, 173–211.

Van Kranendonk, M.J., Bleeker, W., Ketchum, J., 2006. Phreatomagmatic boulder conglomerates at the tip of the ca 2772 Ma Black Range doleerite dyke, Pilbara Craton, Western Australia. Australian Journal of Earth Sciences 53, 617–630. https://doi.org/10.1080/08120090600686777.

Van Kranendonk, M.J., Hickman, A.H., Smithies, R.H., Champion, D.C., 2007. Paleoarchean development of a continental nucleus: the East Pilbara terrane of the Pilbara craton, Western Australia. In: Van Kranendonk, M.J., Smithies, R.H., Bennet, V. (Eds.), Earth's Oldest Rocks. Elsevier, Amsterdam, pp. 307–337.

Van Kranendonk, M.J., Hugh Smithies, R., Hickman, A.H., Wingate, M.T.D., Bodorkos, S., 2010. Evidence for Mesoarchean (~3.2Ga) rifting of the Pilbara craton: the missing link in an early Precambrian Wilson cycle. Precambrian Res. 177, 145–161.

Van Kranendonk, M.J., Kröner, A., Hoffmann, J.E., Nagel, T., Anhaeusser, C.R., 2014. Just another drip: Re-analysis of a proposed Mesoarchean suture from the Barberton Mountain Land, South Africa. Precambrian Res. 254, 19–35.

Van Kranendonk, M.J., Smithies, R.H., Griffin, W.L., Huston, D.L., Hickman, A.H., Champion, D.C., Anhaeusser, C.R., Pirajno, F., 2015. Making it thick: a volcanic plateau origin of Palaeoarchean continental lithosphere of the Pilbara and Kaapvaal cratons. In: Roberts, N.M.W., et al. (Eds.), Continent Formation through Time, Geological Society of London, Special Publications, 389, pp. 83–111.

Van Reenen, D.D., Smit, C., Perchuk, A., Huizenga, J., Safonov, O., Gerya, T., 2019. The Neoarchean Limpopo Orogeny: Exhumation and Regional Scale Gravitational Crustal Overturn Driven by a Granulite Diapir. In: Kröner, A., Hofmann, A. (Eds.), The Archaean Geology of the Kaapvaal Craton, pp. 185–224. https://doi.org/10.1007/978-3-319-78652-0_8. Southern Africa, Regional Geology Reviews.

Vanderhaeghe, O., Teyssier, C., 1997. Formation of the Shuswap metamorphic core complex during late-orogenic collapse of the Canadian Cordillera: role of ductile thinning and partial melting of the mid-to lower crust. Geodin. Acta 10 (2), 41–58.

Vanderhaeghe, O., Burg, J.P., Teyssier, C., 1999. Exhumation of migmatites in two collapsed orogens: Canadian Cordillera and French Variscides. In: Ring, U., Brandon, M.T., Lister, G.S., Willett, S.D. (Eds.), Exhumation Processes: Normal Faulting, Ductile Flow, and Erosion, London, Geological Society Special Publications, 154, pp. 181–204.

Vignaroli, G., Faccenna, C., Jolivet, L., Piromallo, C., Rossetti, F., 2008. Subduction polarity reversal at the junction between the Western Alps and the Northern Apennines, Italy. Tectonophysics 450, 34 50. https://doi.org/10.1016/j.tecto.2007.12.012.

Wakita, K., Metcalfe, I., 2005. Ocean plate stratigraphy in East and Southeast Asia. J. Asian Earth Sci. 24, 679–702.

Wallace, R.E., 1990. The San Andreas Fault System, California. U.S. Geological Survey Professional Paper 1515, 283 pp.

Webb, A.A.G., Muller, T., Zuo, J.W., Haproff, P.J., Ramirez-Salazar, A., 2020. A non-plate tectonic model for the Eoarchean Isua supracrustal belt. Lithosphere 12, 166–179. https://doi.org/10.1130/L1130.1.

Wegmann, E., 1953. Uber gleichzeitige Bewegungsbilder verschiedener Stockwerke. Geol. Rundsch. 41, 21 33.

Weinberg, R.F., Podladchikov, Y.Y., 1995. The rise of solid-state diapirs. J. Struct. Geol. 17, 1183–1195.

White, S.H., Zegers, T.E., Van Haaften, W.M., Kloppenburg, A., Wijbrans, J.R., 1998. Tectonic evolution of the eastern Pilbara, Australia. Geol. Mijnb. 76, 343–347.

Whitehouse, M.J., Dunkley, D.J., Kusiak, M.A., Wilde, S.A., 2019. On the true antiquity of Eoarchean chemofossils-assessing the claim for Earth's oldest biogenic graphite in the Saglek block of Labrador. Precambrian Res. 323, 70–81.

Whitney, D.L., Teyssier, C., Siddoway, C.S., 2004. Gneiss Domes in Orogeny: Boulder, Colorado, Geological Society of America Special Paper 380.

Whitney, D.L., Teyssier, C., Rey, P., Buck, W.R., 2013. Continental and oceanic core complexes. Geol. Soc. Am. Bull. 125, 273–298. https://doi.org/10.1130/B30754.1.

Wiemer, D., Schrank, C.E., Murphy, D.T., Wenham, L., Allen, C.M., 2018. Earth's oldest stable crust in the Pilbara Craton formed by cyclic gravitational overturns. Nat. Geosci. 11 (5), 357–361. https://doi.org/10.1038/s41561-018-0105-9.

Wilcox, R.E., Harding, T.P., Seely, D.R., 1973. Basic Wrench Tectonics. AAPG Bull. 57, 74–96.

Williams, I.S., Collins, W.J., 1990. Granite greenstone terranes in the Pilbara Block, Australia, as coeval volcanoplutonic complexes: evidence from U-Pb zircon dating of the Mount Edgar Batholith. Earth Planet. Sci. Lett. 91, 41–53.

Windley, B.F., 1995. The Evolving Continents, 3rd edition. J. Wiley, Chichester.

Windley, B.F., Bridgwater, D., 1971. The evolution of Archaean low- and high-grade terrains. Geological Society of Australia, Special Publications 3, 33–46.

Windley, B.F., Garde, A., 2009. Arc-generated blocks with crustal section in the North Atlantic craton of West Greenland: Crustal growth in the Archean with modern analogues. Earth-Sci. Rev. 93, 1–30.

Windley, B.F., Bishop, F.C., Smith, J.V., 1981. Metamorphosed layered igneous complexes in Archean granulite-gneiss belts. Annu. Rev. Earth Planet. Sci. 9, 175 198. https://doi.org/10.1146/annurev.ea.09.050181.001135.

Windley, B.F., Kusky, T.M., Polat, A., 2021. Onset of plate tectonics by the Eoarchean. Precambrian Res. https://doi.org/10.1016/j.precamres.2020.105980.

Wright, J.E., Wyld, S.J., 1994. The Rattlesnake Creek terrane, Klamath Mountains, California: an early Mesozoic volcanic arc and its basement of tectonically disrupted oceanic crust. Geol. Soc. Am. Bull. 106, 1033 1056. https://doi.org/10.1130/0016-7606(1994)106<1033:TRCTKM>2.3.CO;2.

Wright, J.E., Wyld, S.J., 2006. Gondwana, Iapetan, Cordilleran interactions: A geodynamic model for the Paleozoic tectonic evolution of the North American Cordillera. In: Haggart, J.W., Enkin, R.J., Monger, J.W.H. (Eds.), Paleogeography of the North American Cordillera: Evidence for and against Large-Scale Displacements: St, John's, Newfoundland, Geological Association of Canada Special Paper, 46, pp. 377–408.

Xu, Z.Q., Li, Y., Jinx, Sh., Li, G.W., Pei, X.Z., Ma, X.X., Xiang, H., Wang, R., 2020. Qinling gneiss domes and implications for tectonic evolution of the Early Paleozoic Orogen in Central China. J. Asia Earth Sci. 188, 104052. https://doi.org/10.1016/j.jseaes.2019.104052.

Yin, A., Brandl, G., Kroner, A., 2020. Plate-tectonic processes at ca. 2.0 Ga: evidence from >600 km of plate convergence. Geology 48, 103–107. https://doi.org/10.1130/G47070.1.

Žák, J., Paterson, S.R., 2005. Characteristics of internal contacts in the Tuolumne batholith, Central Sierra Nevada, California (USA): implications for episodic emplacement and physical processes in a continental arc magma chamber. Geol. Soc. Am. Bull. 117, 1242–1255. https://doi.org/10.1130/B25558.1.

Zegers, T.E., 1996. Structural, kinematic and metallogenic evolution of selected domains of the Pilbara granitoid–greenstone terrain, Ph.D. Dissertation, vol. 146. Utrecht University, Geologica Ultraiectina, 208 pp.

Zegers, T.E., van Keken, P.E., 2001. Middle Archean continent formation by crustal delamination. Geology 29, 1083–1086.

Zegers, T., White, S.H., de Keijer, M., Dirks, P., 1996. Extensional structures during deposition of the 3460 Ma Warrawoona Group in the eastern Pilbara Craton. Western Australia, Precambrian Research 80, 89–105.

Zeh, A., Gerdes, A., 2012. U–Pb and Hf isotope record of detrital zircons from gold-bearing sediments of the Pietersburg Greenstone belt (South Africa)—is there a common provenance with the Witwatersrand Basin? Precambrian Res. 204–205, 46 56.

Zeh, A., Jaguin, J., Poujol, M., Boulvais, P., Block, S., Paquette, J.-L., 2013. Juvenile crust formation in the northeastern Kaapvaal Craton at 2.97 Ga—Implications for Archean terrane accretion, and the source of the Pietersburg gold. Precambrian Res. 233, 20–43.

Zellmer, G.F., Edmonds, M., Straub, S.M., 2015. Volatiles in subduction zone magmatism. Geological Society, London, Special Publications 410, pp. 1–17.